

ARFGEF mutations: A mechanism for breast-to-brain metastasis

Item Type	Thesis or dissertation
Authors	Allamsetty, Naga Harshitha
Citation	Allamsetty, N.H. (2025) ARFGEF mutations: A mechanism for breast-to-brain metastasis. University of Wolverhampton. https://wlv.openrepository.com/handle/2436/625979
Publisher	University of Wolverhampton
Download date	2026-06-11 03:35:35
License	https://creativecommons.org/licenses/by-nc-nd/4.0/
Link to Item	https://wlv.openrepository.com/handle/2436/625979



**ARFGEF Mutations: A mechanism for breast-to-brain
metastasis.**

NAGA HARSHITHA ALLAMSETTY

(Student number:2000501)

**A thesis submitted in partial fulfilment of the requirements of
the University of Wolverhampton for the degree of
Master of Philosophy**

Research Institute in Healthcare Science

Faculty of Science and Engineering

University of Wolverhampton

November 2024

DECLARATION

This work, or any aspect of it has not been previously submitted in any format to the University or any other institution for evaluation, publication, or any other intention. Except for any explicit acknowledgements, references, and/or bibliographies indicated in the work is solely the product of my own efforts and the efforts of others.

The authorship of this work by Naga Harshitha Allamsetty is ensured by sections 77 and 78 of the Copyright, Designs and Patents Act 1988. Currently, the author has the copyright.

Signature: NAGA HARSHITHA ALLAMSETTY

Date: 29/12/24

ACKNOWLEDGEMENTS

I would like to sincerely thank Dr Mark Morris for his guidance and continuous support, without whom the present work would not have been possible. Dr Mark has always been an inspiration, and his thought-provoking questions and in-depth discussions have been instrumental in shaping research. I want to thank Dr Ivonne Olivares for her support and guidance. Special thanks to Amisha and Akshaya for their contributions to my project. It was indeed a pleasure working with them.

I am deeply grateful to Prof Weiguang Wang and Prof Angel Armesilla for their encouragement and support. I would also thank Dr Vinodh Kannappan for being supportive during my research time at the University of Wolverhampton. I would like to extend my thanks to Teja Kola, Raaghavi Aravindan, Yamini Mohan, Joel Varghese, Gautham Rajendran, Leander Santhosh, Yoshitha Lakshmanan, Benjamin Small, Chris Edward, Karim Azar, for making my time in Wolverhampton memorable.

I deeply thank the University of Wolverhampton for providing the necessary resources and unwavering support that were essential for the successful completion of my course.

I extend my heartfelt gratitude to my parents, whose encouragement has enabled me to pursue my aspirations and undertake my research.

Lastly, I offer my sincere thanks to the almighty God, without whom none would have been possible.

TABLE OF CONTENTS

LIST OF FIGURES	VII
LIST OF TABLES	IX
LIST OF ABBREVIATIONS	X
ABSTRACT.....	XV
1. INTRODUCTION.....	1
1.1 Cancer and its Epidemiology	2
1.2 Hallmarks of Cancer.....	3
1.3 Cancer Molecular Biology	5
1.4 Breast Cancer and its Incidence	8
1.4.1 Molecular Basis of Breast Cancer	9
1.5 Metastasis.....	11
1.6 Breast to brain metastasis.....	14
1.7 Neurotransmitters	16
1.7.1 Glutamate and glutamate receptor	18
1.7.2 GABA and GABA receptor	20
1.8 Neurotransmitters, Neurotransmitter Receptors and Brain Tumours.....	22
1.9 Role of ARFGEF3 in Breast cancer progression and brain metastasis	24
2. AIM AND OBJECTIVES.....	27
3. MATERIALS AND METHODS.....	29
3.2 Cell Culture	30
3.2.1 Breast Cancer Cell Lines.....	30
3.2.2 The Parameters for Aseptic Apparatus and Culturing Environment	30

3.2.3 Media Preparation for Cell Culture	30
3.2.4 Reviving Frozen Cells.....	31
3.2.5 Maintenance of Cell Culture	31
3.2.4 Cell Quantification.....	32
3.2.5 Cryopreservation of Cell lines.....	32
3.3 Expression Analysis of Nucleic Acid	32
3.3.1 RNA Isolation.....	32
3.3.2 Quantification of RNA.....	34
3.3.3 Complementary DNA (cDNA) Synthesis	34
3.3.4 Primer Designing for RT PCR	35
3.3.5 Reverse Transcription (RT) PCR.....	38
3.3.6 Quantitative Real-Time PCR.....	39
3.4 Growth Curve Analysis	40
3.5 Western Blot.....	41
3.5.1 RIPA Buffer Preparation.....	41
3.5.2 Protein extraction.....	41
3.5.3 Protein Quantification	42
3.5.4 Gel Preparation	43
3.5.5 Sample Preparation and Gel Electrophoresis	44
3.5.6 Blotting.....	45
3.5.7 Blocking	46
3.5.7 Antibody Staining	47
3.5.8 Image development.....	47
3.6 Flow Cytometry.....	48
3.7 Immunostaining.....	50

3.8 Statistical Analysis	52
4. RESULTS	53
4.1 Confirmation of ARFGEF3 gene mutation using WES data.....	55
4.2 Confirmation of ARFGEF3 gene knockout in MCF-7 cells by PCR and Western Blot Analysis.....	57
4.3 Growth Curve Analysis of ARFGEF3 KO and SCR	58
4.4 Analysis of PHB2 Expression at mRNA and protein levels.....	60
4.5 Expression Analysis of Neurotransmitter Receptors using RT-PCR.....	61
4.6 Expression Analysis of Neurotransmitter Receptors using Western Blot	71
4.7 Expression Analysis of Neurotransmitter Receptors Using Flow Cytometry	72
4.8 Qualitative Analysis of Neurotransmitter Receptors Using Immunofluorescence ...	79
5. DISCUSSIONS	82
6. CONCLUSIONS	95
7. REFERENCES.....	99

LIST OF FIGURES

Figure 1.1 The Hallmarks of Cancer - A Framework of Tumor Progression.	4
Figure 1.2 Classification of glutamate receptors.	20
Figure 1.3 Role of Glutamate Signalling in Synaptic Interactions Between Neurons, Astrocytes, and Metastatic Breast Cancer Cells.	24
Figure 4.1 Sanger sequencing of ARFGEF3 mutation in BBM tumour.	56
Figure 4.2 Confirmation of ARFGEF3 expression in following CRISPR-knockout at the RNA and protein level.	58
Figure 4.3 Microscopic Images of MCF-7 under different conditions.	59
Figure 4.4 Growth Curve analysis of ARFGEF3 KO and SCR.	59
Figure 4.5 Expression analysis of PHB2 in m-RNA level and protein level.	61
Figure 4.6 Expression data of neurotransmitter receptor subunits in Control (SCR) and ARFGEF3 KO clones were analysed using end-point PCR and qPCR (Nanda Gopal's).	64
Figure 4.7 Expression data of neurotransmitter receptor subunits in Control (SCR) and ARFGEF3 KO clone using RT-PCR (conducted by me).	65
Figure 4.8 mRNA expression levels of neurotransmitter receptor subunits in ARFGEF3 KO and Control SCR using qRT-PCR analysis (conducted by me).	67
Figure 4.9 mRNA expression levels of neurotransmitter receptor subunits in ARFGEF3 KO and Control SCR of a previous student, Nandagopal Ajaykumar and current data done by me.	70
Figure 4.10 Confirmation of expression of neurotransmitter receptors at protein level using Western blot.	72
Figure 4.11 Histograms and counterplots illustrate different neurotransmitter receptors' protein expression in MCF-7 cell lines.	76

Figure 4.12 Bar graph shows the population percentage increase in neurotransmitter receptor expression in the MCF-7 cell lines. 78

Figure 4.13 Qualitative analysis of expression of neurotransmitter receptors in MCF-7 cell lines. 81

LIST OF TABLES

Table 3.1 Components of the "High-Capacity cDNA Reverse Transcription Kit" with the required quantities for the RT master mix.....	35
Table 3.2 Thermal cycler setting for cDNA synthesis.....	35
Table 3.3 List of primer sequences.....	38
Table 3.4 Outlines the components required to prepare the master mix for RT-PCR.....	38
Table 3.5 PCR amplification setting on a thermocycler.....	39
Table 3.6 TaqMan Gene Expression Assays Used for Quantitative Real-Time PCR.....	40
Table 3.7 Components required of qRT-PCR for master-mix preparation.....	40
Table 3.8 (A+S) master mix preparation for protein Quantification.....	43
Table 3.9 Master mix preparation for protein Quantification.....	43
Table 3.10 Composition of stacking gel.....	44
Table 3.11 Composition of Resolving Gel or Separating Gel.....	44
Table 3.12 Reagents required for Protein sample preparation.....	45
Table 3.13 List of Antibodies used for Western blot.....	47
Table 3.14 List of Antibodies Used for Flowcytometry.....	50
Table 3.15 List of Antibodies Used for Immunostaining.....	51
Table 4.1 Mutated Sites in ARFGEF33 Gene in Patient-Derived Samples.....	57

LIST OF ABBREVIATIONS

AIM-1 - Absent in Melanoma 1

AKT - Protein Kinase B

AMPA - Alpha-Amino-3-Hydroxy-5-Methyl-4-Isoxazole Propionic Acid

ARF-GEFs - ADP Ribosylation Factor-GTP Exchange Factors

ARFGEF3 - ADP Ribosylation Factor Guanine Nucleotide Exchange Factor 3

ATM - Ataxia Telangiectasia Mutated

BAD - BCL-2-associated Agonist of Cell Death

BAX - BCL-2-associated X Protein

BBB - Blood-Brain Barrier

BCL2 - B-Cell CLL/Lymphoma 2

BCL-w - B-cell Lymphoma-w

BCL-xl - B-cell Lymphoma-extra Large

BDNF - Brain-Derived Neurotrophic Factor

BIG3 - Brefeldin A-Inhibited Guanine Nucleotide Exchange Protein 3

BID - BH3-interacting Domain Death Agonist

BRCA1 - Breast Cancer Gene 1

BRCA2 - Breast Cancer Gene 2

BRIP - BRCA1 Interacting Protein

CAS - Certified Assurance System

CDH1 - Cadherin-1

CDK2 - Cyclin-dependent Kinase 2

CHK2 - Checkpoint Kinase 2

CNS - Central Nervous System

COX-2 - Cyclooxygenase-2

CRISPR - Clustered Regularly Interspaced Short Palindromic Repeats

cDNA - Complementary DNA

c-MYC - Cellular Myelocytomatosis Oncogene

DALYs - Disability-Adjusted Life Years

DCT - Dopachrome Tautomerase

DMSO - Dimethyl Sulfoxide

DMEM - Dulbecco's Modified Eagle's Medium

DNA - Deoxyribonucleic Acid

DNase I - Deoxyribonuclease I

dNTP - Deoxynucleotide Triphosphates

DTT - Dithiothreitol

ECM - Extracellular Matrix

EMT - Epithelial-Mesenchymal Transition

ER - Estrogen Receptor

ERBB2 - Epidermal Growth Factor Receptor 2

Er α - Estrogen Receptor Alpha

FBS - Fetal Bovine Serum

GABA - Gamma-Aminobutyric Acid

GABRA3 - Gamma-Aminobutyric Acid Type A Receptor Subunit Alpha 3

GABRA4 - Gamma-Aminobutyric Acid Type A Receptor Subunit Alpha 4

GABRB - Gamma-Aminobutyric Acid Type A Receptor Subunit Beta

GABRG1 - Gamma-Aminobutyric Acid Type A Receptor Subunit Gamma 1

GATA3 - GATA Binding Protein 3

GFP - Green Fluorescent Protein

GRB7 - Growth Factor Receptor-Bound Protein 7

GTPases - Guanosine Triphosphatases

HER2 - Human Epidermal Growth Factor Receptor 2

HRP - Horseradish Peroxidase

INK4a - Cyclin-dependent Kinase Inhibitor 2A

IVD - In Vitro Diagnostics

Ki67 - A Marker for Proliferation

KO - Knockout

LABC - Luminal A Breast Cancer

LBBC - Luminal B Breast Cancer

MAF - Minor Allele Frequency

MART1 - Melanoma Antigen Recognized by T Cells 1

MCL-1 - Myeloid Cell Leukemia-1

MCF-7 - Michigan Cancer Foundation-7

mGlu - Metabotropic Glutamate Receptors

mGluRs - Metabotropic Glutamate Receptors

MMPs - Matrix Metalloproteins

MITF - Microphthalmia-associated Transcription Factor

mTOR - Mechanistic Target of Rapamycin

NBS1 - Nijmegen Breakage Syndrome 1

NGS - Next-Generation Sequencing

NMDA - N-Methyl-D-Aspartate

PALB2 - Partner and Localizer of BRCA2

PBS - Phosphate Buffered Saline

PCR - Polymerase Chain Reaction

PDQ - Physician Data Query

PHB2 - Prohibitin 2

PI3K - Phosphoinositide 3-Kinase

PMEL17 - Premelanosome Protein 17

PR - Progesterone Receptor

PVDF - Polyvinylidene Fluoride

qPCR - Quantitative Polymerase Chain Reaction

RAR α - Retinoic Acid Receptor Alpha

RB - Retinoblastoma Protein

RNA - Ribonucleic Acid

RNase - Ribonuclease

RT - Reverse Transcription

RT-PCR - Reverse Transcriptase Polymerase Chain Reaction

SDS-PAGE - Sodium Dodecyl Sulfate Polyacrylamide Gel Electrophoresis

SIFT - Sorting Intolerant from Tolerant

SRC - Proto-Oncogene Tyrosine-Protein Kinase

STARD3 - StAR-related Lipid Transfer Domain Containing 3

STAT3 - Signal Transducer and Activator of Transcription 3

TBST - Tris-Buffered Saline with Tween 20

TBX2 - T-Box Transcription Factor 2

TBS - Tris-Buffered Saline

TEMED - Tetramethylethylenediamine

TGF- β - Transforming Growth Factor Beta

TNBC - Triple-negative Breast Cancer

TP53 - Tumor Protein 53

TSGs - Tumour Suppressor Genes

TYR - Tyrosinase

TYRP1 - Tyrosinase-related Protein 1

WHO - World Health Organization

WES - Whole Exome Sequencing

WT - Wild Type

ZR-75 - ZR-75 Breast Cancer Cell Line

ABSTRACT

Cancer is one of the most devastating and major causes of death worldwide. In 2018, there were an estimated 18.1 million new cases and 9.6 million deaths globally. Most cancer-related fatalities, over 90%, are caused by the spread of cancer cells to other parts of the body, known as metastasis. Similarly, around 80% of deaths resulting from breast cancer are due to metastasis. Approximately 15-25% of breast tumours metastasise to the brain, and the outlook for patients with breast-to-brain metastasis is poor. Although it is established that mutations are responsible for driving metastasis, the specific gene alterations that promote brain metastasis remain unknown. Breast-to-brain metastasis occur when primary breast tumour cells disseminate to the brain, proliferating to form secondary tumours. Recent research has shown that metastatic brain cancer expresses neurotransmitter receptors and forms synaptic-like connections with neurons, contributing to tumour growth and survival. Exome sequencing of 26 breast-to-brain metastasis (BBM) cancers identified *ARFGEF3* mutations in the BBM samples. This suggests that the absence of *ARFGEF3* in breast cancer cells plays a role in the development of brain metastasis. The research presented here aims to uncover the molecular mechanisms underlying the metastatic process and identify potential therapeutic targets for preventing or treating brain metastasis in breast cancer patients.

The knockout of *ARFGEF3* by CRISPR Cas9 gene editing results in the regulation of several neurotransmitter receptors in a breast cancer cell line. The results presented here suggest a mechanism where mutations in *ARFGEF3* may facilitate metastasis to and proliferation in the brain. Understanding this mechanism could facilitate the development of new therapeutic drugs targeting these pathways, potentially improving the treatment outcomes for metastatic breast cancer patients.

1. INTRODUCTION

1.1 Cancer and its Epidemiology

Cancer is one of the most destructive categories of human diseases, characterised by a wide range of distinctive clinical symptoms and resulting in millions of deaths worldwide each year (Upadhyay, 2021a). The worldwide prevalence of cancer has significantly increased. The World Health Organisation (WHO) forecasts an alarming 70% surge in new cancer cases over the next 20 years. Although there have been advancements in treatment and prognosis in recent decades, cancer now ranks as the second leading cause of death (Arem and Loftfield, 2018). According to WHO, malignancies have the highest global burden, with 244.6 million disability-adjusted Life Years (DALYs), affecting both men (137.4 million DALYs) and women, surpassing that of ischemic heart disease and stroke. Among women, breast cancer is the prevailing form of cancer, with a total of 2.09 million cases. It has the highest age-standardised incidence rate, namely 46.3 % of 100,000 women (Mattiuzzi and Lippi, 2019).

Cancer encompasses a diverse spectrum of diseases, which are categorised according to their primary site of origin in the body, in addition, they are also classified by the specific type of cell from which they originated. There are 5 main types: Carcinoma, sarcoma, leukaemia, lymphoma and myeloma, and brain & spinal cord cancers (Cancer Research UK, 2024). Carcinomas constitute approximately 90% of human malignancies and are tumours that originate from epithelial cells. Sarcomas are relatively rare in humans, which are cohesive tumours originating in connective tissues such as muscle, bone, cartilage, and fibrous tissue. Leukaemia and lymphoma, which make up approximately 8% of all human cancers, originate from hematopoietic cells and immune system cells. Tumours can be characterised by the specific cell type affected; for example, fibrosarcoma arises from fibroblasts, whereas erythroid leukaemia originates from erythrocyte precursors (IncCooper GM., 2000).

Cancer is a pathological condition characterised by altered signalling and metabolism, resulting in the uncontrolled proliferation and survival of the mutated cells (Brown *et al.*, 2023). Benign tumours are non-cancerous growths that remain localised and do not spread to other body parts. They do not metastasise to adjacent anatomical structures or to distant anatomical sites. Benign tumours exhibit a modest growth rate and possess well-defined boundaries. Malignant tumours consist of cells that undergo uncontrolled growth and have the ability to spread both locally and to distant locations. Malignant cells spread to distant sites via the circulation or lymphatic system, a phenomenon referred to as metastasis (Patel, 2020)

Cancer development is a multistage process that occurs due to mutations in several genes responsible for regulating cell proliferation, apoptosis, and metabolic pathways (Kontomanolis *et al.*, 2021). These mutations disrupt the regular signalling pathways (Sever and Brugge, 2015). Mutations in proto-oncogenes can alter them into oncogenes and however, mutations in tumour suppressor genes result in suppression of function, enabling the cancer cells to evade regulatory control and proliferate (Dakal *et al.*, 2024). This activation/inactivation can trigger dysregulated cell cycling and cell death (Sarkar *et al.*, 2013). The loss of proliferative and structural control enables the movement of cancer cells through the bloodstream and lymphatic vessels to distant areas of the body, which results in migration and invasion (Hanahan and Weinberg, 2011; Sarkar *et al.*, 2013; Fares, Fares, *et al.*, 2020). Cancer progression is affected by an intricate interplay among the tumour cells, adjacent non-cancerous cells, and the extracellular matrix (ECM) (Sever and Brugge, 2015).

1.2 Hallmarks of Cancer

The hallmarks of cancer were originally proposed as six biological capabilities that are developed throughout the complex and gradual development of human cancers. These hallmarks serve as a fundamental framework for simplifying the intricacies of neoplastic

disease (Hanahan and Weinberg, 2011). It was initially proposed by Weinberg and Hanahan and was eventually broadened to ten distinct capacities and four enabling characteristics. The current hallmarks (Figure 1.1) consist of maintaining evading growth, suppressors proliferative signalling, initiating or accessing vasculature, resisting cell death, enabling replicative immortality, activating invasion and metastasis, changing cellular metabolism, unlocking phenotypic plasticity, and avoiding immune destruction (Hanahan, 2022). In a recent review, Hanahan established a correlation between cancer hallmarks and the neurological system, which states that the nervous system significantly impacts tumour innervation and the functioning of neuronal regulatory circuits in cancer (Hanahan and Monje, 2023).



Figure 1.1 The Hallmarks of Cancer - A Framework of Tumor Progression.

The conceptual framework known as the “Hallmark of Cancer” is a fundamental and distinguishing characteristic of cancer. This schematic representation outlines the ten hallmarks of cancer, which are key biological processes enabling tumour development and survival (Hanahan and Weinberg, 2011).

1.3 Cancer Molecular Biology

Carcinogenesis is a multistage process in which the genes involved in maintaining the balance between cell proliferation and apoptosis are mutated, thus causing uncontrolled cell growth, breakdown of the general metabolic cycle, cell invasion, and metastasis (N Kontomanolis *et al.*, 2021). Numerous genetic alterations have been documented that can transform healthy human cells, leading to the development of tumours and the onset of cancers (Upadhyay, 2021b). Mutations in these cellular protooncogenes can transform them into oncogenes by activating them. This conversion can occur due to point mutations, chromosomal abnormalities, deletions, or insertions, base substitutions, (Markowitz and Bertagnolli, 2009). The common alteration in oncogenes is point mutation, where one amino acid of the protein is changed (Botezatu *et al.*, 2016). There are more than 40 oncogenes identified and studied so far, and the most notable oncogenes are RAS and BRAF (Adamson, 1987; Torry and Cooper, 1991; Botezatu *et al.*, 2016; N Kontomanolis *et al.*, 2021).

One of the most studied proto-oncogenes is the RAS family, which comprises K-RAS, N-RAS, and H-RAS, where each RAS has its own designated mutation site (Singh, Thakur and Kumar, 2023). These encode small GTPases involved in cell signalling transduction pathways that regulate cell proliferation, differentiation, and survival (Motoi *et al.*, 2000). When proto-oncogenes such as one of the RAS proteins, c-MYC, or Cyclin-D, is activated into an oncogene, it often mutates only one allele. This mutation commonly arises at certain specific codons, leading to constant activation of RAS protein that continuously signals cell proliferation, even in the absence of growth factors (Motoi *et al.*, 2000; Fares, Fares, *et al.*, 2020). Proto-oncogene

can also be activated through chromosomal abnormalities like chromosomal rearrangement, chromosomal translocation, gene amplification and gene fusion (Torry and Cooper, 1991).

Gene amplification refers to the gene amplification of a restricted chromosomal arm region, (Albertson, 2006). Some examples of such amplicons are GRB7 ((StAR)-related lipid transfer domain containing 3), RAR α (Retinoic acid receptor alpha), MITF targets genes involved in cell-cycle arrest (*INK4a* and *p21*), cell survival (B-cell CLL/lymphoma 2, *BCL2*) and cell proliferation (*CDK2* and *TBX2*), and differentiation (*TYRP1*, *TYR*, *DCT*, *PMEL17*, *AIM-1*, and *MART1*), which are found in patients of different breast, lung, gastric, oesophageal and other types of cancers (Matsui *et al.*, 2013). An increase in the number of copies leads to an increase in the expression, affecting the cellular process involved (Albertson, 2006). In cell proliferation, c-MYC amplification is typically associated with a 20-fold increase in lung carcinoma or leukaemia, whereas amplification of 5 to 1000-fold in N-MYC can contribute to the development of neuroblastoma or retinoblastoma and erbB-2 amplification of about 15-30-fold is observed in some instances of breast cancer or ovarian cancer (Botezatu *et al.*, 2016).

Inhibition of apoptosis leads to uncontrolled growth, resulting in cancer formation. It occurs through two main pathways: the intrinsic and extrinsic pathways, where several disruptions have been observed in both (O'Brien and Kirby, 2008). The path significantly depends on the pro-apoptotic and anti-apoptotic signal equilibrium (Power, Fanning and Redmond, 2002). In some cancers, it is observed that p53, which is the apoptosis-controlling factor, is mutated or has disrupted function, whereas in some other cancers, Bcl-2 is overexpressed (O'Brien and Kirby, 2008). Bcl-2 regulates apoptosis with pro-apoptosis and pro-survival proteins as subgroups (Power, Fanning and Redmond, 2002). Abnormally high expression of BCL-2 is frequently observed in different cancers, and it is noted that this overexpression renders the malignant cell resistant to many anti-cancer agents that cause cell death (Kaloni *et al.*, 2023).

In the BCL-2 family, BCL2, BCL-w, BCL-xl, and MCL-1 are anti-apoptotic members, whereas pro-apoptotic members include BAD, BID, and BAX. Overexpression of pro-apoptotic proteins makes cells more susceptible to apoptosis, while overexpression of anti-apoptotic proteins makes them more resistant (Kaloni *et al.*, 2023).

Tumour suppressor genes (TSGs) are often mutated or downregulated, leading to protein degradation or inactivation (Liu *et al.*, 2015). Examples of commonly dysregulated TSGs products include the retinoblastoma protein (*RB*), BRCA1 and 2, p53, ATM, CHK2, NBS1, RAD50, PALB2, and BRIP (Lee and Muller, 2010). Most of the genes mentioned here are frequently disrupted in breast cancer. Additionally, it has been observed that a mutation in one gene might impact the gene expression of other associated tumour suppressors (Liu *et al.*, 2015). The RB pathway is commonly disrupted in cancer by either the inactivation of RB and CDK inhibitors or by amplification of cyclin D. RB regulates the G1-S phase transition, and alteration of RB causes disruption of the cell cycle, thus producing cancerous cells (Lee and Muller, 2010).

p53 activation generally induces protein transcription involved in cell cycle regulation, DNA repair, senescence, apoptosis, autophagy and metabolism of tumour cells. In most cancers, p53 is observed to have single base-pair substitution in the central and most conserved DNA-binding domain of p53, thus disrupting transcription of the said protein and resulting in cancer cell production (Liu *et al.*, 2015). The tumour suppressor genes *BRCA1*, and *BRCA2* are found to be mutated in more than 10% of patients with breast-ovarian cancer syndrome. This mutation is somatic dominant in inheritance (Lynch, Marcus and Rubinstein, 2008). Cancer patients tend to develop different tissue cancers based on the BRCA type mutated. Cancer development heavily depends on various factors and genes and vastly differs between patients, thus causing the complexity in diagnosis and treatment of the disease itself (De Talhouet *et al.*, 2020).

1.4 Breast Cancer and its Incidence

Breast cancer is the second most common cancer reported so far (Maughan, Lutterbie and Ham, 2010). One in twelve females between 1 and 85 years old tends to get breast cancer in Britain (Akram *et al.*, 2017). The global incidence rate is 48/1000000, ranging from < 30/1,00,000 in sub-Saharan Africa to >70/1,00,000 in Western Europe and North America. Based on these criteria, it can be inferred that the outcome may depend on variables like overall population. The other risk factor is age. Over a third of breast cancer in UK is observed in females over the age of 70 and less than one in five under the age of 50 females. Factors can be classified as reproductive and non-reproductive factors. Risk is high before menarche and after the menopause period due to less breast-feeding incidence. Non-reproductive risks are obesity and alcohol consumption. 5-10% of patients have genetic or hereditary causes; eight out of nine female patients are not due to hereditary causes. In 2020, over 685,000 females worldwide have died due to breast cancer (Wilkinson and Gathani, 2022). 25-30% of patients develop cancer recurrence and are at risk of death from disease dissemination. In 2020, breast cancer constituted over 24.5% of all cancer cases and 15.5% of cancer-related fatalities among women, ranking first in both incidence and mortality in most nations worldwide (Lei *et al.*, 2021). 5-10% of patients tend to develop metastasis at the initial stage of cancer itself, and over 20% develop disease recurrence at a later stage. It also noted that the 5-year survival rate is 27% in the metastatic disease stage. Generally, it is said that 53.2% of patients have luminal A (LABC) subtype, 18.5% have luminal B (LBBC), 18.5% have triple negative, and 9.8% have HER2+. Within triple-negative breast cancer (TNBC), 30.6% accounted for brain metastasis, while in HER2+, 42.3% of patients had neural metastasis (Courtney *et al.*, 2022).

It is noted that developing brain metastasis has one of the worst treatment outcomes and has a high risk of recurrence (Courtney *et al.*, 2022). Even though there is a significant improvement

in diagnosis and treatment techniques, it is still a challenge when it comes to advanced-stage cancer treatment, resulting in a high mortality rate (Ivanova *et al.*, 2023). Breast cancer is broadly divided into invasive and non-invasive. In non-invasive is either lobular carcinoma in situ or ductal carcinoma in situ, where the cancer usually does not have metastasis tendency. Invasive can be infiltrating ductal carcinoma, infiltrating lobular carcinoma, inflammatory breast cancer, mucinous carcinoma, tubular carcinoma, medullary carcinoma, Paget's disease of the breast, phyllodes tumour or triple-negative breast cancer based on the part of the organ where the cancer cells form (*Breast Cancer Treatment (PDQ®)–Patient Version*, no date). The treatment heavily depends on stage, histology and biomarkers assessment results. The most common therapies include chemotherapy, radiotherapy, and surgery. Each subtype is based on the chemical biomarker, tumour position, shape, size and invasive nature. After the treatment, the cancer can recur locally, in nodes or at a distant metastatic site (Maughan, Lutterbie and Ham, 2010). The prevailing issue associated with cancer is metastasis. The most common metastasis sites are bone, liver, lung and brain, where brain metastasis causes significant mortality (Hosonaga, Saya and Arima, 2020; Ivanova *et al.*, 2023). Over 10-30% of breast cancer observed to develop brain metastasis (Hosonaga, Saya and Arima, 2020). It is also noted that brain metastasis is more frequent in patients with HER2+ or triple-negative BC (Hosonaga, Saya and Arima, 2020; Ivanova *et al.*, 2023). Specific therapies targeting brain metastasis in breast cancer are yet to be established and are needed to develop an efficient treatment for the patients (Hosonaga, Saya and Arima, 2020).

1.4.1 Molecular Basis of Breast Cancer

Breast cancer arises from the uncontrolled proliferation of epithelial cells in the mammary ducts or lobules due to the genetic and epigenetic alterations that disrupt normal cell growth and division. It comprises different subtypes based on the presence or absence of hormone

receptors (ER-oestrogen and PR-progesterone receptors), the levels of HER2 (human epidermal growth factor receptor 2), and the presence of proliferation markers like ki-67 which are Luminal A, Luminal B, HER2- enriched, and triple-negative/basal-like (Barzaman *et al.*, 2020; Manore *et al.*, 2022; Nolan, Lindeman and Visvader, 2023). Luminal A tumours exhibit ER and/or PR positivity, which lack HER2 expression with low levels of Ki67. Luminal B tumours exhibit ER and/ or PR expression, but they can be either positive or negative for HER2 and show high levels of Ki67. HER-2 enriched shows positivity for HER2 and are negative for both ER and PR. Triple-negative or basal-like tumours lack the expression of all three receptors (ER, PR, and HER2). These molecular subtypes exhibit variations not only in their gene expression profiles but also in their clinical behaviour, which includes different patterns of metastasis. HER2-positive and triple-negative breast cancers exhibit a greater tendency for brain metastasis compared to luminal subtypes (Kaleem *et al.*, 2022). Breast cancer frequently exhibits genetic alterations, which results in hyperactivation of the PI3K/AKT/mTOR pathway, which are the most common genetic alterations in breast cancer, occurring in approximately 30-40% of cases (Miricescu *et al.*, 2020).

TP53 mutations are prevalent in triple-negative and HER2-positive breast cancers, often resulting in the loss of p53's essential roles in maintaining genome stability and regulating cell cycle progression. Frequent occurrence of PTEN loss, which acts as a suppressor of the PI3K/AKT/mTOR pathway, is also commonly observed in cases of breast cancer. CDH1 and GATA3 mutations (ER-positive) are also widely observed in breast cancers. These mutations impact a transcription factor that plays a role in the differentiation of luminal cells (Miricescu *et al.*, 2020). BRCA1 and BRCA2 act as tumour suppressor genes and are essential for maintaining stability by repairing double-stranded DNA breaks through homologous recombination (Nolan, Lindeman and Visvader, 2023). Inherited Mutations in these genes significantly increase the risk of developing ovarian and breast cancers, especially among

young women (Manore *et al.*, 2022). BRCA1 is often linked to triple-negative breast cancer, whereas BRCA2 mutations are more prevalent in Luminal-type tumours (Damrauer *et al.*, 2014). Alterations in the microenvironment of the mammary gland, such as extracellular matrix and fibroblasts, can promote cancer (Wu and Crowe, 2019). The intricate interactions between cancer cells and different constituents of the tumour microenvironment, such as immune cells, fibroblasts, and the extracellular matrix, profoundly impact tumour characteristics.

Oestrogen receptor (ER) signalling is crucial in approximately 70% of breast cancers. ER-positivity is a hallmark of Luminal breast cancers and is a crucial promoter of tumour growth and progression (Yoshimaru, Aihara, *et al.*, 2017a; Manore *et al.*, 2022). The ER pathway is vital in these subtypes, as oestradiol binds to $ER\alpha$ and stimulates the transcription of genes that regulate cell proliferation and survival (Nolan, Lindeman and Visvader, 2023). An area of growing interest in the field of breast cancer biology is the role of BIG3 (Brefeldin A-inhibited guanine nucleotide exchange protein 3) and its PHB2 (Prohibitin 2) complex interaction in the regulation of $ER\alpha$ activity (Yoshimaru, Aihara, *et al.*, 2017b; Toki *et al.*, 2021a). Recent research has demonstrated that BIG3 inhibits the nuclear translocation of PHB2, thereby preventing PHB2 from repressing $ER\alpha$ -mediated transcription (Kim *et al.*, 2009; Yoshimaru *et al.*, 2015). This interaction enhances the proliferative effects of oestrogen in breast cancer cells, specifically in those with high expression of $ER\alpha$, contributing to tumour growth and progression (Li *et al.*, 2014; Yoshimaru *et al.*, 2015).

1.5 Metastasis

Metastasis is an intricate, multistep process by which cancer cells spread from the primary tumour to form secondary tumours at distant sites. Metastatic Cascade initiates with local invasion, where cancer cells penetrate the basement membrane and invade the adjacent extracellular matrix, which is aided by the degradation of ECM components by proteolytic

enzymes such as matrix metalloproteins (MMPs) (Pickup, Mouw and Weaver, 2014a; Fares, Fares, *et al.*, 2020). This poses a significant challenge in cancer treatment due to its contribution to the death rate among cancer patients (Krakhmal *et al.*, 2015; Suhail *et al.*, 2019). Tumour cell colonisation involves cell proliferation, dormancy, cell death, and angiogenesis (Friedl and Wolf, 2003a). Cancer cells undergo morphological and molecular changes during migration to interact with the external tissue environment, specifically the extracellular matrices (ECM) (Chambers, Groom and MacDonald, 2002). During epithelial-mesenchymal transition (EMT), these changes involve the downregulation of epithelial markers, such as E-cadherin, and the upregulation of mesenchymal markers, such as vimentin and N-cadherin (Canel *et al.*, 2013; Craene and Berx, 2013).

E-cadherin is a transmembrane protein which mediates cell-cell adhesion in epithelial tissues. It is often inhibited during EMT through the action of transcription factors like Snail, Slug, and Twist, which bind to the promoter of E-cadherin, and its expression is repressed (Craene and Berx, 2013). The loss of E-cadherin reduces the cell-cell adhesion strength, allowing the cancer cells to detach from the primary tumour and invade the ECM (Canel *et al.*, 2013; Craene and Berx, 2013). As cancer cells migrate, they frequently remodel the ECM by secretion of MMPs, which degrade ECM components and facilitate pathways for cell invasion (Adams, 2001; Pickup, Mouw and Weaver, 2014b). The migrating cell's leading edge attaches to the ECM through integrin receptors, which transduce signals that enhance actin polymerisation and facilitate cell mobility (Adams, 2001; Chaffer and Weinberg, 2011). After infiltrating the nearby stroma, cancer cells can enter the bloodstream or lymphatic system, called intravasation (Krakhmal *et al.*, 2015; Suhail *et al.*, 2019). Cancer cells need to withstand the shear stress to survive in circulation, evade immune detection, and avoid apoptosis, often by acquiring stem cell-like properties through EMT. CTCs (circulating tumour cells) that overcome these challenges have the ability to extravasate at distant sites and interact with the surrounding

microenvironment to form micrometastasis (Chambers, Groom and MacDonald, 2002; Friedl and Wolf, 2003b; Quail and Joyce, 2013; Suhail *et al.*, 2019).

The metastatic cascade is a complex, multi-step process by which cancer spreads from its primary site to distant organs. It begins with invasion, where tumour cells breach the surrounding extracellular matrix and basement membrane. During intravasation, these cells infiltrate the circulation or lymphatic channels. Once in circulation, cancer cells must endure the adverse conditions of the circulatory system while escaping immune detection. They then undergo extravasation, exiting the blood vessels to infiltrate distant tissues. In colonisation, the cells adapt to the new microenvironment and establish secondary tumours, completing the metastatic cycle and enabling the growth of new malignancies (Fares, Fares, *et al.*, 2020). For cancer cells to successfully migrate to other organs, they are required to go through a mesenchymal-to-epithelial transition (MET), which establishes cell-cell contacts and integrates into the tissue morphology for the macro metastasis growth (Craene and Berx, 2013). Several key signalling pathways, including TGF- β , Wnt/ β -catenin, Notch, and Hedgehog, regulate EMT and MET during metastasis (Zhang, Tian and Xing, 2016).

TGF- β induces EMT, transitioning from a tumour suppressor in the initial stages to promoting metastasis. The Wnt/ β -catenin pathway induces EMT by increasing the expression of mesenchymal genes, while the Notch and Hedgehog signalling promotes cancer stemness, cell survival and invasiveness during metastasis (Craene and Berx, 2013; Fares, Fares, *et al.*, 2020). The increased expression of vimentin in breast cancer is associated with poor prognosis and heightened metastatic potential (Canel *et al.*, 2013). The upregulation of vimentin and N-cadherin and the loss of E-cadherin is a crucial indicator of EMT, showing the transition to a more invasive state. Snail, Slug, and Twist transcriptional factors are vital in regulating the EMT by suppressing the E-cadherin and promoting mesenchymal traits, where Snail binds to

E-box elements in epithelial gene promoters, driving EMT (Serrano-Gomez, Maziveyi and Alahari, 2016). The plasticity between MET and EMT facilitates the cancer cells to adapt to different microenvironments (Canel et al., 2013; Craene and Berx, 2013). Perineural invasion, the infiltration and proliferation of cancer cells along nerves is a significant factor in the spread of cancer (Chen *et al.*, 2019). Research suggests that EMT can be significantly influenced by essential epigenetic modifications like DNA methylation and histone modifications, which are significant drivers of EMT (Bornman et al., 2001). Transcription factors such as SNAIL, SLUG, ZEB1, and ZEB2 bind to the CDH1 promoter, which effectively represses E-cadherin activity (Friedl and Wolf, 2003b; Canel *et al.*, 2013; Pickup, Mouw and Weaver, 2014b).

1.6 Breast to brain metastasis

Breast cancer is a prevalent form of cancer in women and has a high potential to metastasise to the brain, with brain metastasis occurring in 10%-30% of breast cancer patients (Simsek *et al.*, 2022; Ivanova *et al.*, 2023). Triple-negative breast cancer (TNBC) and HER2-positive subtypes have a significant chance of developing brain metastasis (Das *et al.*, 2023a). The incidence of brain metastasis in breast cancer patients is rising, most likely due to improved systemic control of extracranial disease and increased patient survival, but it remains associated with poor prognosis and limited treatment options (Maughan, Lutterbie and Ham, 2010; Das *et al.*, 2023a). The metastatic cascade from breast cancer to the brain consists of several stages, beginning with the detachment of cancer cells from the primary tumour and their subsequent migration into the circulation or lymphatic system (Bos *et al.*, 2009; Fares, Kanojia, *et al.*, 2020). Upon infiltrating the bloodstream, breast cancer cells need to endure the challenging environment of the bloodstream, evade immune detection, and eventually adhere to the endothelial cells of distant organs, including the brain (Brastianos *et al.*, 2015; Fares, Kanojia, *et al.*, 2020). After travelling through circulation, these cells cross the blood-brain barrier (BBB) by disrupting tight junctions and interacting with astrocytes, pericytes, and endothelial

cells. Upon entering the brain, they extravasate into neural tissue, inciting neuroinflammatory responses and enlisting local cells such as astrocytes and microglia. Cancer cells adapt to the brain microenvironment, inducing neo-angiogenesis for sustained growth and establishing metastatic colonies (Corti *et al.*, 2022).

Specific genetic and molecular changes facilitate the earliest stages of metastasis, such as the increased expression of HER2 and cyclooxygenase-2 (COX-2). These modifications enhance the cells' ability to invade, survive and establish at distant sites (Bos *et al.*, 2009). The interplay between cancer cells and the neural niche consisting of neurons, astrocytes, microglia and other supportive cells in the brain is vital in the development of brain metastasis (Neman *et al.*, 2014a; Termini, Neman and Jandial, 2014a). The blood-brain barrier poses a significant challenge for breast cancer cells that attempt to metastasise to the brain (Arvanitis, Ferraro and Jain, 2020; Terceiro *et al.*, 2023). The BBB is formed by endothelial cells, tight junction proteins, pericytes, and astrocyte end-feet, which collectively limit the passage of many substances, including therapeutic agents, into the brain (van Tellingen *et al.*, 2015; Arvanitis, Ferraro and Jain, 2020). Various factors impact the ability of the breast cancer cells to cross the BBB, which include the expression of adhesion molecules like integrins and selectins, which aid in attachment to brain endothelium, and proteolytic enzymes such as MMPs which degrade the extracellular matrix and disrupt the tight junction of the BBB (Hamester *et al.*, 2022; Terceiro *et al.*, 2023).

Furthermore, breast cancer cells can exploit either the transcellular or paracellular pathways to transmigrate through the BBB. The permeability changes in the barrier facilitate this migration process (Hamester *et al.*, 2022; Zhao *et al.*, 2023). Chemokines, cytokines and growth factors produced by both tumour cells and brain stromal cells substantially impact and activation of specific signalling pathways such as PI3K/Akt, Src, and STAT3, which promote the survival

and proliferation of metastatic cells (Brosnan and Anders, 2018). It can exploit neurotrophic factors, such as brain-derived neurotrophic factor (BDNF), to enhance their growth within the brain (Termini, Neman and Jandial, 2014b; Wang *et al.*, 2021a).

The interaction between metastatic breast cancer cells and neurones in the brain can significantly influence progression. Breast cancer cells may adopt neuronal-like properties to integrate into the neural niche, including the GABA receptors, which enables them to utilise neurotransmitters for growth and survival (Neman *et al.*, 2014a). These cancer cells can release factors that promote neuronal excitability and disrupt neuronal function, leading to seizures and cognitive decline observed in patients with brain metastasis (Osswald *et al.*, 2015; Dubey *et al.*, 2023).

1.7 Neurotransmitters

Neurotransmitters are chemical messengers that transmit signals across a chemical synapse, between a neuron and another neuron or a neuron and a terminal effector such as a muscle cell, facilitating communication throughout the nervous system (Venkataramani *et al.*, 2019). They are released from the presynaptic terminal of a neuron when an action potential occurs and traverse the synaptic cleft to bind to specific receptors on the postsynaptic membrane to initiate or inhibit response in the receiving cell (Traynelis *et al.*, 2010). They are classified into several types: amino acids, monoamines, peptides, and acetylcholine. Each of these neurotransmitters has a distant role in brain function (Sigel and Steinmann, 2012). The amino acid neurotransmitters include glutamate, gamma-aminobutyric acid (GABA), and glycine, which are crucial for rapid excitatory and inhibitory synaptic transmission in the brain (Sigel and Steinmann, 2012; Neman *et al.*, 2014a). Glutamate is the primary neurotransmitter that stimulates activity in the central nervous system. It plays crucial in synaptic plasticity, learning and memory by activating ionotropic glutamate receptors, such as NMDA, AMPA, and kainite

receptors (Venkataramani *et al.*, 2019). GABA is the primary inhibitory neurotransmitter, crucial for reducing neuronal excitability and maintaining a balance between excitation and inhibition in the brain (Neman *et al.*, 2014a; Pin and Bettler, 2016a).

Neurotransmitters often exert their effects through G-protein-coupled receptors (GPCRs), such as mGlu (metabotropic glutamate receptors) and GABA B receptors, which regulate neuronal activity indirectly via intracellular signalling cascade. Acetylcholine impacts ionotropic nicotinic and metabotropic muscarinic receptors (Pin and Bettler, 2016). The neuronal transmission of neurotransmitters begins with synthesising and packaging neurotransmitters into synaptic vesicles within the presynaptic neuron (Venkataramani *et al.*, 2019). Once an action potential shows up, voltage-gated calcium channels open, causing an influx of calcium ions into the presynaptic terminal, which triggers the fusion of synaptic vesicles with the presynaptic membrane and the release of neurotransmitters into the synaptic cleft (Traynelis *et al.*, 2010). The released neurotransmitters then diffuse across the synaptic cleft and bind to specific receptors on the postsynaptic membrane, which can be either metabotropic or ionotropic receptors, leading to either excitatory or inhibitory postsynaptic potentials depending on the receptor type and neurotransmitter involved (Neman *et al.*, 2014a; Zeng, *et al.*, 2019). Ionotropic receptors, such as NMDA and AMPA, open channels when neurotransmitter glutamate binds to them. This allows ion flow through the cell membrane, causing a quick shift in the electric charge of the receiving cell (Venkatesh *et al.*, 2019). Neurotransmitter receptors are generally composed of multiple subunits, significantly affecting their synaptic activity. The number of receptor types and synaptic contexts is vast due to the complex variety of neurotransmitters, receptor subtypes, and the specificity of neuronal signalling (Sanfilippo *et al.*, 2024).

Glutamatergic synaptic input has a notable impact on tumour progression. Research indicates that glioma cells integrate into neural circuits and receive glutamatergic synaptic input, which can drive tumour growth by activating NMDA receptors and signalling (Venkataramani *et al.*, 2019; Venkatesh *et al.*, 2019). Glioma cells enable the activation of NMDA receptors by the release of glutamate from synapses, which are in the proximity of glioma cells, promoting tumour cell proliferation and invasion. This process of tumour activation by release of glutamate is also true of metastatic breast cancer (Zeng, *et al.*, 2019). Breast cancer cells that metastasise to the brain can also exhibit GABAergic characteristics, interacting with neural niches and potentially utilising neurotransmitter signalling for survival and proliferation in the brain microenvironment (Neman *et al.*, 2014a). Neuroglins, a group of molecules that adhere to the postsynaptic region, are implicated in neuronal activity-regulated growth of gliomas (Venkatesh *et al.*, 2015; Humsa S. Venkatesh, 2017). The interaction between tumour cells and neurones can occur through neurotrophic factors, neurotransmitters and other neuroactive molecules secreted by nerves. This interaction allows the tumour cells to engage with the receptors of the TME, promoting proliferation, invasion, and metastasis of cancerous cells (Wang *et al.*, 2021b).

1.7.1 Glutamate and glutamate receptor

Glutamate is the primary excitatory neurotransmitter in the CNS, and it plays a crucial role in synaptic transmission, plasticity, and neural development (Traynelis *et al.*, 2010). Its effects are mediated through the binding to specific glutamate receptors, which are classified into two main types: ionotropic receptors, like NMDA (N-methyl-D-aspartate), AMPA (α -amino-3-hydroxy-5-methyl-4-isoxazole propionic acid), and kainite receptors, and metabotropic receptors, referred to as mGlu receptors (Traynelis *et al.*, 2010; Pin and Bettler, 2016a). Ionotropic glutamate receptors, specifically NMDA receptors, are ligand-gated ion channels that allow the influx of Calcium (Ca^{+2}) and sodium (Na^{+2}) ions, enabling depolarisation and

synaptic plasticity. Metabotropic glutamate receptors (mGluRs) are G-protein-coupled receptors (GPCRs) that regulate neuronal excitability and the transmission of signals between the synapses via second messenger systems, which in turn affect intracellular signalling cascades (Pin and Bettler, 2016a).

Glutamate receptors, specifically ionotropic receptors, possess intricate structures that modulate their function and localisation at synapses. NMDA receptors consist of many subunits, including GluN1, GluN2, and GluN3, which collectively contribute to ion permeability, voltage dependency, and sensitivity to co-agonists like glycine (Traynelis *et al.*, 2010). Metabotropic glutamate receptors (mGluRs) are categorised into three classes (I, II and III) according to their sequence homology and signal transduction pathways and regulate synaptic transmission. Group I mGluRs (mGluR1 and mGluR5) activate phospholipase C (PLC) to increase intracellular Ca^{+2} levels, whereas groups II and III (mGluR2-4, mGluR6-8) suppress adenylate cyclase, decreasing cyclic AMP (cAMP) levels (Figure 1.2) (Pin and Bettler, 2016a). Post-translational modifications (phosphorylation, ubiquitination, and palmitoylation) closely regulate glutamate receptor signalling, which impacts receptor trafficking, localisation, and degradation, eventually influencing synaptic strength (Traynelis *et al.*, 2010). Glutamate signalling has a significant impact on tumour progression, specifically in brain tumours like glioma, through mechanisms involving neuroligin-3, a neuron-secreted protein that promotes glioma growth (Venkatesh *et al.*, 2015; Humsa S. Venkatesh, 2017).



Figure 1.2 Classification of glutamate receptors.

This diagram categorizes glutamate receptors into ionotropic receptors (ligand-gated ion channels) and metabotropic receptors (G-protein-coupled receptors). Ionotropic receptors are further divided into NMDA (N-methyl-D-aspartate), AMPA (α -amino-3-hydroxy-5-methyl-4-isoxazolepropionic acid), and kainate receptors, each with associated gene subunits. Metabotropic receptors are classified into three groups: Class I (mGluR1, mGluR5), Class II (mGluR2, mGluR3), and Class III (mGluR4, mGluR6, mGluR7, mGluR8), representing distinct signalling pathways. (Eduardo Flores-Soto *et al.*, 2013)

1.7.2 GABA and GABA receptor

Gamma-aminobutyric acid (GABA) is the primary neurotransmitter in the CNS that inhibits neuronal activity and helps maintain the balance between excitation and inhibition in the brain.

GABA is synthesised in the brain from L-glutamic acid catalysed by L-glutamate decarboxylase (GAD) (Roberts, 2007). GABA exerts its effects via two primary receptors: ionotropic GABA receptors (GABA_A and GABA_C) and metabotropic GABA receptors (GABA_B). GABA_A and GABA_C receptors are ion channels that are activated by ligands and play a role in fast-inhibiting synaptic activity by allowing the influx of chloride ions (Cl⁻) to enter neurones, which leads to hyperpolarisation and a reduction in neuronal firing (Sigel

and Steinmann, 2012). GABA_B receptors are GPCRs that regulate slower inhibitory signals through second messenger pathways, inhibiting adenylyl cyclase and activating potassium channels (Pin and Bettler, 2016a). GABA_A receptors exhibit significant diversity in both their structure and function due to their multiple subunit compositions, which consist of five subunits: alpha (α), beta (β), gamma (γ), delta (δ), and other subunits. These subunits combine to create a heteropentameric structure surrounding a central ion channel (Pin and Bettler, 2016a). GABAergic signalling is mediated by GABA_A and GABA_B receptors, which play a role in the TCA (tricarboxylic acid) cycle through the GABA shunt pathway, which is an alternative metabolic route that bypasses two steps of the TCA cycle to convert glutamate to succinate by GABA transaminase (ABAT). The GABA shunt route starts with converting glutamate to GABA by decarboxylation, catalysed by the enzyme glutamate decarboxylase (GAD) (Jayachandran *et al.*, 2023). This shunt maintains the glutamate and GABA levels in the cells, affecting energy metabolism, proliferation, stress such as tumour microenvironment and redox balance in cancer cells (R. Q. Li *et al.*, 2023a). The delta subunit of the GABA_A receptor is necessary for certain forms of breast cancer metastasis, as it facilitates tumour progression by interacting with other signalling pathways such as glutamic pyruvate transaminase 2 (GPT2)-activated Sonic Hedgehog signalling (N. Li *et al.*, 2023).

The GABA_A receptor's expression in breast cancer cells is linked to metastasis with specific isoforms activating oncogenic pathways like Akt (Gumireddy *et al.*, 2016a). GABA_B receptors regulate neurotransmitter release and neuronal excitability by inhibiting adenylyl cyclase, decreasing cAMP levels, and activating potassium channels, leading to neuron hyperpolarisation. The organisation of GABA_B receptor complexes is critical for maintaining synaptic balance (Pin and Bettler, 2016b). The GABA R is a GABA_B receptor involved in prostate and breast cancer invasion and is overexpressed in breast cancer cell lines (Drell *et al.*, 2003).

1.8 Neurotransmitters, Neurotransmitter Receptors and Brain Tumours

Neurotransmitter receptors substantially impact the progression and metastasis of various cancers, such as breast cancer, to the brain by influencing tumour cell behaviour and their interaction with the neural microenvironment. Glioma cells can integrate into neural circuits by forming synaptic-like structures, enabling them to receive excitatory glutamatergic inputs from neurons (Venkatesh *et al.*, 2019). Tumour cells interact with neurons by receiving and transferring glutamatergic signals (Radin and Tsirka, 2020). Glioma cells interact actively with adjacent neurones, particularly glutamatergic signal-transferring (Pei *et al.*, 2020). Glutamate receptors have been shown to contribute to the tumour development and invasiveness of gliomas and brain metastasis, where the activation of glutamatergic signalling through AMPA and NMDA receptors enhances the synaptic input into tumour cells with neuron forms synapses that results in an electrically coupled system (Venkataramani *et al.*, 2019; Zeng, *et al.*, 2019).

The proximity of tumour cells to the synaptic sites enables the activation of the NMDA receptor. Further, it promotes tumour growth by enhancing the calcium influx, which in turn leads to the activation of the oncogenic pathways such as those involving MAPK and PI3K/Akt (Zeng, *et al.*, 2019). Electron microscopy observation showed synapse formation between presynaptic neurons and postsynaptic tumour cells in glioma. The excitatory current of a post-synaptic signal in glioma cells shows similarities to the signals present between two functional neurons (Venkataramani *et al.*, 2019; Venkatesh *et al.*, 2019). NMDA and AMPA are essential for communication between tumour cells, neurones, and breast-to-brain metastasis. Metastatic breast cancer cells that invade the brain increase these receptors' expression and adapt to the new environment by expressing glutamate receptors. This promotes tumour growth by activating oncogenic pathways mediated by calcium signalling, which is necessary for the

tumour cell's proliferation, migration and invasion (García-Gaytán *et al.*, 2022; Koda *et al.*, 2023).

NMDA receptor signalling has been implicated in promoting the metastasis of breast cancer. Research studies suggest that NMDA receptor antagonists have the potential to inhibit this process by disrupting the calcium influx and following signalling cascades (Morelli *et al.*, 2019; Gallo, Vitacolonna and Crepaldi, 2023). These properties in metastatic cells may form functional synaptic-like connections with neurons, facilitating their integration into the brain microenvironment and further tumour growth development (Neman *et al.*, 2014a). Specific subunits of the GABA_A receptors, such as the delta subunit, are crucial for breast cancer metastasis, facilitating cell migration and invasion through signalling pathways involving GTP2 and Sonic Hedgehog signalling (Cao *et al.*, 2017; N. Li *et al.*, 2023). They initiate signalling pathways that include the GluN2B subunit of the NMDAR when tumour cells metastasise to the brain, which enhances their communication capacity with neurons. This process is linked with an increased expression of neuroligin and other postsynaptic signalling proteins that enable the non-neuronal cells, like cancer cells, to form pseudo-synapses (Zeng, Zhang, *et al.*, 2019).

Astrocytes are specialised cells in the brain and CNS which maintain neurotransmitter balance and provide metabolic support to neurons (Hamester *et al.*, 2022). Presynaptic neurons release glutamate during synaptic transmission, which is then received by post-synaptic neurons expressing NMDARs. Astrocytes in the synaptic cleft prevent glutamate-induced neurotoxicity and absorb excess glutamate released by neurons (Wilhelm *et al.*, 2013) Breast cancer cells metastasise to the brain and can displace astrocytes by forming pseudo-tripartite synapses and allowing them to access glutamate and NMDAR signalling pathways, thereby promoting proliferation and metastasis in the brain environment (Neman *et al.*, 2014a; Hosonaga, Saya

and Arima, 2020). Figure 1.3 shows the pseudo-tripartite synapse, where metastatic tumour cells replace astrocytes, enabling glutamate uptake from the synaptic cleft. This distinctive synaptic configuration between neurons and. Metastatic breast cancer cells facilitate an enhanced glutamate supply to the tumour cells (Neman *et al.*, 2014a; Hosonaga, Saya and Arima, 2020).

These recent discoveries have described the existence of pseudo synapses as a key feature of brain tumours. However, the mechanisms that enable these tumour cells to express the cellular structures necessary to form pseudo-synapses are still to be determined.

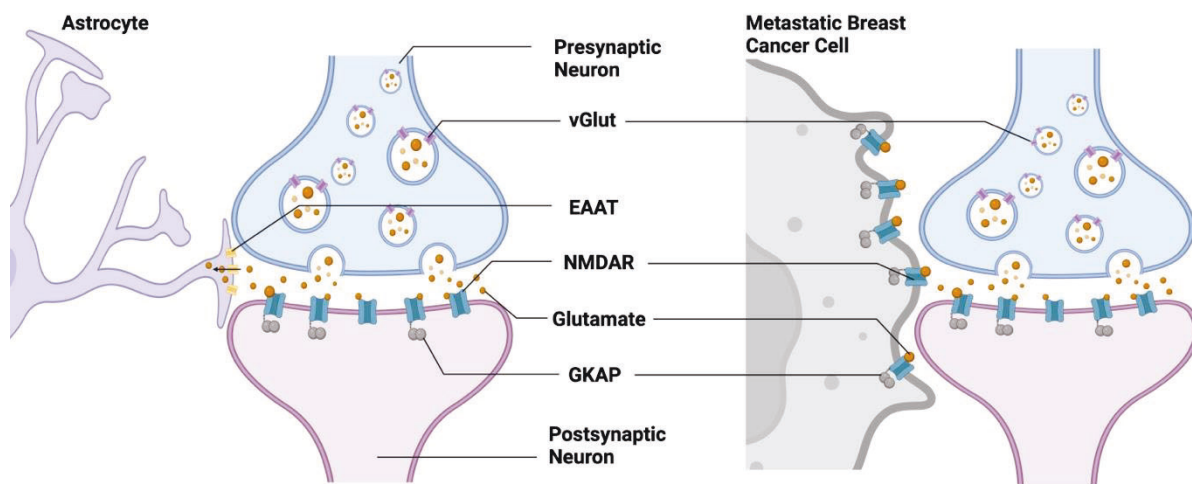


Figure 1.3 Role of Glutamate Signalling in Synaptic Interactions Between Neurons, Astrocytes, and Metastatic Breast Cancer Cells.

Brain-metastatic cancer cells replace the astrocytes at the neuronal synapse, enabling NMDAR-dependent colonisation. The tripartite synapse comprising pre- and postsynaptic neurons and astrocytes (left) is disrupted by metastasising breast cancer cells, which resemble astrocytes and form pseudo-tripartite synapse (right) that provide a source of glutamate ligand, which activates NMDAR signalling and promotes tumour growth in the brain (Zeng, Zhang, *et al.*, 2019). Created in <https://BioRender.com>.

1.9 Role of ARFGEF3 in Breast cancer progression and brain metastasis

ARFGEF3, also known as BIG3 (Brefeldin A-inhibited guanine nucleotide-exchange protein 3), is a multifunctional protein implicated in cellular signalling pathways. In primary breast cancer, ARFGEF3 plays a pivotal role in modulating estrogen signalling by interacting with

PHB2 (Prohibitin 2), a protein that regulates transcriptional activity and mitochondrial function (Toki *et al.*, 2021a). In the presence of BIG3, this protein binds PHB2, effectively sequestering it and preventing its interaction with estrogen receptors (ERs). This inhibition allows the estrogen-ER complex to activate downstream signalling pathways, promoting cell proliferation and survival (Yoshimaru, Ono, *et al.*, 2017). The structural integrity of this interaction is influenced by the non-conserved loop region of BIG3, which stabilizes its binding to PHB2, enhancing its capacity to modulate estrogen signalling (Chigira *et al.*, 2019a). In the absence of BIG3, PHB2 interacts with Era disrupting estrogen signalling and thereby reducing transcriptional activation of genes associated with cell growth and survival. The BIG3-PHB2 interaction represents a critical determinant in the regulation of estrogen signalling in breast cancer cells. Its presence facilitates oncogenic signalling, while its absence reinstates the tumour-suppressive effects of PHB2 (Yoshimaru *et al.*, 2013).

Previous studies by Li *et al.* (2014, 2015) show that BIG3, a protein containing a SEC7 domain, negatively regulates the biogenesis and secretion of insulin and glucagon granules (Li *et al.*, 2014, 2015). Notably, BIG3 is predominantly expressed in pancreatic islets and the brain. Beyond pancreatic islets, the brain is the only organ where BIG3 is abundantly expressed, emphasising its potential role in neural and metabolic processes (Li *et al.*, 2014).

The study by Li *et al.* (2016) investigated the function of BIG3 in the brain using hippocampal neurons as a model system. BIG3 is predominantly localised within lysosomes in hippocampal neurons. Furthermore, the loss of BIG3 selectively impacted inhibitory synaptic transmission, indicating its specific influence on neuronal signalling (Liu *et al.*, 2016a). Building on these findings, a recent exome sequencing study by our group identified frequent mutations of ARFGEF3 (BIG3) in breast-to-brain metastasis (BBM), further underscoring its significance in breast-to-brain metastasis (Olivares, 2023). **These previous studies by Liu *et al.*, *et al.* 2016,**

and Zeng et al.,2019 allow to establish a connection between neuronal synaptic regulation and breast cancer brain metastasis. Formation of Pseudosynapses is critical for tumour survival and proliferation within the brain microenvironment, as they enable tumour cells to exploit neuronal signalling for their growth (Venkataramani *et al.*, 2019; Zeng, Zhang, *et al.*, 2019). While previous studies have documented the presence of neurotransmitter receptors in brain-metastatic tumours, the underlying mechanisms facilitating their formation remain unclear. This leads to the hypothesis that these mutations may contribute to brain metastasis by promoting the formation of structures that facilitate pseudo-synapses. This hypothesis forms the basis of our investigation, aiming to determine whether *ARFGEF3* mutations facilitate brain metastasis by regulating neurotransmitter receptor components and enabling the formation of pseudo-synapses.

2. AIM AND OBJECTIVES

This study aims to determine the function of *ARFGEF3* in breast-to-brain metastasis. Specifically, does loss of *ARFGEF3* contribute to the expression of neurotransmitter receptors in a breast cancer cell line.

1. To validate the successful knockout expression of *ARFGEF3* expression in the knockout MCF-7 cells by CRISPR-CAS9, using RT-PCR and Western Blot analysis, where the knockout model was performed earlier by Ivonne Olivares.
2. Characterisation of the *ARFGEF3* function in cellular growth and proliferation under normoxia conditions by growth curve assay.
3. Examining the PHB2 levels in *ARFGEF3* KO and scrambled (control) cells using RT-PCR and Western Blot.
4. Comparative analysis of *ARFGEF3*-KO and control cells to determine the role of *ARFGEF3* in controlling the neurotransmitter receptor expression by:
 - RT-PCR validation of neurotransmitter receptors in scrambled (control) and *ARFGEF3* KO
 - Validating the expression of neurotransmitter receptors in both control and KO cells using TaqMan qPCR
 - To quantify the expression of neurotransmitter receptors (GABRG1, GABRA3, GABRA4, GRIN2B, GRIN2C, GRIN2D and GABRB3) in *ARFGEF3* KO clone and scrambled (control) using flow cytometry and Western Blot.
 - Comparing the expression of neurotransmitter receptors (GABRG1) in *ARFGEF3* KO clone and scrambled (control) using the immunostaining technique.

3. MATERIALS AND METHODS

The experiments in this study solely used adherent cell lines MCF-7. MCF-7 cells were cultured in DMEM media (Dulbecco's Modified Eagle's Medium, Gibco), supplemented with 10% FBS (fetal bovine serum, Gibco), 1% L-Glutamine (Bio-whittaker) and a penicillin-streptomycin antibiotic combination to prevent the growth of contaminants. Isogenic MCF7 clones edited to knock out *ARFGEF3* had previously been isolated in our lab by Ivonne Olivares (Olivares, 2023). The Ethics Committee at the University of Wolverhampton has approved this project - LSEC/2024-25/MM/52.

3.2 Cell Culture

3.2.1 Breast Cancer Cell Lines

Primary breast cancer cell line MCF7 was utilised for tissue culture and experimental studies. The Research Institute of Healthcare Sciences at the University of Wolverhampton (RIHS) and Prof. Weiguang Wang's team contributed to all cell lines.

3.2.2 The Parameters for Aseptic Apparatus and Culturing Environment

All cell culture methods were completed in a Bio MAT 2 class II biological safety cabinet (CAS, UK). Before each usage, the safety cabinet was cleaned using a 70% ethanol and 1% Trigene solution supplied from Sigma-Aldrich UK to avoid cell culture contamination. Before usage, all the chemicals required for tissue culture were first allowed to defrost at room temperature. The cells are maintained in vented flasks that have a special Nunclon Delta coating that helps the cells adhere to the surface. The cells were grown at 37°C with 5% CO₂ while suspended in the appropriate volume of media in the suitable-sized flask.

3.2.3 Media Preparation for Cell Culture

The breast cancer cell lines (MDA-MB231, MCF7, T47-D, ZR-75, and BT-549) were maintained in DMEM (Corning) supplemented with 1% penicillin/streptomycin, 1% L-glutamine and 10% foetal bovine serum (FBS) (Sigma Aldrich) at 37°C and 5% CO₂.

3.2.4 Reviving Frozen Cells

Cryovials of cells were taken out of the liquid nitrogen and allowed to thaw at 37°C in order to recover them. To prevent cell damage, cells were resuspended in a 1:10 cell to tissue medium ratio. The supernatant was carefully removed after 5 minutes of centrifugation of cells at 1200g. The cell pellet was re-suspended in new cell culture media and were transferred to an appropriate-sized flask and cultured at 37°C with 5% CO₂.

3.2.5 Maintenance of Cell Culture

All experiments in this study were carried out on adherent cell lines: MCF7. Cells were frequently examined for any changes to the cultured medium or the cell population. For in vitro research and maintenance, cells were consistently passaged at 80–90% confluence. The cell monolayer was first washed with Phosphate Buffered Saline 1x (PBS 1x, Corning) after decanting the media. Trypsin 1x (Lonza, Biowhittaker) was used in an adequate volume to remove the cells from the tissue culture flask. The flask was lightly tapped to hasten the separation once the monolayer was separated from it. To check if cells were detached, they were observed using a Nikon Eclipse Ts100 Inverted Phase Contrast Microscope (Nikon, Japan). In order to neutralise the trypsin, detached cells were resuspended in a fresh complete DMEM medium (Corning). After being transferred to a sterile tube, the cell solution was centrifuged at 1,200 g for 5 minutes. The cell pellet was resuspended in new media after the supernatant was removed to remove any remaining trypsin traces. The cell suspension was separated into tissue culture flasks with an adequate volume of media in order to amplify the cell lines. The media was then changed every 1-2 days or whenever there was a change in the

colour, a sign that the media pH had dropped. The cells were cultured at 37 C with 5% CO₂ until confluency was attained.

3.2.4 Cell Quantification

Thermo Invitrogen Countess II FL Automated Cell Counter was used to count the cells for any in vitro experiments. 10µl of cell suspension was added to the chambers of the counting slide and then the slide is placed in the Countess II FL. The computer provided live cell density ranges from 1×10^4 – 1×10^7 cells/mL.

3.2.5 Cryopreservation of Cell lines

The cells were trypsinised to separate the cells from the flask. The cell suspension was centrifuged at 1,200 g for 5 minutes, and the pellet was then re-suspended in 1 mL of freezing solution, which included 90% (v/v) FBS and 10% (v/v) DMSO. A cryovial (Nalgene Cryovial™ Labware, Denmark) was then used to transfer the solution, and it was kept at -80°C. Cryovials were kept at -80°C for three days before being moved to a container of liquid nitrogen, which was kept at -196°C, for long-term storage.

3.3 Expression Analysis of Nucleic Acid

3.3.1 RNA Isolation

The cells that were modified by CRISPR technology were grown in a T75 flask until they reached 75% to 90% confluent and then were trypsinized to detach them from the flask. After trypsinising, it was instantly inactivated by adding DMEM media. The cell suspension was centrifuged for 5 minutes at 1200 g. The supernatant was aspirated, and the cell pellet was washed with PBS. The supernatant was removed completely by aspiration. 350 µl of Lysis solution and 3.5 µl of β-mercaptoethanol were added to the cell pellet, which was pipetted up and down to re-suspend the cell pellet and to directly lyse the cell. RNA extraction was

performed using Amersham™ RNAspin Mini RNA Isolation Kit 250 prep. The RNA Mini Filter was placed in a collection tube and the lysate was added to the RNA Mini Filter and was centrifuged at 11,000xg for 1min. The RNA Mini Filter was discarded and 350 µl of 70% molecular grade ethanol was added to it and was mixed by vortexing it twice, each for 5s. There may be a stringy precipitate evident after the ethanol has been added. This has no impact on the isolation of RNA, and the lysate was pipetted up and down before being transferred to the RNAspin Mini Column and centrifuged at 8000xg for 30s. Following centrifugation, transfer the column to a new collection tube. The RNAspin Mini column was loaded with 350 µl of desalting buffer, and the membrane was dried by centrifuging it for 1 minute at 11,000xg. When it was evident that all of the lysates had passed through after centrifugation, the flow through was discarded and the RNAspin Mini Column was returned to the collecting tube. Eliminating salt will greatly improve the efficiency of the DNase digestion that follows. The flowthrough was discarded and centrifuged again for 30 seconds at 11000 g if the column outlet had come into touch with it for any reason. For every isolation, a sterile microcentrifuge tube containing 90 µl DNase Reaction Buffer and 10 µl of reconstituted DNase I is used to creating the DNase I reaction mixture, which is then mixed by flipping the tube. To the silica membrane of the column, 95 µl of the DNase I reaction mixture was added directly and was incubated for 15 min at room temperature. The RNA mini-Spin Column holding the RNA was washed with 200 µl of wash buffer I which will inactivate DNase and centrifuged for 1 min at 11,000xg. The column was placed into a new collection tube. 600 µl of wash buffer II was added to the RNA spin Mini column and was centrifuged for 1min at 11,000xg. The flowthrough was discarded, and the column was placed back into the collection tube. To the RNA spin Mini Column, 250 µl of wash buffer II was added and centrifuged again at 11,000xg for 2min to dry the membrane completely. In the instance that, following centrifugation, the liquid level in the collecting tube reaches the RNA spin Mini Column, the flowthrough was discarded off and

centrifuged once more. Checked that the column outlet had no residual flowthrough left, it was re-centrifuged if any remains were found and then the column was placed into a sterile nuclease-free 1.5mL Microcentrifuge Tube. The RNA was eluted by adding 40 µl of RNase-free H₂O and centrifuged for 1 min at 11,000xg. Eluted RNA was kept at -20°C or -80°C for short-term or long-term storage, respectively, after being promptly placed on ice to prevent any degradation.

3.3.2 Quantification of RNA

The isolated concentration of total RNA (µg/mL) was measured with a Thermo Scientific, UK, Nanodrop 2000 spectrophotometer. 1.5µl of blank control was applied to the read head for calibration. The RNA concentration, protein contamination, and organic solvent contamination were noted. The purity was determined using the A260/A280 ratio.

3.3.3 Complementary DNA (cDNA) Synthesis

After RNA quantification, cDNA was synthesised using a High-Capacity cDNA Reverse Transcription Kit from Thermo Fisher. Prior cDNA synthesis, RNA was standardised by using a normalisation coefficient determined by the concentration of extracted RNA. The RNA was normalised for cDNA synthesis using a normalisation coefficient value of 1000. The formula for calculating the RNA dilution is:

Volume of RNA used for cDNA synthesis = Normalisation coefficient t / Concentration of RNA

Samples were then diluted with nuclease-free water (Invitrogen, UK) to 1000 ng of total RNA in a final volume of 10 µl. The cDNA synthesis kit contains: Reverse Transcription (RT) mixture including 10x Transcription Buffer, 25x dNTP mix (100 mM, 0.2 mL), 10x Random Primers, MultiScribe reverse transcriptase (0.2 mL at 50 U/ µl), and RNase Inhibitor (2 × 0.1

mL at 20 U/ μ l) is combined with 10 μ l of total RNA. A master mix was prepared according to the number of samples. Each sample was combined with this RT master mix to yield a final volume of 20 μ l. Using a pipette, the components were gently mixed to prevent bubbles. In a thermal cycler, reverse transcription was carried out at 25°C for 10 minutes, 37°C for 120 minutes, and 85°C for 5 minutes and a hold stage at 4°C. 80 μ l of nuclease-free water was added to the reaction once it was completed. For short-term usage, the cDNA was kept on ice; for longer-term storage, it was stored at -20°C. Table 3.1 provides a summary of the quantities and reaction components.

Components	Volume/ μ l
10x RT Buffer	2.0
25x dNTPS	0.8
10x Random Primers	2.0
MultiScribe Reverse Transcriptase	1.0
RNase Inhibitor	1.0
Nuclease Free Water	3.2

Table 3.1 Components of the "High-Capacity cDNA Reverse Transcription Kit" with the required quantities for the RT master mix.

Steps	Temperature	Time
Denaturation	25°C	10 minutes
Annealing	37°C	120 minutes
Elongation	85°C	5 minutes
Storage	4°C	Hold

Table 3.2 Thermal cycler setting for cDNA synthesis.

3.3.4 Primer Designing for RT PCR

Primers spanning several exons were constructed for RT-PCR expression analysis in order to ensure that the amplification product was free of contaminating gDNA. The parameters were altered so that the primer's maximum length was limited to 18-20 base pairs, the GC content was restricted to under 50% (40-60%), and the melting temperature difference between the

forward and reverse primers was specified to be less than 1°C is ideal for the optimal primer-template annealing. The primers for the neurotransmitter receptors and ARGEF3 were created manually. Each primer's annealing temperature was determined using the following formula:

$$[(\% \text{ CG} \times 0.41) + 64.9 - (600/N)]$$

where the %CG is obtained by dividing the primer's total C and G content by its length (N) and OligoCalc (<http://biotools.nubic.northwestern.edu/OligoCalc.html>) was used for cross-referencing. The programme was run to produce the optimal primer for the target sequence once the parameters were established.

The primers were received in a lyophilised state, and Table 3.3 provides the list of the primer sequences. Thus, before using them, they needed to be dissolved into a solution. The primer stocks were prepared in Nuclease-free water. The stock was made in accordance with the datasheet given by the company. The primers were diluted with nuclease-free water to create a stock solution of 200µM and a working solution of 20µM.

Gene	Primer	Sequence
GRIA1	Forward	CTGGAAGAGACCCAAGTACACC
	Reverse	CTCGTAACGGTCATTGCCCTC
GRIA2	Forward	CGGAAGATTGGCTACTGGAGTG
	Reverse	GATATCCCGAGGCTCATGAAGG
GRIA3	Forward	CTTTCTGCTCCCAGTTCTCGAG
	Reverse	CCCTAGGATCACAACTGTTCC
GRIA4	Forward	GGGGATACTCGATACTCCAAGC
	Reverse	GATGGAGTCCTTGTGATGGCTG
GRIK1	Forward	GATGACAACCTGAAGCGGCTCTG
	Reverse	GTCCACCATTCTGGAAGAACCC
GRIK2	Forward	CCACTCTGGACCTCTTTGCTC
	Reverse	CTGTGAGGCCTTCCCAATGTG
GRIK3	Forward	CGGAGGAATCTTCGAGTATGCG
	Reverse	GATGAGCCCTGTACTGTCGTC
GRIK4	Forward	CTCCTTGAGGATCGCTGCTATC
	Reverse	GATAGCAGCGATCCTCAAGGAG
GRIK5	Forward	CACGGACACCATGTGTCAGATC
	Reverse	CTGTTCGTC AACATCCTCACTG
GABBR2	Forward	GTTCTCTGAGGTGCGGAATGAC
	Reverse	CTCCATGGCAGCAAGCAGATTC
GABRA1	Forward	CTGGAAGAAGCTATGGACAGC
	Reverse	CTCATGGTGTACAGCAAGGTG
GABRA5	Forward	TCCCTGCATAATGACCGTGA
	Reverse	CCGTGGCAAACCTCTATCAGC
GABRA6	Forward	GGCTGTGCATTATTCTGTGGCTAG
	Reverse	CAGACTCAGAATCTCAGTTGGC
GABRB2	Forward	GGACTCAGAATCACAACCACAG
	Reverse	GGTAATCAGGATGGAAGGCATG
GABRB3	Forward	CTCAGAATCACCACGACAGCAG
	Reverse	GGCAA CTCTAGCAGCAGATGC
GABRE	Forward	CTGGCATTGGAGAGAAGCCCAC
	Reverse	GCATCCGGCATCAATGGTCATC
GABRG2	Forward	CCTGATATAGGAGTGAAGCCAACG
	Reverse	CCTGATATAGGAGTGAAGCCAACG
GABRG3	Forward	CGTGACAACGTCTGCAGGTGATTATG
	Reverse	CGATGTTGTCTTCTTCGTGGTGG
GABRR1	Forward	CGATGTTGTCTTCTTCGTGGTGG
	Reverse	GTAGTTGCCGTCCAGCATCG
GABRR2	Forward	GGACATGGACTTCACTATGACCC
	Reverse	CAGCCAGTGCTGCTGTAGAAG
GABRR3	Forward	CTCTCCTTTCTAGCACAGC
	Reverse	CTATTGTACCAACCTGTGC
GABRQ	Forward	GCATCCGACTCACCCTACAG
	Reverse	CAATTGTCACCCTGGCTGCAG
GRIN1	Forward	CATCTACTCGGACAAGAGCATC
	Reverse	GTGATGTTCTCCTTCTCGAG
ARFGEF 3	Forward	AGAACAGTCTCAAGTCGCCA

	Reverse	GCAGTTTTAGAGACAGGGCG
--	---------	----------------------

Table 3.3 List of primer sequences.

3.3.5 Reverse Transcription (RT) PCR

RT-PCR was used to determine the mRNA expression analysis. Section 3.2 provides a prior description of the extraction and reverse transcription of RNA from samples. The PCR amplification was carried out using reagents from Thermo Fisher Scientific, which included 10x PCR buffer, Taq polymerase enzyme, and a 25x DNTP mix. The reaction mixture composition for a single reaction is presented in Table 3.4. The reaction mixture was prepared based on the number of samples, and a pipette was used to dispense 20.5 μ l of the mixture into labelled PCR tubes. Each PCR tube was filled with 4.5 μ l of previously synthesised cDNA. Before being placed in a thermocycler, the obtained mixture was stored on ice. The thermocycler was set up based on the primers' melting temperature, and the reaction was initiated after adjusting the reaction mixture's final volume to 25 μ l. The reaction mixture is placed on ice until it is ready to be placed into a thermocycler. The thermocycler was programmed based on the amplification settings of each primer (Table 3.5). Subsequently, the PCR tubes containing the reaction mixture are inserted into the thermocycler and initiated. The amplified product was then run on the agarose gel via electrophoresis at 100 V for 20 minutes and then the gel was examined under UV light.

Components	Volume/ μ l
PCR Reaction Buffer	2.5
25x dNTPS	2.5
Forward Primer	1.0
Reverse Primer	1.0
Fastart Taq Polymerase	0.2
Nuclease Free Water	12.3
cDNA sample	4.5

Table 3.4 Outlines the components required to prepare the master mix for RT-PCR.

Steps	Temperature	Time
Initial denaturation (hold)	94°C	5 minutes
Denaturation	95°C	30 seconds
Annealing	50-65°C	40 seconds
Elongation	72°C	40 seconds
Final elongation (hold)	72°C	5 minutes
Storage	4°C	Infinite

Table 3.5 PCR amplification setting on a thermocycler.

3.3.6 Quantitative Real-Time PCR

The measurement of gene-specific mRNA expression was determined by qRT-PCR with FAM reporter and TaqMan Gene Expression Assays (Thermo Scientific, UK); Table 3.6 shows the specific probe-sets used. As previously mentioned in section 3.2, RNA was isolated from the samples and reverse transcribed. a master mix is prepared according to the ratio shown in Table 3.7. In every experiment, 5.5 µl of a 2x real-time qRT-PCR master mix (Applied Biosystems) was added with 2 µl of NFW and 0.5 µl of the TaqMan probe with FAM on the 5' end and non-fluorescent quencher (NFQ) on 3' end. This resulted in a final volume of 8 µl for every reaction. This reaction is set up by adding 8 µl prepared reaction mixture to a single well of a MicroAMP® fast optical 96-well reaction plate (Applied Biosystems, UK) with 2 µl of cDNA sample. As a component of the experimental controls, a negative control sample comprising 2µl of nuclease-free water was added in the place of the cDNA sample to the well with reaction to confirm the scientific validity of the PCR amplification and they were sealed with optical adhesive film. Once any air bubbles were eliminated from the plate, it was centrifuged, and the sealed plates were placed in the QuanStudio6 qRT-PCR System (Applied Biosystems, UK). The RT-PCR technique was executed in compliance with pre-established guidelines. For two minutes, there was an initial incubation (hold) stage at 50°C. After that, a hold (polymerase activation step) was carried out for two more minutes at 50°C. The 40 cycles that made up the PCR cycling phase that followed each included denaturation for 1 second at 95°C and

annealing/extension for 20 seconds at 60°C. The $\Delta\Delta CT$ method was chosen as the data analysis methodology to provide a quantified comparison of data (Rao *et al.*, 2013).

Gene Expression Assay	Assay ID	Lot
<i>GABRA3</i>	Hs00968130_m1	4331182
<i>GABRA4</i>	Hs00608034_m1	4331182
<i>GABBR1</i>	Hs00559488_m1	4331182
<i>GABRG1</i>	Hs00921822_m1	4448892
<i>GRIN1</i>	Hs00609557_m1	4453320
<i>GRIA2</i>	Hs00181331_m1	4453320
<i>ARFGEF3</i>	Hs00415641_m1	4331182
<i>GAPDH</i>	Hs02786624_m1	4331182
<i>B ACTIN</i>	Hs01060665_G1	4331182

Table 3.6 TaqMan Gene Expression Assays Used for Quantitative Real-Time PCR.

Components	Volume per reaction (10 μ l)
TaqMan Gene Expression Assay	0.5 μ l
TaqMan Gene Expression PCR master Mix (2X)	5.5 μ l
Nuclease Free Water	2.0 μ l
cDNA	2.0 μ l
Total	10 μ l

Table 3.7 Components required of qRT-PCR for master-mix preparation.

3.4 Growth Curve Analysis

Initially, cells were collected from T75 flasks when they reached 80% confluency and were quantified using Thermo Invitrogen Countess II FL Automated Cell Counter. Subsequently, 200,000 cells were plated into T25 flasks and were maintained for a week. The cells were counted at the end of the week. This process was reiterated over the course of 7 weeks. The cumulative population doubling level at each sub-cultivation was determined by calculating the cell count using the given equation.

$$N_H/N_I = 2^X$$

$$\text{Or } [\log_{10} (N_H) - \log_{10} (N_I)] / \log_{10}^{(2)} = X$$

Where N_I = inoculum number, N_H = cell harvest number, and X = population doubling.

The calculated increase in the population doubling was subsequently combined with the previous population doubling level (PDL), to yield the cumulative population doubling level (Cristofalo *et al.*, 1998).

3.5 Western Blot

Various samples of the MCF7 cell line were utilised to extract and quantify total protein for Western Blot analysis. Cellular protein was extracted from each sample using RIPA buffer.

3.5.1 RIPA Buffer Preparation

Thermo Fisher's RIPA buffer contains 25 mM Tris-HCl (pH 7.6), 150mM NaCl, 1% NP-40, 1% sodium deoxycholate, and 0.1% SDS. To the RIPA buffer a protease inhibitor cocktail tablet (cOmplete, Roche Diagnostics.) and a phosphatase inhibitor cocktail tablet (PhosSTOP EASY pack, Roche.) are added to it. Both inhibitors are provided in tablet form and are dissolved in deionized water. The phosphatase inhibitor pill is dissolved in 1 mL of deionized water and split into two equal quantities of 500 μ l each, which are thereafter labelled and stored at -20°C. The protease inhibitor pill is dissolved in 2 mL of deionized water and then aliquoted into ten equal portions, each labelled and stored at -20°C. To prepare RIPA buffer, combine 500 μ l of phosphatase inhibitor and 200 μ l of protease inhibitor with 5 mL of Pierce RIPA Buffer from Thermo Scientific. The prepared solution is labelled and stored at -20°C for future use.

3.5.2 Protein extraction

The CRISPR-modified cells were cultured in a T75 flask until they achieved 75 to 90% confluency. When the cells reached the desired confluency, they were removed from the flask

using trypsin. Trypsin activity was stopped immediately by adding DMEM media right after trypsinization. The cell suspension was centrifuged at 1200 g for 5 minutes. Following centrifugation, the supernatant was removed, and the cell pellet was washed with PBS. The cleaned cell pellet was combined with 70 μ l-100 μ l of RIPA buffer (based on the pellet size) using a pipette. The mixture was sonicated in an ultrasonic machine for 60 seconds using a 50% pulse. The suspension was centrifuged at 14,000 g at 4°C for 10 minutes after sonication. The supernatant containing the desired protein was collected and transferred to an entirely fresh Eppendorf tube that was labelled accordingly. The extracted protein was stored at -20°C for further analysis or research.

3.5.3 Protein Quantification

Protein quantification is a process used to measure the amount of protein extracted from cells. The Bio-Rad Protein Assay kit (Protein estimation kit: DC protein assay reagent A, DC protein assay reagent B, DC protein assay reagent S; BIO-RAD, Hertfordshire, UK) is used to perform this experiment. The Bio-Rad DC Protein Assay is a colourimetric test used for determining protein concentration after detergent solubilisation. The test is similar to the well-known Lowry assay but with some enhancements. The colour development reaches 90% of its peak within 15 minutes. The reaction produces a characteristic blue colour, with the highest absorbance at 750 nm and the lowest absorbance at 405 nm. The kit consists of three reagents, namely, reagent A, reagent S, and reagent B. To quantify proteins using the Bio-Rad Protein Assay kit, a preparation of Reagent A and Reagent S in a 50:1 proportion is required to create a master mix for three replicates of each sample, as shown in Table 3.8. The master mix is then added to a 96-well plate by aliquoting 25 μ l into each well. After that, 2.5 μ l of the protein sample is added to each well, followed by 200 μ l of Reagent B. The plate is then incubated to allow the colourimetric reaction to occur. Once the reaction is finished, the absorbance or fluorescence of each well is measured at 650nm by a Multiskan plate reader, and the protein concentration

is calculated by comparing these readings to a standard curve. This protein quantification method delivers accurate protein concentration measurements, which is critical for various biochemical and molecular analyses.

Reagents	Volume (μ l)
Reagent A	200
Reagent S	4

Table 3.8 (A+S) master mix preparation for protein Quantification.

Reagents	Volume (μ l)
A+S Master Mix	25
Sample	2.5
Reagent C	200

Table 3.9 Master mix preparation for protein Quantification.

3.5.4 Gel Preparation

In Western blotting, the gel matrix used for protein separation comprises two main components: the stacking gel and the resolving gel. The function of the stacking gel is to concentrate and align the protein samples as they enter the resolving gel. This ensures that they all enter the separating portion of the gel at approximately the same time, which is crucial for obtaining sharp and well-defined protein bands during electrophoresis. The stacking gel typically has the same acrylamide concentration as the resolving gel and a buffering system to maintain the appropriate pH for protein migration. On the other hand, the resolving gel is responsible for separating the proteins based on their molecular weights. The composition of the resolving gel is optimised based on the expected molecular weight range of the proteins being analysed. For proteins with higher molecular weights, a lower percentage gel (e.g., 6% or 8%) is used, allowing better separation of larger proteins. Conversely, a higher percentage gel (e.g., 10% or 12%) is employed for proteins with lower molecular weights to achieve better resolution of smaller proteins. The resolving gel also contains a suitable buffering system to maintain the pH and ionic strength necessary for efficient protein separation.

10% (APS) Ammonium per sulphate (Sigma Aldrich Company Ltd., Dorset, UK) was prepared by dissolving 0.1g of APS in 1 mL of distilled water.

Reagents	Volume (μ l)
Stacking Buffer	4.2mL
40% Acrylamide	1.6mL
Distilled Water	6.2mL
APS	250 μ l
TEMED	20 μ l

Table 3.10 Composition of stacking gel.

Reagents	Volume (μ l) 6%	Volume (μ l) 10%
Separating Buffer	5.5mL	5.5mL
40% Acrylamide	3.2mL	4.4mL
Distilled Water	7.2mL	6.5mL
APS	120 μ l	120 μ l
TEMED	20 μ l	20 μ l

Table 3.11 Composition of Resolving Gel or Separating Gel.

The BioRad glass plates were cleaned and firmly fastened, showing no evidence of leaking. The next step was to add the separating gel solution between the set plates once it had been made. 120 μ l to 200 μ l of isopropanol was added to the top of the separating gel solution to prevent the formation of bubbles. The stacking gel was prepared, ensuring the thorough removal of isopropanol before its addition. The separating gel was allowed to solidify before the stacking gel was added on top of the gel and the comb was quickly inserted to form wells for loading the samples. For 15 minutes the gel was set aside.

3.5.5 Sample Preparation and Gel Electrophoresis

After protein quantification, the concentration was calculated using this formula: (mean of absorbance value -0.1662)/ 0.1065×2 . The protein samples were prepared with 4x loading buffer, 0.5mm DTT solution, and distilled water. **β -mercaptoethanol is added for GABRG1,**

GABRB3, and GABRA4 samples. The samples were heated at 95°C by using a block heater for 10 minutes and then can be stored on ice until use. The SDS-PAGE gel was inserted into the electrophoresis tanks using the cassette and soaked in 1x running buffer (0.025M Tris, 0.129M Glycine, 0.1% SDS) (diluted from 10x Tris/Glycine/SDS), Gene flow. Before loading samples, the comb was taken out, and the wells were cleaned with a syringe to remove any remaining gel particles. The following loading sequence was used throughout the experiments: ladder (5 µl/10 µl), negative control, ARGEF3-knockout clones, and scrambled clone (control). The tank was filled with 1x running buffer according to the number of gels to the required level. The electrophoresis was run at 200V and 400mA for 60 minutes until the clear differentiation of the ladder relative to the size of the band of the primary antibody.

Reagents	Volume (µl)
Sample Concentration (30µg)	5
4x loading buffer	4
DTT	1
<i>β-mercaptoethanol</i>	3
Distilled Water	3
Total	16

Table 3.12 Reagents required for Protein sample preparation.

3.5.6 Blotting

After electrophoresis, the gel was transferred using a semi-dry method and wet transfer based on the size of the target protein.

SEMI-DRY:

To perform the semi-dry transfer, 4 extra thick filter papers (20x20) by Thermo Scientific, USA were used to cut. These papers were cut evenly into 10 x 5 cm sizes. PVDF membrane from GE Healthcare Life Sciences, Buckinghamshire, UK, which was cut into 4 x 8 cm size. The 4 filter papers were soaked in the 1x transfer buffer made from 5x Power Blotter Transfer Buffer,

Thermo Fisher, USA. Then the 2 filter papers were placed on the Power Blotter, Thermo Fisher Scientific. For activation of the PVDF membrane, it was immersed in 100 % methanol for 30 seconds, followed by washing with distilled water and then with transfer buffer. After that, it was placed on blotting papers, by adding a little transfer buffer on top of the membrane. The SDS-PAGE gel was placed on the top of the PVDF 74 membrane, and it was evenly rolled to avoid air bubbles. The two filter papers were placed, and the remaining transfer buffer was poured on top of it. It was set for transfer at 25 Volts and 155mA for 20 mins.

WET-TRANSFER:

For the wet transfer method, 6 filter papers were cut into 8 x 11 cm each, and a 4 x 8 cm PVDF membrane was used. The proteins that were earlier separated using SDS-PAGE were transferred onto a polyvinylidene difluoride (PVDF) membrane using 1x Tris-Glycine Transfer Buffer (0.025M Tris, 0.129M Glycine, 20% Methanol). The PVDF membrane was then dipped in 100% methanol for 30 seconds, followed by washing with distilled water and transfer buffer. After the completion of gel electrophoresis, the stacking gel was removed, and the PVDF membrane was placed on top of the resolved SDS-PAGE gel. In the BioRad Transfer kit, a polyacrylamide gel and the PVDF membrane were placed between 6 thick extra-filter papers and 2 sponge pads, all soaked in transfer buffer. The transfer was performed at 35 V and 200 mA for 90 min.

3.5.7 Blocking

The membrane was blocked in a blocking solution following the transfer from the gel to the PVDF membrane to avoid non-specific binding. The blocking solution contains 5% skimmed milk powder in TBST and was left to incubate for an hour at 4°C on a rocker. Skimmed milk powder, which lacks lipid content, was used to ensure no interference with antibody binding.

After incubation, the blocking solution was removed, and the membrane was briefly washed with TBS-T (0.05% Tween 20 in TBS).

3.5.7 Antibody Staining

The membrane was next incubated with the primary antibody overnight at 4°C on a rocker. The concentration of the primary antibody was appropriately diluted in TBS-T, as specified in the Table below. After the overnight incubation, the membrane was washed with a washing solution (0.05% Tween 20 in TBS) for 30 minutes, with the washing solution being replaced every 15 minutes. Subsequently, the membrane was treated with the suitable HRP-conjugated secondary antibody in TBST for a minimum of 2 hours at room temperature. Following this, the membrane underwent another round of washing using TBS-T for 30 minutes.

Antibody (1:1000 μl)	Company
BIG3/ARFGEF3	Novous, NBP1-9075
PHB2 (E1Z5A)	Cell Signalling-14085S
GABRG1	Thermo Fisher - PA5-119791
GABRA3	Thermo Fisher – PA5-40998
GABRA4	Thermo Fisher - PA5-97765
GABRB3	Thermo Fisher- AB98968
GRIN2C	Thermo Fisher- NB300-107
GRIN2D	Thermo Fisher-PA5-101608
Anti-Rabbit IgG, peroxidase-linked species-specific whole antibody (from donkey) Secondary Antibody, Cytvia.	Thermo Fisher- 10794347
Monoclonal Anti- β -Actin antibody produced in mouse.	Sigma Aldrich-A228-100UL
Monoclonal Anti- α -Tubulin antibody produced in mouse.	Sigma Aldrich-T5168-100UL

Table 3.13 List of Antibodies used for Western blot.

3.5.8 Image development

The detection process used an “EZ-Chemiluminescence Detection Kit for HRP” from GeneFlow, UK. To prepare the EZ-ECL solution, 1.5mL of reagent A was combined with 1.5mL of reagent B. The membrane was placed on cling film, and the solution was gently applied drop by drop to ensure it was completely soaked. It was then left at room temperature for 2-3minutes. After that, the excess solution was removed using tissue paper, and the membrane was wrapped in cling film before it was exposed to CL -Xposure film 5x7 inches, in a dark room. The exposure time varied, once the exposure was complete, the film was developed by immersing it in “Developer Solution” from Science Laboratory Supplies, UK. Any extra developer solution was rinsed off with water, and then it was fixed in “Fixer Solution” from Science Laboratory Supplies, UK. Lastly, the film was washed with water and allowed to dry. The ladder markings were made to the film after it was dried.

3.6 Flow Cytometry

Protein expression levels may be measured precisely and quantitatively using flow cytometry. Immunocytochemistry is used to stain the protein with a fluorescent marker in order to do this. It takes 3 days to complete the process, which involves culturing cells, fixing, and labelling.

Day 1:

The initial step involved harvesting cells from a T75 flask that had reached 80% confluence. The cells were then counted using a cell counting slide on a Thermo Invitrogen Countess II FL Automated Cell Counter. The count was adjusted based on the desired number of samples (each sample has a duplicate), and 1000,000 cells were plated in each well of 6-well plates. The cells were then incubated overnight at 37°C with 5% CO₂ and 20% oxygen.

Day 2:

The next day, the cells were harvested and transferred to a 10 mL tube using a pipette. The suspension was then subjected to centrifugation and washed with 2 mL of PBS. After the centrifugation step, the PBS was removed, and the cells were resuspended in 200µl of PBS

using a pipette and vortexed. The cells were then fixed by slowly adding 2mL of ice-cold methanol while vortexing, followed by incubation at room temperature for 15 minutes. Post-fixation, the cells were washed with PBS twice to remove any residual solvent. The cells were then blocked using 200µl of a 3% blocking solution and incubated at room temperature for 1 hour to prevent nonspecific binding of the primary antibody. Afterwards, the cells were washed with PBS and resuspended in a mixture of prepared primary antibody (1:1000 µl) and blocking solution, adjusted according to the concentration specified in the provided table. Preparation of the primary antibody involved adding 2 µL of primary antibody to 1000 µl of blocking solution. The cells were then incubated overnight in a cold room.

Day 3:

After completing the incubation period, the cells were washed twice with PBS to remove any excess primary antibody. Next, the cells were suspended in a solution containing the secondary antibody (FITC Anti-Rabbit IgG SigmaF0382) (1:5000 µl) and incubated at room temperature for 2 hours on a rocker. After that, the cells were washed twice with PBS to remove any remaining secondary antibody. Finally, the cells were suspended in 200 µl of PBS and transferred into a FACS tube for analysis. The detection of the resulting fluorescence reflects the level of receptor expression.

Antibody (1:500 µl)	Company	Catalogue Number
PHB2 (E1Z5A)	Cell Signalling	14085S
GABRG1	Thermo Fisher	PA5-119791
GABRA3	Thermo Fisher	PA5-40998
GABRA4	Thermo Fisher -	PA5-97765
GABRB3	Thermo Fisher	AB98968
GRIN2B	Proteintech	2190-1-AP
GRIN2C	Thermo Fisher	NB300-107
GRIN2D	Thermo Fisher	PA5-101608
Donkey anti-Rabbit IgG (H+L) Highly Cross-Adsorbed Secondary Antibody, Alexa Fluor™ 488	Thermo Fisher	A-21206
Secondary Antibody (FITC Anti-Rabbit IgG)	Merck	F9887-1ML

Table 3.14 List of Antibodies Used for Flowcytometry.

3.7 Immunostaining

Immunostaining is a technique used to visually assess the expression levels of a specific protein of interest. The procedure takes three days and involves cell culturing, fixation, and staining on a slide. The visualisation is done using an Evos FL Cell Imaging System and Confocal Microscope. The experiment utilised the Image-iT™ Fixation/Permeabilization Kit from Thermo-Fisher Scientific Inc, UK.

Day 1:

On the first day of the experiment, cells were harvested from a T75 flask once they reached 80% confluence. The cells were then quantified using a Thermo Invitrogen Countess II FL Automated Cell Counter. The count was adjusted accordingly for the desired number of samples by plating 200,000 cells in each well in a 6-well plate. 22/26 mm, 1,5 coverslips were sterilised in 75% ethanol and allowed to air-dry. These coverslips were then transferred into each well of the 6-well plate, and 200,000 cells were meticulously seeded in each well with 3 mL of media. The cells were then incubated overnight at 37°C with 5% CO₂ and 20% oxygen.

Day 2:

The cells were fixed and stained using a series of procedures. First, the media was removed using a glass Pasteur pipette and the coverslip containing cells was transferred to a fresh six-well plate containing 1 mL of wash buffer. After washing the cells, the wash buffer was removed, and 200 µL of fixative solution was added to the well. The cells were then incubated for 15 minutes at room temperature. Next, the coverslip was subjected to three washes with wash buffer for 5 minutes each. After washing, 250 µL of permeabilization solution was added and incubated for 15 minutes at room temperature. The cells were washed three times with wash buffer to remove any residual permeabilization solution. Following this, 200 µL of

blocking solution was applied to the coverslip and incubated for 60 minutes at room temperature. Primary antibody labelling was conducted post-blocking, with the primary antibody diluted in the blocking solution at a ratio of 1:500. The antibody staining solution was then transferred into the six-well plates and incubated overnight in a cold room at 4°C.

Day 3:

After primary antibody staining, the cells underwent three washes with wash buffer for five minutes each. The secondary antibody (FITC Anti-Rabbit IgG SigmaF0382) was diluted in the blocking solution at a ratio of 1:500. Once added to the six-well plates, the solution was incubated for 120 minutes at room temperature while being covered in foil to prevent light exposure, as the secondary stain is light-sensitive. Finally, the slides were washed three times with a wash buffer for five minutes each. Actin staining (ActinRed™) was performed as post-secondary staining. According to the manufacturer's instructions, the stain was prepared by aliquoting one drop of Actin Red in 1 mL blocking buffer. The cells were incubated with 1 mL of Actin Red and incubated for 30 minutes before undergoing three washes with wash buffer. DAPI (ProLong™ Diamond Antifade Mountant with DAPI) was used for nucleus staining. One drop of DAPI stain was added to a slide, and the coverslip with cells was carefully placed onto the slide. The images were captured using a Confocal Microscope.

Antibody	Company	Catalogue Number
GABRG1	Thermo Fisher	PA5-119791
Donkey anti-Rabbit IgG (H+L) Highly Cross-Adsorbed Secondary Antibody, Alexa Fluor™ 488	Thermo Fisher	A-21206
Secondary Antibody (FITC Anti-Rabbit IgG)	Merck	F9887-1ML
ProLong™ Diamond Antifade Mountant with DAPI	Thermo Fisher	P36962

Table 3.15 List of Antibodies Used for Immunostaining.

3.8 Statistical Analysis

All data analyses were conducted using Microsoft Excel 360 and GraphPad Prism 9 software programs. A significance threshold of $p=0.05$ was applied to determine statistical significance. The data was deemed significant if the p-value was less than 0.05. If the p-value was greater than 0.05, then the data was labelled as non-significant (ns). Student's t-test was used to compare two samples, whereas one-way analysis of variance (one-way ANOVA) was utilised when analysing two or more samples.

4. RESULTS

ARFGEF3 interacts with and hinders PHB2 (prohibitin 2) to control tumour growth (Chigira *et al.*, 2019b). This interaction is essential for regulating the activation of oestrogen signalling in breast cancer cells. The expression of ARFGEF 3 is significantly upregulated in most oestrogen receptor alpha positive primary breast cancer cases and the regulation is crucial for the growth and survival of primary breast cancer cells with oestrogen receptor alpha (Toki *et al.*, 2021b). ARFGEF3 is highly expressed in pancreatic islets; it is a negative regulator of insulin granule formation in pancreatic beta-cells (Li *et al.*, 2014). Moreover, ARFGEF3 has a significant role in regulating the expression of GABA activity and lysosomal function in hippocampus neurons (Liu *et al.*, 2016a). Recent research shows that cancer cells are capable of establishing connections with neurons by expressing neurotransmitter receptors. These interactions emphasise the intricate connection between cancer cells and neurons, emphasising the significance of the tumour microenvironment in the development of metastases (Venkataramani *et al.*, 2019; Zeng *et al.*, 2019). The interaction between neurons and metastatic cancers is an intricate process that includes important receptors like the N-methyl-D-aspartate (NMDA) receptor and the gamma-aminobutyric acid (GABA) receptor (Venkataramani *et al.*, 2019; Zeng, *et al.*, 2019). This research aimed to study the involvement of ARFGEF3 Mutations, (a potential driver in breast-to-brain metastasis) and its regulation of neurotransmitter receptors using the CRISPR-Cas9 MCF-7 knockout model. In Dr. Mark Morris's research group, previous researcher Dr Ivonne Olivares sequenced the protein-coding regions from genomes of metastatic breast cancers from patients to find molecular changes that drive breast-to-brain metastasis were identified. The project commenced with the Whole Exome Sequencing of 26 patient-derived samples of breast cancer that had metastasized to the brain conducted by Dr. Olivares, identifying distinct genomic alterations that are rarely observed in the general population or primary breast cancer patients. These alterations are believed to occur as late-stage genetic events necessary for tumor adaptation and brain

colonization. Notably, mutations in the BIG3 gene were detected in breast-to-brain metastatic tumors after WES. These mutations are hypothesized to facilitate tumor-neuronal network integration by upregulating neurotransmitter receptor subunits— a mechanism previously reported in both primary and metastatic brain tumors to enhance adaptation to the tumor microenvironment, thereby promoting tumor growth and colonization to the brain (Olivares, 2023). Our current research has focused on one of these: ARFGEF3, which is mutated in 27% of breast-to-brain metastasis. The project commenced with the analysis of 26 patient-derived samples of breast cancer that had metastasised to the brain. To focus specifically on mutations related to metastasis and those that are likely to result in protein damage, Dr. Olivares utilised multiple filtering stages. At first, the WES data eliminated intronic variations that were synonymous, non-coding RNA variants, and variants in the promoter region. Prevalent polymorphisms were excluded by applying a filter based on the minor allele frequency (MAF) score. Only variants with an MAF score below 1% were kept for further study. Later, Dr. Olivares identified frequently mutated genes in the BBM samples, notably those with five or more mutant variations among at least five individuals and had mutation frequencies in primary breast cancer below 1%, according to the cosmic database. This suggests an evolutionary selection of these mutations in the metastases (Olivares, 2023).

Additional optimisation of missense mutations was conducted using the SIFT and PolyPhen-2 tools. Among the 846 missense variants, 454 were shown to have a detrimental effect on the protein. ARFGEF3 was mutated in 7/26 individual brain metastatic tumours, whereas it is mutated in less than 1% of primary breast tumours (COSMIC) tumours. In 2020, as part of my master's international exchange program (IREX), I collaborated with Dr. Olivares on this project work involving the sequencing of ARFGEF3 (Olivares, 2023).

4.1 Confirmation of ARFGEF3 gene mutation using WES data

Exome sequencing identified ARFGEF3 mutations in 7/26 individual breast-to-brain metastasis (BBM) tumours. Chain termination sequencing was utilised to validate the exon sequencing data of the ARFGEF3 gene. As predicted by exome sequencing the findings revealed mutations in 7 exons (figure 4.1). Table 4.1 shows data for all 7 ARFGEF3 mutations and the specific exon locations for each tumour. The sequencing analysis confirmed the substitution mutations in exons 19, 28 and 29 of the ARFGEF3 gene (Olivares, 2023).

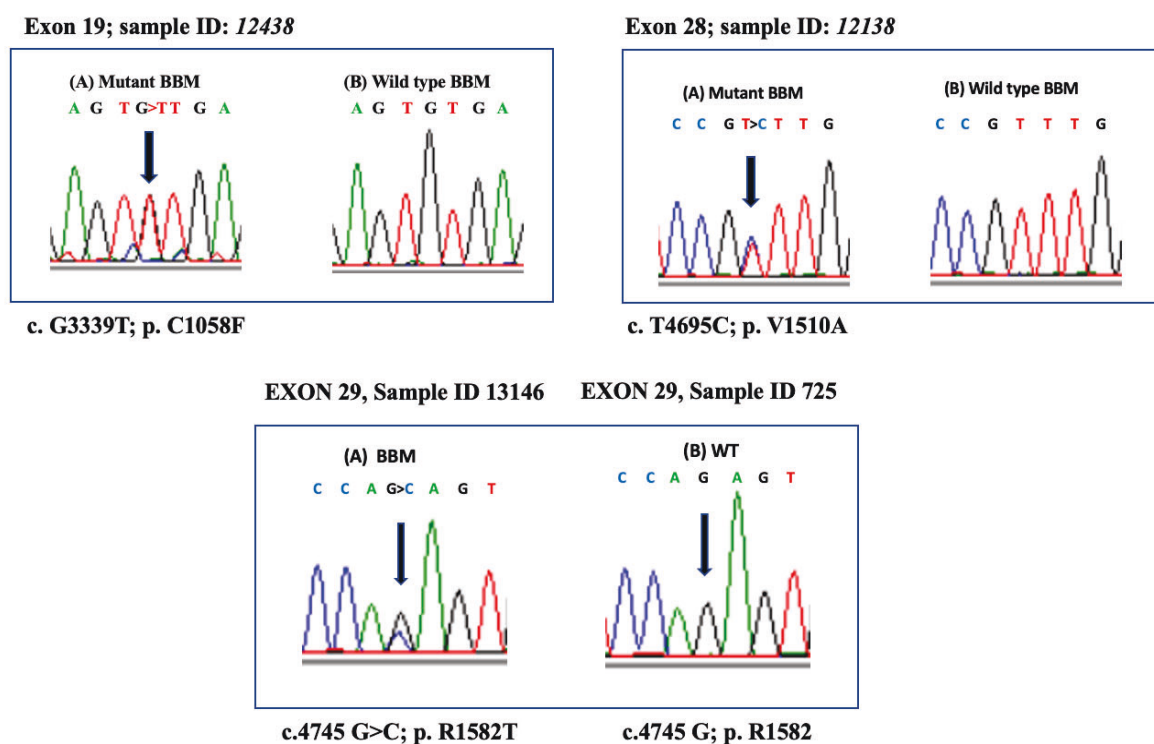


Figure 4.1 Sanger sequencing of ARFGEF3 mutation in BBM tumour.

Sequencing was conducted to identify the mutations specific to brain metastasis in ARFGEF3. A) The sequencing analysis of tissue samples from breast-to-brain metastasis has confirmed the substitution mutation on exons 19, 28, and 29 of the BIG3 gene sequence. B) The identified mutation sites in BIG3 were validated, along with the details of mutations, amino acid sequences and nucleotide sequences (Olivares, 2023). Below provided are the validated mutated sites found on various exons of ARFGEF33, along with corresponding sample numbers and the specific type of mutations. Three mutations were identified in 26 patient-derived samples at specific locations, and other potential mutation sites in the ARFGEF3 gene were additionally examined.

Sample ID	Exon	Mutation in amino acid sequence	Mutation in nucleotide sequence	Mutation type
12438	19	C1058F	G3339T	Substitution
12138	28	V1510A	T4695C	Substitution
13146	29	R1582T	G4745C	Substitution
2613	21	V1203G	T3774G	Substitution
712	24	A1329V	C4152T	Substitution
119	30	V1510A	T4695C	Substitution
756	34	V2162L	C6484G	Substitution

Table 4.1 Mutated Sites in ARFGEF33 Gene in Patient-Derived Samples.

4.2 Confirmation of ARFGEF3 gene knockout in MCF-7 cells by PCR and Western Blot Analysis

The functions of ARFGEF3 were investigated using CRISPR-Cas9 gene editing. Specifically, the CRISPR knockout (KO) was performed to mimic the ARFGEF3 mutation commonly observed in breast cancer cells. This CRISPR-Cas9 transfection of ARFGEF3 in the MCF-7 cell line was performed by Dr. Olivares. MCF-7 cells were transfected with CRISPR plasmid containing either guide RNA targeting ARGEF3 or a scrambled (SCR) control sequence. After the transfection, the cells were then cultured under puromycin selection, and 47 KO clones were picked and transferred to the well plates. Each clone was given a number for identification purposes. The scrambled (SCR) serves as the control and is similar to the wild-type MCF-7 cells, having undergone the same transfection procedure as the experimental group. RNA was isolated from the clones, and cDNA was synthesised from KO and SCR clones to perform RT-PCR. The RT-PCR results have confirmed the successful gene editing as clone number 28 and clone 47 showed no expression of ARFGEF3 at the transcript level, indicating a complete knockout, known as ARFGEF3 KO. I was involved in this work as part of the master's international exchange program (IREX) (Olivares, 2023). At the beginning of my MPhil study, I chose to continue this work. To ensure the validity of the project, I first revived all the stored cell lines and confirmed that these were the appropriate knockouts before proceeding further.

I have now confirmed these clones, and I continued the work from this point forward, as shown in Figure 4.2. SCR clone 3, referred to as the control in this thesis, showed expression of ARFGEF3 at the transcript level. The ARFGEF3 KO (clone 28) was further confirmed through Western Blot analysis. ARFGEF3 expression in the control clone was observed as 240kDa band, whereas the knockout clone exhibited no expression of the ARFGEF3 protein, confirming the successful knockout of the gene.

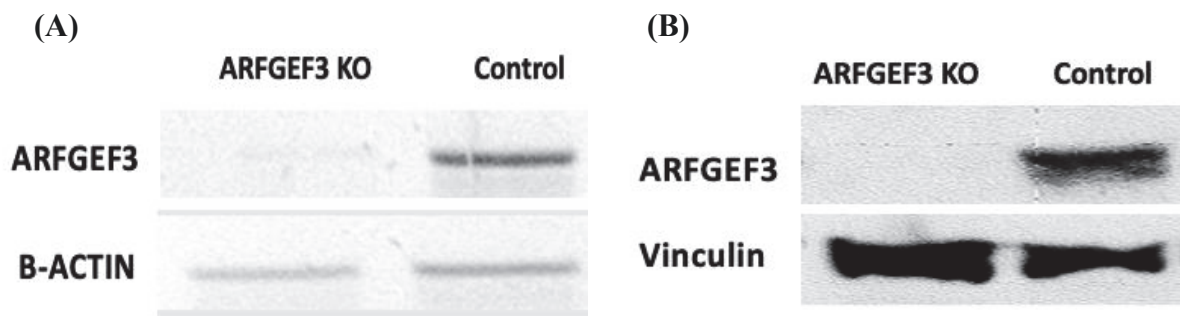


Figure 4.2 Confirmation of ARFGEF3 expression in following CRISPR-knockout at the RNA and protein level.

A) The RT-PCR analysis confirms the complete loss of ARFGEF3 expression in the ARFGEF3 KO clone compared to the control (SCR). The loading control used for this experiment was Beta-Actin. B) Knockout confirmation was performed using western blot analysis, which validated the loss of ARFGEF3 expression in the ARFGEF3 KO clone compared to the control (SCR). Vinculin was used as a loading control in the western blot analysis.

4.3 Growth Curve Analysis of ARFGEF3 KO and SCR

Despite transfection, the morphology of MCF-7 WT and SCR cells remains unchanged (Fig 4.3b). Conversely, the ARFGEF3 KO clones with loss of ARFGEF3 expression exhibit a clear physiological difference (Fig 4.3c). They tend to form clustered colonies in contrast to the growth patterns of the WT and SCR cells. To further investigate, a growth curve assay was performed on the MCF-7 cell line to evaluate the role of ARFGEF3 in breast cancer proliferation. Both SCR and ARFGEF3 KO cells were cultured, and their growth was assessed every seven days, which was continued for seven weeks. Although the morphology of SCR

and KO cells exhibited differences, their overall growth rates were comparable (Fig 4.4). This finding indicated that although loss of ARFGEF3 expression may affect cellular structure and morphology, it may not significantly impact the proliferation rate under the specific conditions examined.

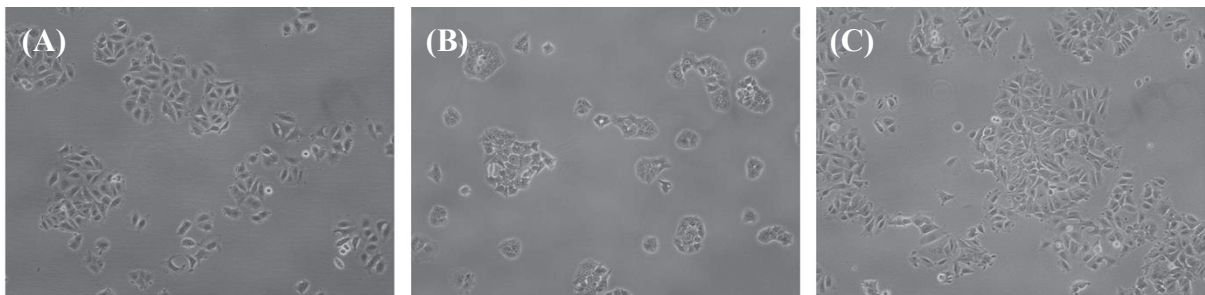


Figure 4.3 Microscopic Images of MCF-7 under different conditions.

A) Un-transfected MCF-7 Wild Type (WT) cells-this image shows MCF-7 Wild Type cells in their normal state, without any genetic modifications or transfection. B) ARFGEF3 KO clone cells; this image illustrates the morphology of MCF-7 cells following loss of ARFGEF3 expression. The cells display changes in their appearance, which include variations in cell size, shape, and clumping. C) SCR control cells; these cells have undergone the same transfection procedure but with a non-targeting SCR sequence instead of BIG3 and their morphology remains like the WT cells.

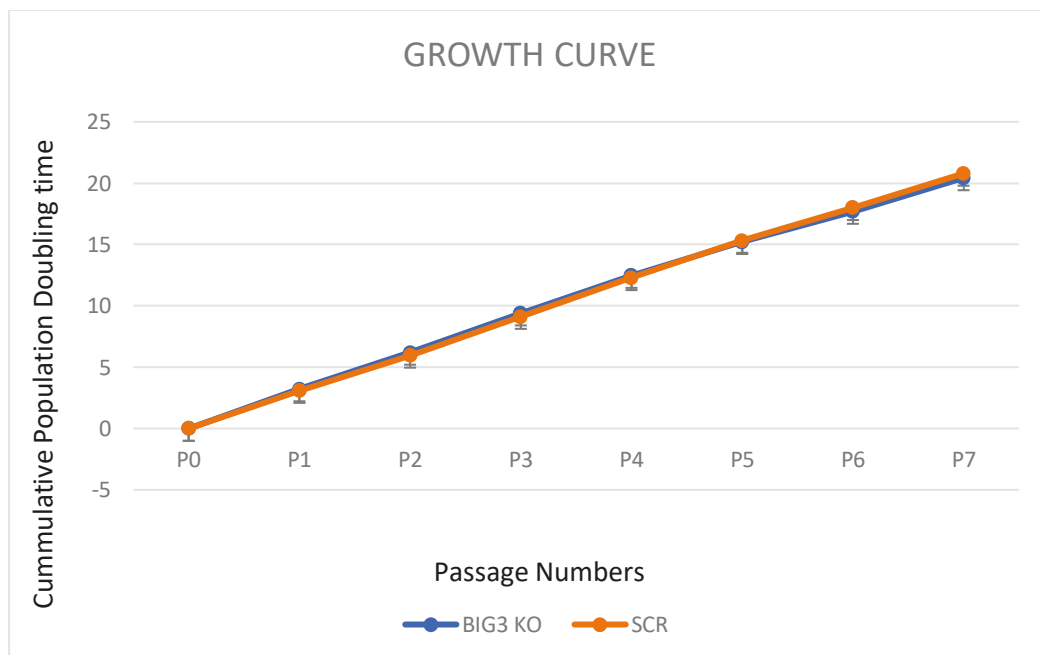


Figure 4.4 Growth Curve analysis of ARFGEF3 KO and SCR.

This graph was plotted using a cumulative population doubling level. It represents the growth rate of MCF-7 cells with ARFGEF3 KO compared to SCR control cells were measured over 7 passages. The cell number was recorded every seven days to monitor the cumulative population doubling levels. The blue line represents the cell growth rate of the ARFGEF3 KO clone. The KO cells follow a steady growth trend identical to the SCR control cells (orange line).

4.4 Analysis of PHB2 Expression at mRNA and protein levels

ARFGEF3/BIG3 has previously been reported to regulate the activity of PHB2 (Chigira *et al.*, 2019b). So, the expression of PHB2 was analysed at the transcript level and protein level in ARFGEF3 KO clones and SCR control using RT-PCR and Western blot. This analysis aimed to provide insight into the regulatory interplay between BIG3 and PHB2. The BIG3-PHB2 binding complex prevents PHB2 from interacting with and inhibiting oestrogen receptors in the presence of BIG3. This lack of inhibition of ER by PHB2 promotes the proliferation of breast cancer cells (Yoshimaru, Ono, *et al.*, 2017; Toki *et al.*, 2021c). Conversely, PHB2 binds to oestrogen receptors in the absence of BIG3, inhibiting its activity and reducing cell proliferation. This interaction between BIG3 and PHB2 plays a crucial role in the regulation of oestrogen signalling pathways within breast cancer cells (Yoshimaru *et al.*, 2013).

PHB2 plays a vital role in regulating oestrogen-dependent processes in the cytoplasm and nucleus of cells and functions as a regulator in the cytoplasm, maintaining mitochondrial integrity and function, which is crucial for cell survival and energy production (Toki *et al.*, 2021c). PHB2 can directly bind to oestrogen receptors, inhibiting their transcriptional activity and suppressing oestrogen signalling pathways. This nuclear inhibition is significant during the loss of BIG3 and has been shown to result in decreased cell growth and increased apoptosis (Yoshimaru, Ono, *et al.*, 2017; Toki *et al.*, 2021c). Therefore, the disruption of the BIG3-PHB2 interaction has a major impact on oestrogen signalling and cell proliferation. PHB2 expression was validated in ARFGEF 3 KO clones and SCR control using RT-PCR and western blot. In RT-PCR analysis, the expression of PHB2 is similar in both the ARFGEF3 KO clone and SCR.

In Western blot analysis, PHB2 protein levels were notably elevated in ARFGEF3 KO clones compared to SCR in both total cells and cytoplasmic-only extracts (Fig 4.5). This upregulation of PHB2 expression in the absence of BIG3 may have significant implications for cell proliferation and survival, specifically considering PHB2's ability to directly bind oestrogen receptors, thereby inhibiting their transcriptional activity and suppressing oestrogen signalling (Yoshimaru *et al.*, 2013; Yoshimaru, Ono, *et al.*, 2017).

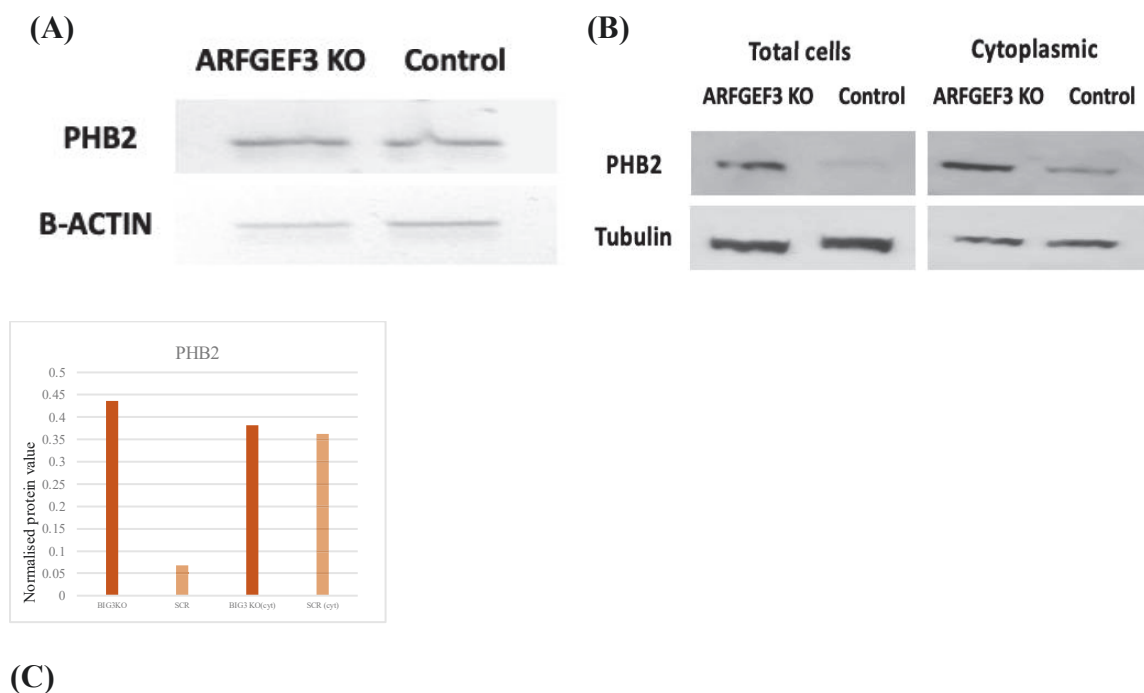


Figure 4.5 Expression analysis of PHB2 in m-RNA level and protein level.

A) RT-PCR analysis confirms the presence of PHB2 expression in the ARFGEF3 KO clone and control (SCR). Beta-Actin was used as the loading control for this experiment. B) PHB2 expression is elevated in the ARFGEF3 KO clone in comparison with the SCR control in both total cell lysate and the cytoplasmic component. This was performed by western blot analysis. Tubulin was used as a loading control for the experiments in the western blot analysis. (C) Shows the Western blot quantification bar graph of PHB2 levels in total cells and cytoplasmic compartment.

4.5 Expression Analysis of Neurotransmitter Receptors using RT-PCR

The expression levels of certain GABA and glutamate receptors were examined with an emphasis on how these receptors are regulated and expressed. Neuronal interactions with brain

tumours have been widely examined, demonstrating that pseudosynapse activity is associated with glioma proliferation and invasion (Humsa S. Venkatesh, 2017; Venkatesh *et al.*, 2019). Brain tumours like gliomas engage in additional interactions with neural circuits through electric and synaptic pathways. These interactions highlight the significance of neurotransmitter receptors in promoting tumour growth and metastasis. Neuronal activity influences the progression of glioma through glutamatergic signalling through AMPA receptors, which induce depolarising currents in cancer cells and stimulate proliferation (Venkataramani *et al.*, 2019). The synaptic connections highlight the crucial importance of neuronal activity in the dynamics of brain tumours. Additionally, breast cancer cells that metastasise to the brain are involved in glutamatergic signalling, forming pseudo-tripartite synapses, and activating NMDA receptors to facilitate brain metastasis (Zeng, et al., 2019). Loss of BIG3 expression was considered a potential mechanism for regulating neurotransmitter receptors in breast cancer as previous work has shown that loss of BIG3 in neurons by RNA interference increased gabergic signalling (Liu *et al.*, 2016a).

Previously, Nanda Gopal Ajay Kumar, an MPhil student supervised by Dr. Mark Morris, analysed the expression of several neurotransmitter receptors at the RNA level in breast cancer cells. The receptors exhibited higher expression in ARFGEF3 KO, as evidenced by RT-PCR and qPCR (Fig. 4.6). I then continued to validate whether these RNA-level expressions were observed at the protein level. In addition to that, I continued investigating other neurotransmitter receptors. This research presents a continuation and extension of the initial study by integrating a combination of neurotransmitter receptor genes that both Nanda Gopal Ajyakumar and I have investigated. These genes were chosen based on their role in the formation of receptor complexes, particularly those involving GABA and glutamate signaling pathways. I present here data generated by Mr Ajyakumar (Fig4.6) and then work conducted

by myself (Fig 4.7) and finally a figure combining the work is presented to facilitate an overview (Fig 4.8).

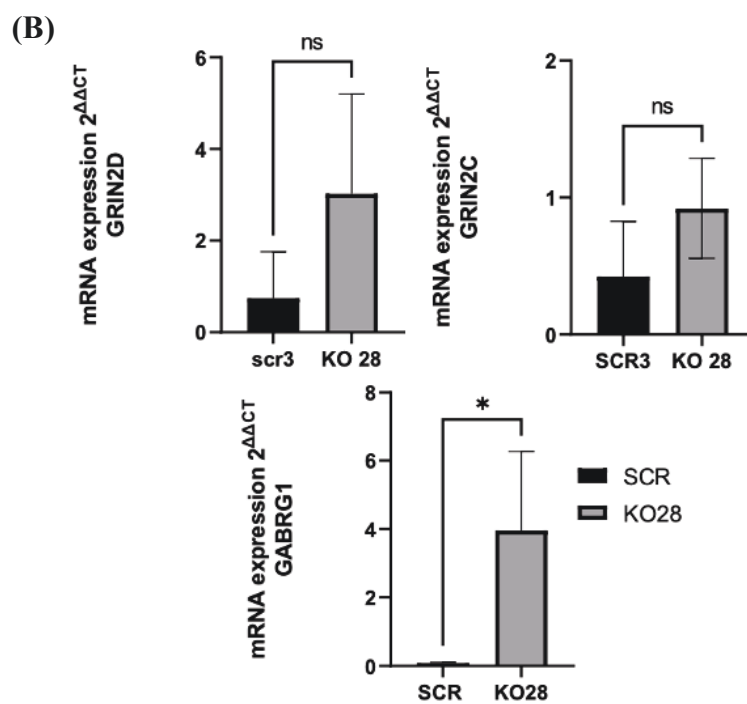


Figure 4.6 Expression data of neurotransmitter receptor subunits in Control (SCR) and ARFGEF3 KO clones were analysed using end-point PCR and qPCR (Nanda Gopal's).

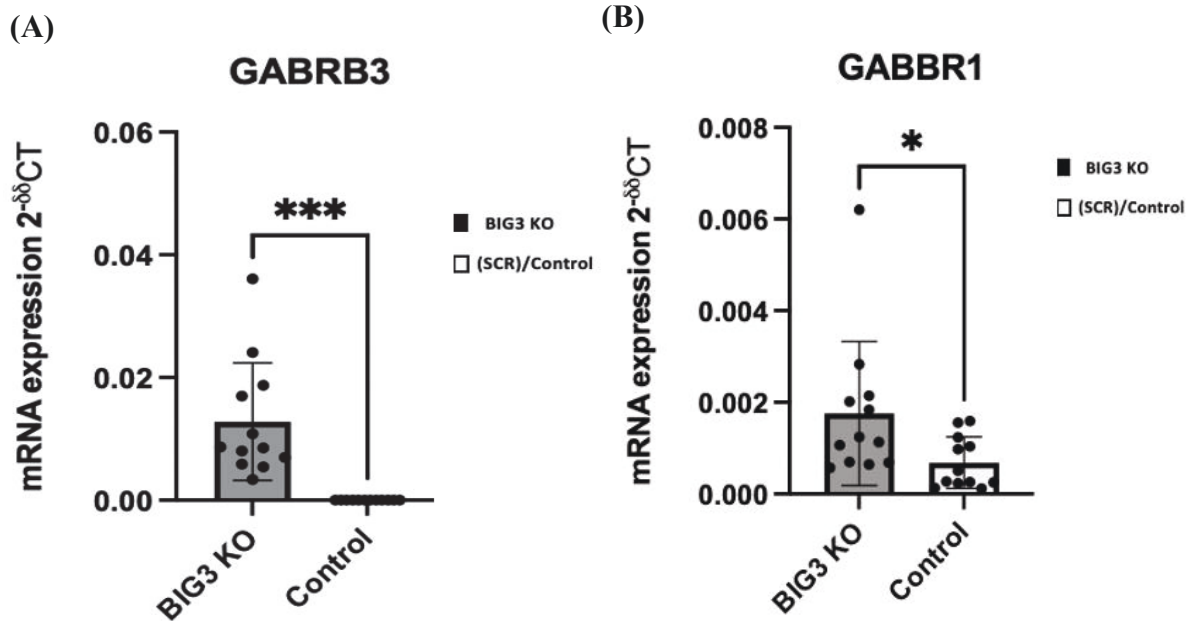
The data from both endpoint and qPCR analyses provide insight into the differential expression of neurotransmitter receptor subunits in ARFGEF3 KO clones compared to SCR control cells. A) The neurotransmitter receptor subunits GABRG1, GRIN2C, and GRIN2D exhibited significant upregulation in the ARFGEF3 KO clone compared to the control at the transcript level. The expression of GABRA2 and GABRA4 were only expressed in the ARFGEF3 KO clone. No significant change was observed in GABBR1 expression between the ARFGEF3 KO clone and control samples. GRIN2B was expressed in the control. Beta-actin was used as a loading control for the end-point PCR. B) These findings were validated using qPCR, where GABRG1 showed significant upregulation in ARFGEF3 KO samples, and GRIN2C and GRIN2D also showed increased expression in ARFGEF3 KO clones compared to the SCR. GAPDH was used as a control for qPCR.

I have conducted an analysis on the expression of the following neurotransmitter receptors, GABA receptors: GABRG2, GABRB2, GABRB3, GABRE, GABRA3, GABRA5, and GABRA6; AMPA receptors: GRIA1 and GRIA2, and NMDDA receptors: GRIN1 at the RNA level, where they were differentially expressed. The analysis was conducted using end-point PCR (Fig 4.7) and qRT-PCR (Fig 4.8). qPCR was conducted for the neurotransmitter receptors where end-point PCR did not produce clear results, allowing for more precise quantification of gene expression levels. For the GABA receptor GABRB3, I initially performed end-point PCR, which provided preliminary confirmation of its expression. To further validate, I followed up with qPCR to ensure consistency and accuracy of the results at a quantitative level. The complete analysis obtained a more detailed understanding of the differentially expressed various neurotransmitter receptors in ARFGEF3 KO cells as compared to the SCR control.



Figure 4.7 Expression data of neurotransmitter receptor subunits in Control (SCR) and ARFGEF3 KO clone using RT-PCR (conducted by me).

The RT-PCR analysis shows that the GABA receptors GABRA5 and GABRB3 were only expressed in ARFGEF3 KO clones, in which GABRB3 was very prominently shown, indicating an upregulation. The other GABA receptors, GABRA3 and GABRA6, show downregulation or absence of expression in ARFGEF3 KO compared to the control (SCR). There is no notable difference in the expression of GABRE between ARFGEF3 KO and the control (SCR). Beta-actin was used as a loading control.



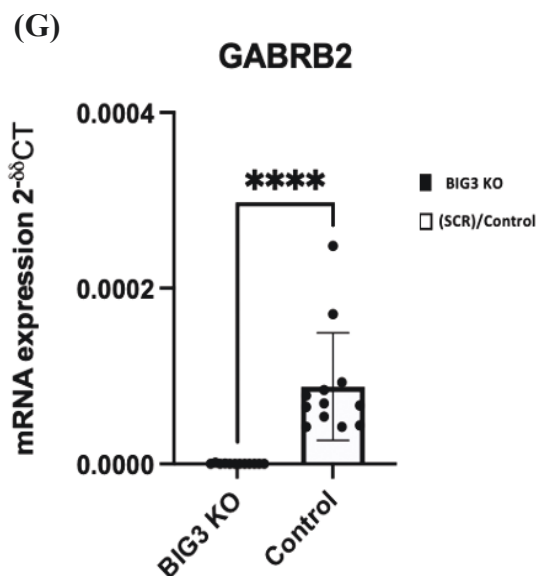


Figure 4.8 mRNA expression levels of neurotransmitter receptor subunits in ARFGEF3 KO and Control SCR using qRT-PCR analysis (conducted by me).

The relative mRNA expression of neurotransmitter receptors between ARFGEF3 KO cells and control (SCR) cells. The data is presented as mean \pm standard deviation (SD). Statistical significance was determined using the t-test. The significance levels are: * = $p < 0.05$, ** = $p < 0.01$, *** = $p < 0.001$ and ns= statistically not significant. A) The mRNA expression of GABRB3 was increased in the ARFGEF3 KO clone compared to the control SCR. This difference was statistically significant, yielding a p-value of 0.0364 and a t-value of 2.229. This indicates a statistically significant upregulation of GABRB3 expression in the ARFGEF3 KO clone (*** = $p < 0.001$). B) GABBR1 expression was significantly upregulated in the ARFGEF3 KO compared to the control SCR, with a p-value of 0.0364 and a t-value of 2.229. C) There is no significant difference in GRIA1 mRNA expression between ARFGEF3 KO and the control SCR however, there is a slight increase in the ARFGEF3 KO clone; $p = 0.1321$ and $t = 1.564$. D) There is no significant difference in the mRNA expression of GRIN1 in ARFGEF3 KO and the control SCR, with a $p = 0.6310$, $t = 0.487$. E) GRIA2 expression was significantly downregulated in the ARFGEF3 KO clone compared to the control (SCR), which provides a p-value of 0.0015 and a t-value of 3.632. F) The expression levels of GABRG2 show a downregulation in the ARFGEF3 KO clone compared to the control SCR; $p = 0.00044$, $t = 3.175$. G) The relative mRNA expression levels of GABRB2 in ARFGEF3 KO compared to the control SCR show a significant downregulation in ARFGEF3 KO compared to the control SCR, with a p-value of < 0.0001 , and a t-value of 4.967.

The data from both endpoint and qPCR analyses provide insight into the differential expression of neurotransmitter receptor subunits in ARFGEF3 KO clones compared to SCR control cells.

In Figure 4.6, conducted by previous student Ajaykumar, there was a significant differential

expression at the transcript level in the ARFGEF3 KO clone and SCR control cells. More precisely, GABA receptors: GABRG1, GABRA2 and GABRA4, and NMDAR receptors: GRIN2C and GRIN2D, exhibited significant upregulation in the ARFGEF3 KO clone compared to the control. No significant change was observed in GABBR1 expression between the ARFGEF3 KO clone and control samples. GRIN2B was expressed in the control, which shows a downregulation in ARFGEF3 KO. These findings were validated using qPCR, where GABA receptor: GABRG1 showed significant upregulation in ARFGEF3 KO samples. NMDAR receptors: GRIN2C and GRIN2D also showed increased expression in ARFGEF3 KO clones compared to the control SCR.

In addition to this, I have analysed several more neurotransmitter receptors, GABA receptors: GABRA3, GABRA5, GABRA6, GABRE, GABRB3, GABBR1, GABRB2, GABRG2, AMPA receptors: GRIA1, GRIA2, and the NMDA receptor: GRIN1 using end-point PCR and qPCR, which are shown in figure 4.7 and 4.8. Figure 4.7 shows that the loss of BIG3 differentially regulates the expression of the neurotransmitter receptors. The GABA receptors GABRA5 and GABRB3 receptors were only expressed in ARFGEF3 KO clones, in which GABRB3 was very prominently shown, suggesting an upregulation. The other GABA receptors, GABRA3 and GABRA6, show downregulation or absence of expression in ARFGEF3 KO compared to the control (SCR). There is no notable difference in the expression of GABRE between ARFGEF3 KO and control (SCR). Figure 4.8 depicts the relative mRNA expression levels of neurotransmitter receptors of which GABA receptor: GABBR1 and GABRB3, and AMPA receptor: GRIA1 show significant upregulation in the ARFGEF3 KO clone compared to SCR. Other GABA and AMPA receptors (GABRG2, GABRB2, and GRIA2) show downregulation in ARFGEF3 KO. Whereas another AMPA receptor: GRIA2 does not show any significance between the ARFGEF3 KO and the control SCR expression. The combined data in Figure 4.9 shows the previous student Nanda Gopal Ajay Kumar's and

my current work, which illustrates the differential expression of neurotransmitter receptor subunits at the transcript level between ARFGEF3 KO and control SCR at the transcript level. To summarise, the previous student's findings, in addition to my current data, show that GABRG1, GRIN2C, GRIN2D, GABRB3, GABRA5, GABRE, GABBR1, and GRIA1 exhibited significant upregulation in the ARFGEF3 KO clone, whereas GRIA2, GABRG2, GABRB2, GABRA3, GABRA6, GRIN1, and GRIN2B showed downregulation in the ARFGEF3 KO clone. This suggests that the ARFGEF3 mutation in metastatic breast cancer may regulate these receptor subunits at the transcript level. Examining the protein expression of neurotransmitter receptors is crucial for understanding their functional significance in breast cancer. To quantify and analyse neurotransmitter receptors' protein expression in breast cancer cell lines, western blot and flow cytometry experiments were conducted.



(B)

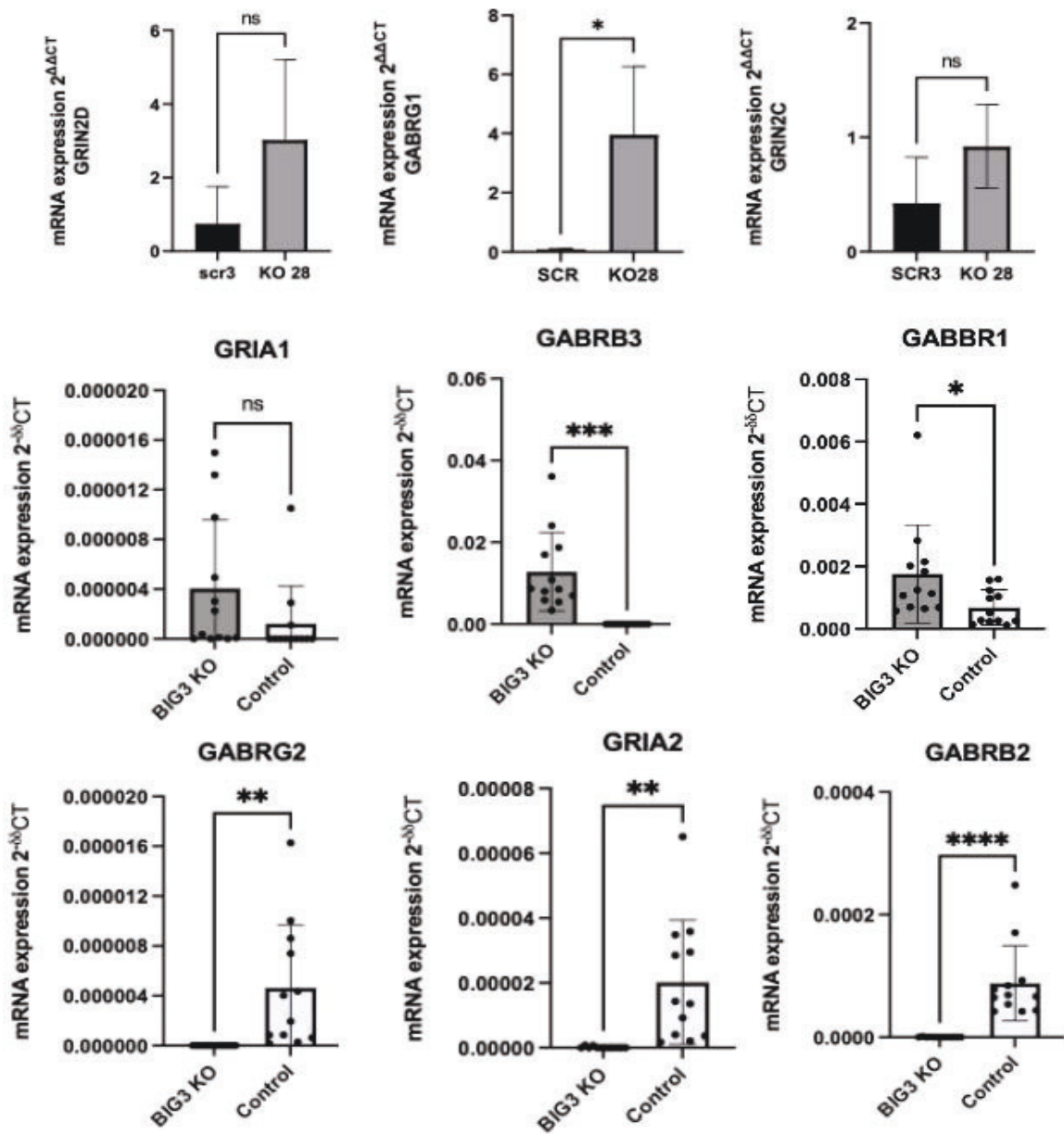
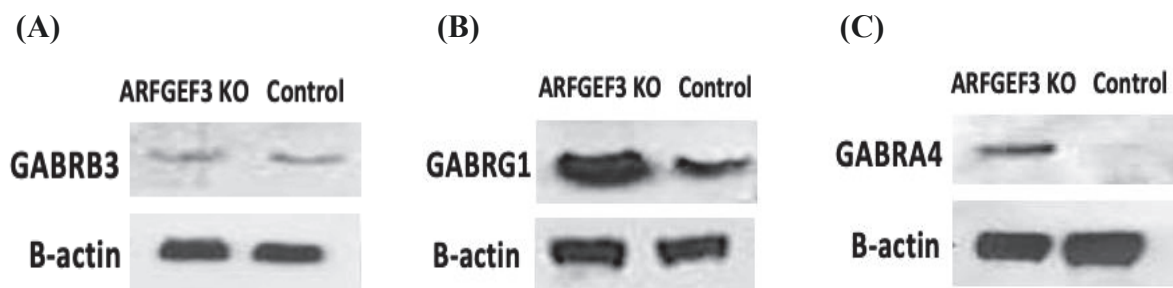


Figure 4.9 mRNA expression levels of neurotransmitter receptor subunits in ARFGEF3 KO and Control SCR of a previous student, Nandagopal Ajaykumar and current data done by me.

The endpoint (A) and qPCR(B) data represent the differential expression of neurotransmitter receptor subunits in ARFGEF3 KO and control SCR at the transcript level. To summarise the combination of all analyses, it shows that GABRG1, GRIN2C, GRIN2D, GABRB3, GABRA5, GABRE, GABBR1, and GRIA1 exhibited significant upregulation in the ARFGEF3 KO clone, whereas GRIA2, GABRG2, GABRB2, GABRA3, GABRA6, GRIN1, and GRIN2B showed downregulation in the ARFGEF3 KO clone.

4.6 Expression Analysis of Neurotransmitter Receptors using Western Blot

Following the analysis of mRNA, protein expression levels were validated by western blotting to confirm the differential expression of neurotransmitter receptor subunits in ARFGEF3 KO cells and the control SCR cells. In this study, western blotting was used to analyse the expression of several neurotransmitter receptors in metastatic breast cancer cells with ARFGEF3 KO and in the control SCR cells. Target-specific antibodies were used for the protein analysis of neurotransmitter receptors GABRB3, GABRG1, and GABRA4 (Figure 4.11). The expression levels of GABRB3 show similar levels of protein in ARFGEF3 KO and the control SCR; no significant difference was observed between the ARFGEF3 KO and the control SCR. Both the GABA receptors: GABRG1 and GABRA4, show an upregulation in ARFGEF3 KO cells compared to the control SCR cells. The presence of prominent bands for GABRG1 and GABRA4 in ARFGEF3 KO cells indicates higher protein expression levels of these neurotransmitter receptors than the control SCR. The differential expression can suggest the potential involvement of BIG3 in regulating the neurotransmitter subunit expression in breast cancer cells. Further expression analysis of these and other receptor components was carried out quantitatively by flow cytometry.



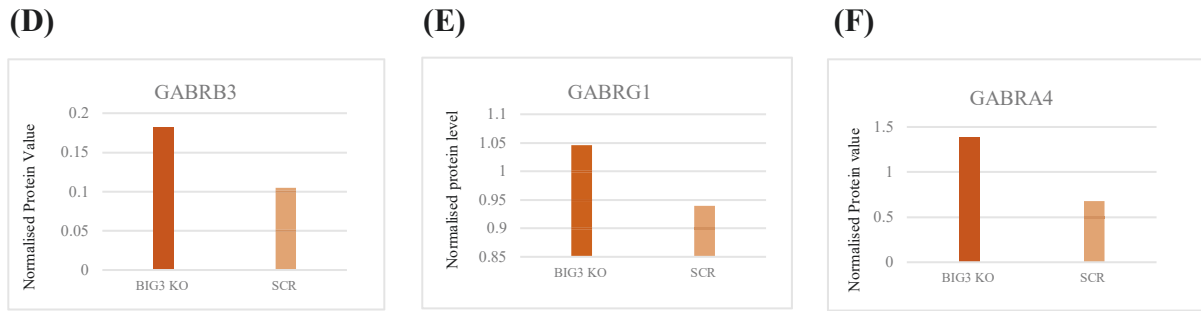


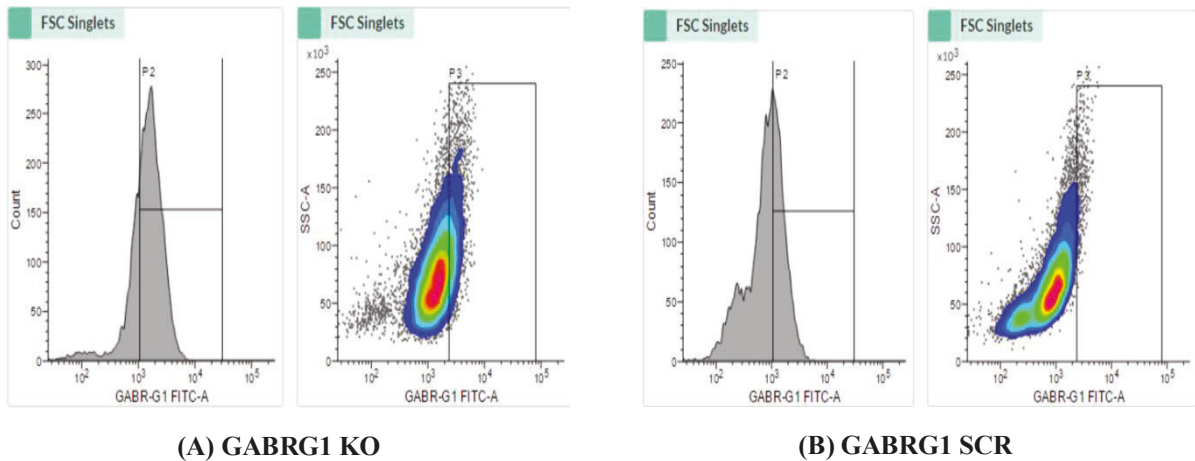
Figure 4.10 Confirmation of expression of neurotransmitter receptors at protein level using Western blot.

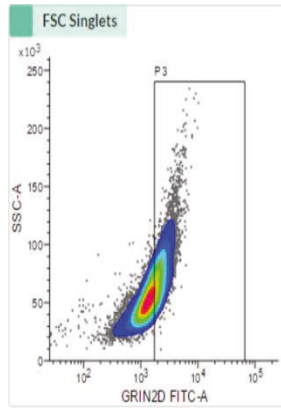
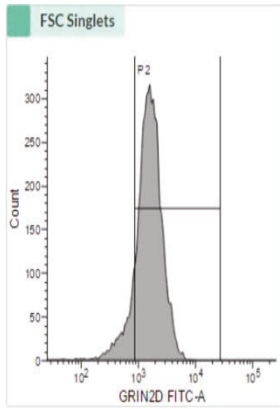
The following data depict the western blot analysis of neurotransmitter receptors in ARFGEF3 KO cells and the control SCR cells. Beta-actin was used as the loading control, which confirms the equal protein loading across the samples. A) The protein levels of the GABRB3 subunit in ARFGEF3 KO and the control SCR show similar protein expression levels. B) GABRG1's protein expression was more prominent in ARFGEF3 KO than in SCR, indicating an upregulation at the protein level. C) ARFGEF3 KO showed an upregulation compared to the control SCR in correspondence to GABRA4 expression, where there was no expression at the control SCR. D), E), and F) show the Western blot quantification graph for GABRB3, GABRG1 and GABRA4.

4.7 Expression Analysis of Neurotransmitter Receptors Using Flow Cytometry

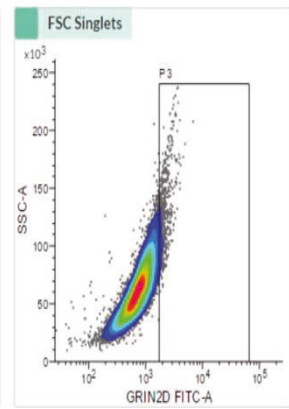
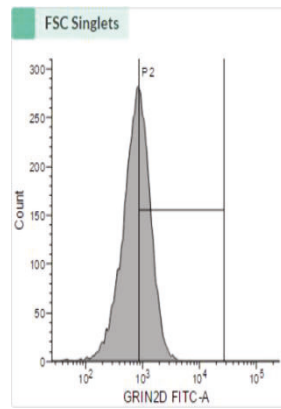
A quantitative analysis was conducted to analyse the expression of selected neurotransmitter receptors at the protein level in the ARFGEF3 KO clone and SCR. This analysis was conducted after confirming their expression at transcript level, based on antibody availability. Initially, experiments were carried out using antibodies for GABRG1, GRIN2D, and GRIN2C. Subsequently, additional receptor antibodies were ordered, resulting in a sample count difference from 10 to 4. In this flow cytometry analysis, the expression of neurotransmitter receptors in the breast cancer cell line MCF-7 was quantitatively assessed, comparing ARFGEF3 KO cells to control cells. Figure 4.11 depicts the immunostaining of the neurotransmitter receptors in ARFGEF3 KO, and the SCR. Figures A and C show the GABRG1 and GRIN2D ARFGEF3 KO results where the drift in cell populations towards the

gate is greater than that of the control SCR (B and D), indicating a notable upregulation of GABRG1 and GRIN2D in ARFGEF3 KO cells. Similar results are seen in Figures E, G, I, and K which show elevated GRIN2B, GRIN2C, GABRA3, and GABRA4 staining in ARFGEF3 KO, resulting in a shift of cell populations towards the gate compared to the control SCR. This shows a higher expression of GRIN2B, GRIN2C, GABRA3, and GABRA4 in ARFGEF3 KO when compared to the control SCR (F, H, J, and L). Figures M and N depict ARFGEF3 KO and the control SCR for GABRB3, showing a similar shift towards the gating region. However, this shows no significant difference in expression between the ARFGEF3 KO (M) and the control SCR (N). Figures O and P serve as controls, showing cells stained only with secondary antibodies to check the presence of background staining, which is crucial to validate the primary antibody's binding specificity.

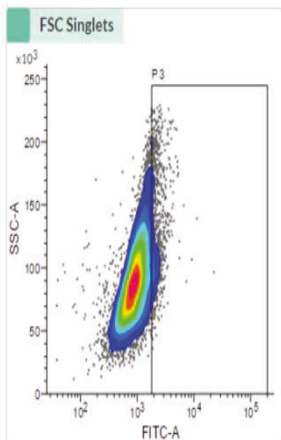
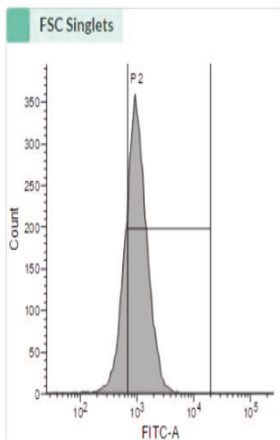




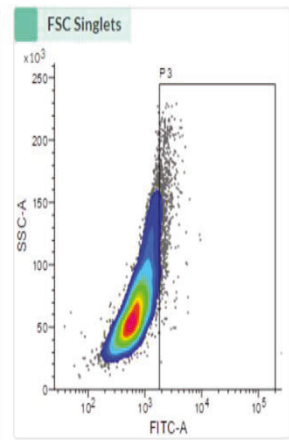
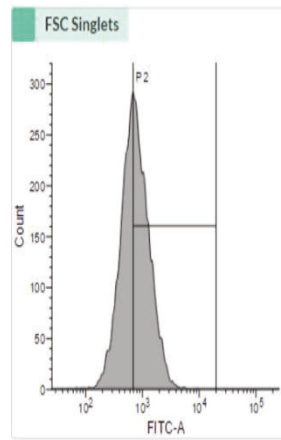
(C) GRIN2D KO



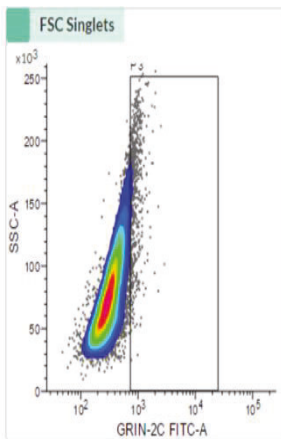
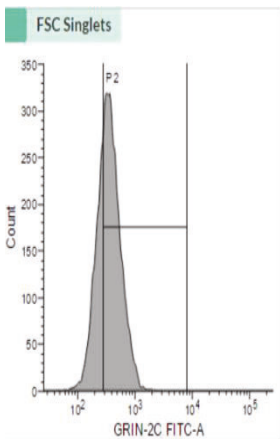
(D) GRIN2D SCR



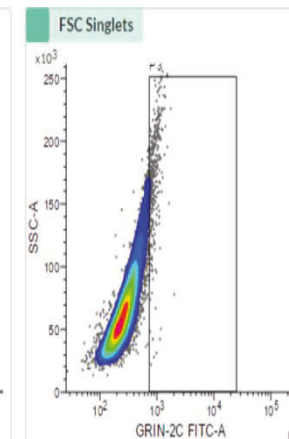
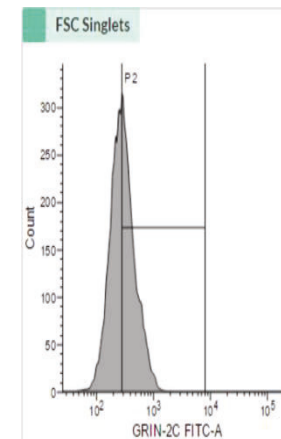
(E) GRIN2B KO



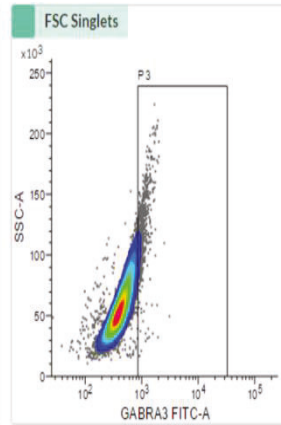
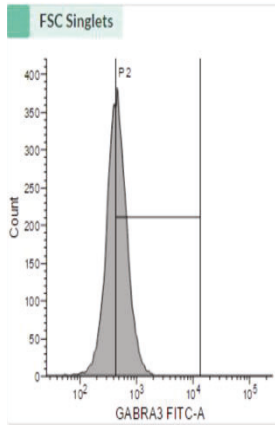
(F) GRIN2B SCR



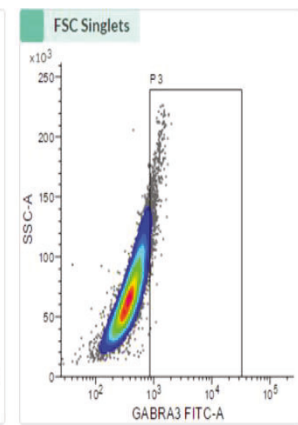
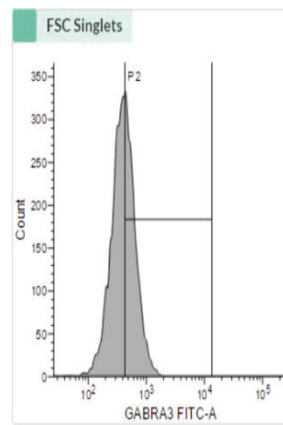
(G) GRIN2C KO



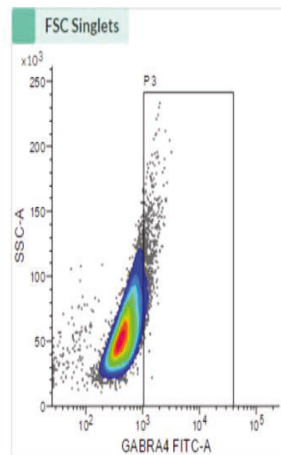
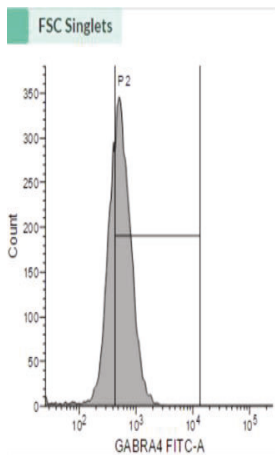
(H) GRIN2C SCR



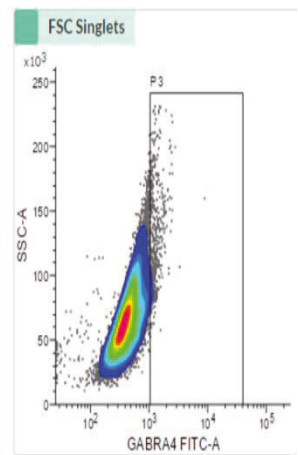
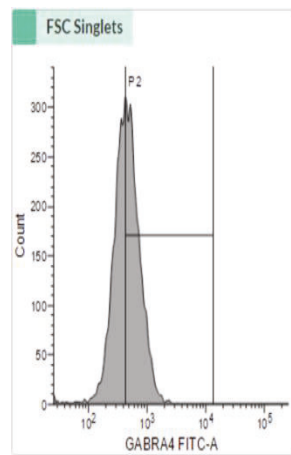
(I) GABRA3 KO



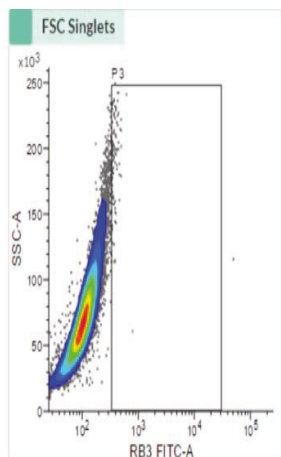
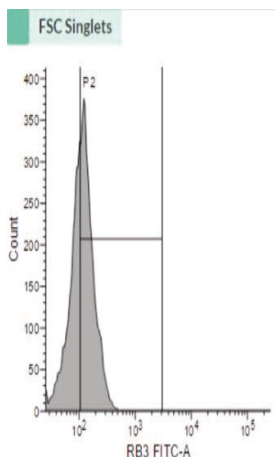
(J) GABRA3 SCR



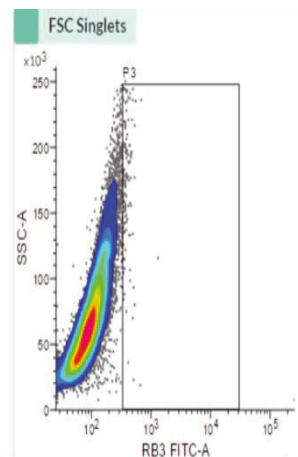
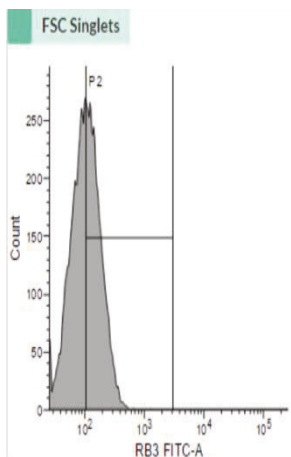
(K) GABRA4 KO



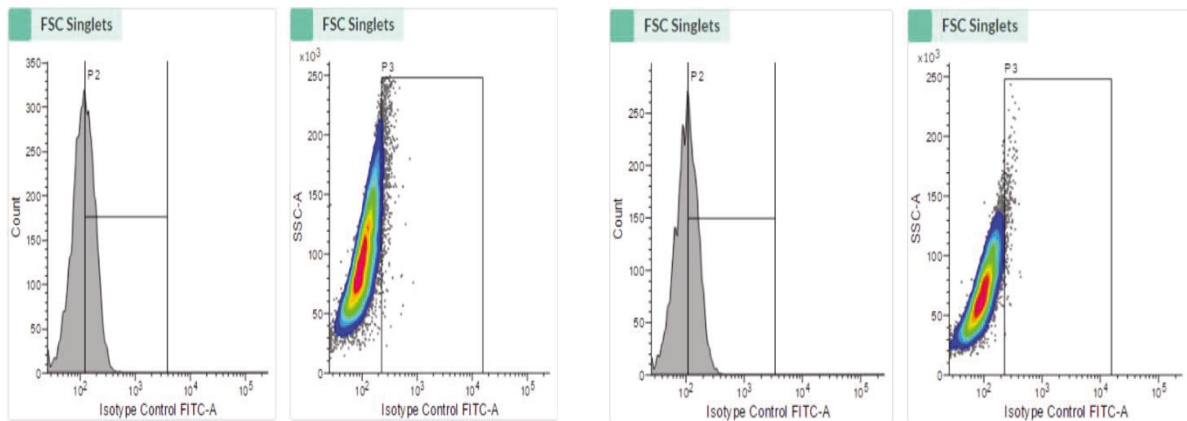
(L) GABRA4 SCR



(M) GABRB3 KO



(N) GABRB3 SCR

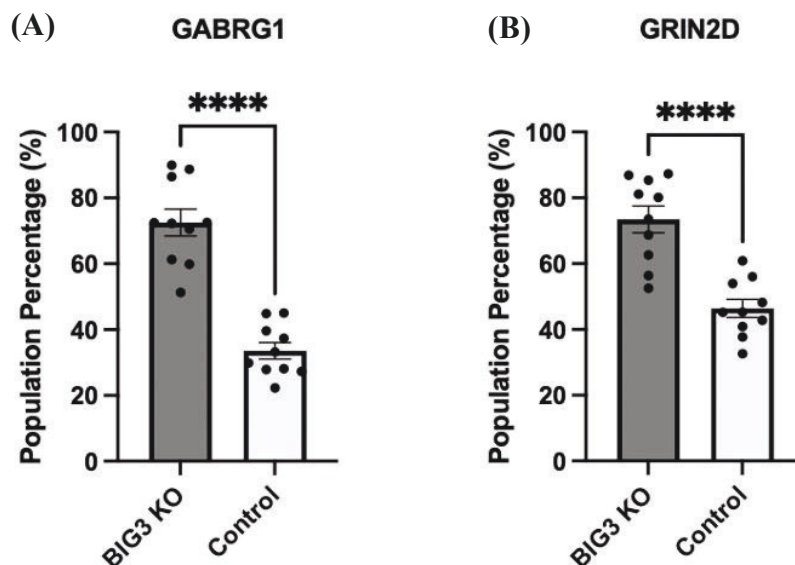


(O) ISOTYPE CONTROL KO

(P) ISOTYPE CONTROL SCR

Figure 4.11 Histograms and counterplots illustrate different neurotransmitter receptors' protein expression in MCF-7 cell lines.

These histograms and counterplots present flow cytometry data, comparing the expression of neurotransmitter receptors in ARFGEF3 KO to the control cells. Figures A and C demonstrate a more significant shift in cell populations towards the gating region for GABRG1 and GRIN2D ARFGEF3 KO, respectively than when compared to the control SCR of GABRG1 (B) and GRIN2D (D), indicating an upregulation of GABRG1 and GRIN2D in ARFGEF3 KO. Figures E, G, I, and K exhibit shifts in population for GRIN2B, GRIN2C, GABRA3, and GABRA4 ARFGEF3 KO cells compared to control the SCR cells in figures F, H, J and L, which shows an increase in the expression of these receptors in BIG3KO compared to the control SCR cells. Figures M and N depict ARFGEF3 KO and the control SCR for GABRB3, showing a similar shift of cell populations towards the gating region. This shows no significance in expression between the ARFGEF3 KO (M) and the control SCR (N). Figures O and P serve as isotype controls.



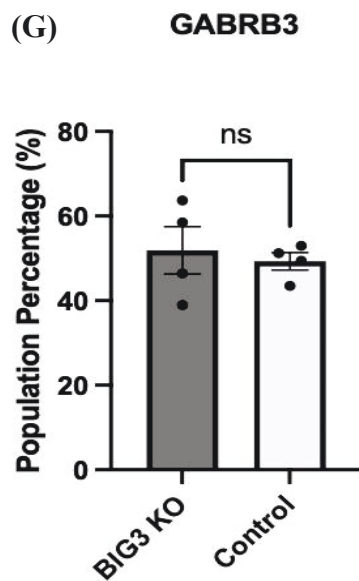
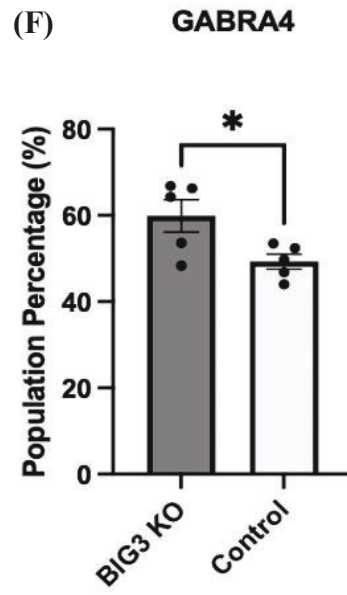
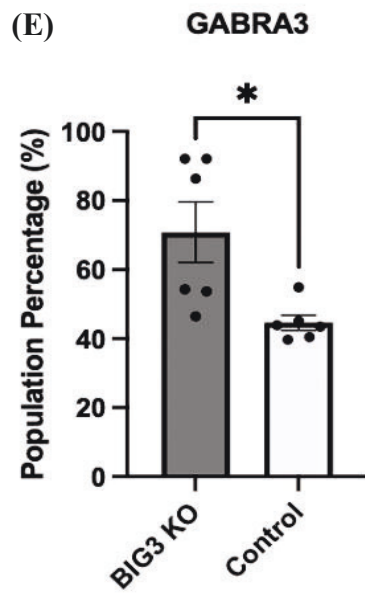
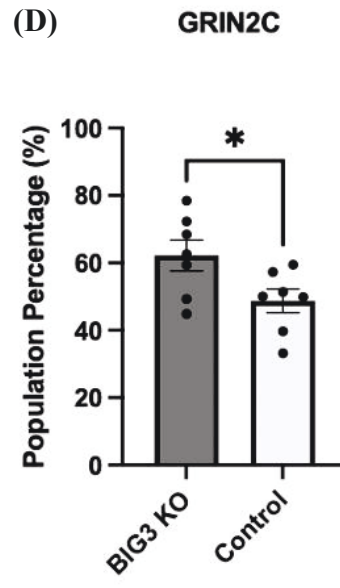
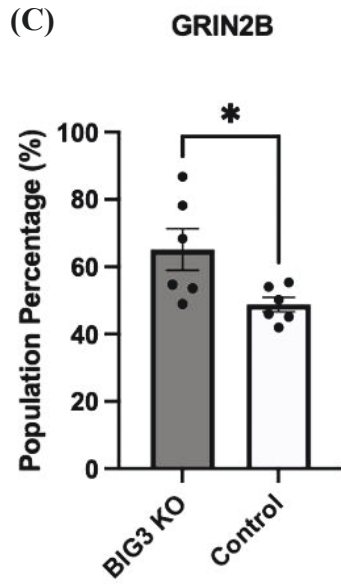


Figure 4.12 Bar graph shows the population percentage increase in neurotransmitter receptor expression in the MCF-7 cell lines.

This graph represents the flow cytometry data, which compares the protein expression of the neurotransmitter receptors in ARFGEF3 KO and the control cells. ARFGEF3 KO cells show a significantly higher percentage of the population expressing GABRG1 and GRIN2D than the control SCR. This statistically significant difference with a p-value <0.0001 for both and t-value = 8.162, and 5.538, respectively, suggests upregulation of GABRG1 and GRIN2D expression in ARFGEF3 KO compared to the control SCR. GRIN2B (p = 0.0321, t-value = 2.488), GRIN2C (p = 0.0374, t-value = 2.339), GABRA3 (p = 0.0158, t-value = 2.901) and GABRA4 p = 0.0339, t-value = 2.556) show a higher expression in ARFGEF3 KO cells compared to the control SCR. The expression of GABRB3 (p = 0.6777, t-value = 0.4365) in ARFGEF3 KO is expressed but also expressed in the control, which shows no significance of expression between them.

Figure 4.12 shows bar graphs, that represent the flow data for the neurotransmitter receptors in ARFGEF3 KO and the control SCR MCF-7 cells. Notably, ARFGEF3 KO cells exhibit a substantially higher expression of GABRG1 and GRIN2D, indicating a significant upregulation in expression compared to the control. Additionally, receptor components GRIN2B, GRIN2C, GABRA3, and GABRA4 also show higher expression in ARFGEF3 KO cells compared to the control SCR, though to a lesser extent in comparison with the other receptors. Conversely, GABRB3 expression remains consistent between ARFGEF3 KO, and the control SCR cells, exhibiting no significant difference. These differences are statistically significant, suggesting that the loss of ARFGEF3 leads to the increased expression of these receptor components. These findings indicate that ARFGEF3 significantly regulates the expression of specific neurotransmitter receptors, this finding is crucial for comprehending its broader biological functions. To further validate our findings, we aimed to determine whether the upregulated proteins were correctly localised on the cell surface; a prerequisite for them to act as functioning receptors. To do this immunofluorescence studies were conducted on neurotransmitter receptors.

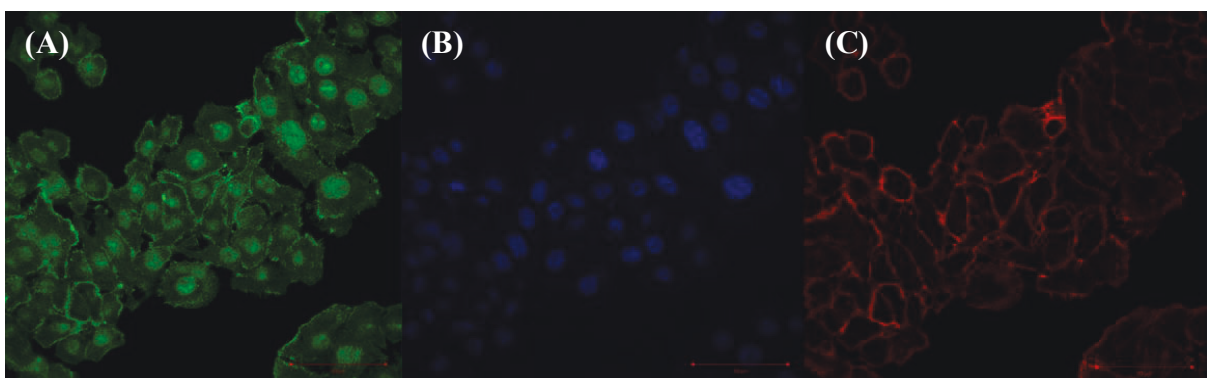
4.8 Qualitative Analysis of Neurotransmitter Receptors Using Immunofluorescence

To further validate our findings, we aimed to determine whether the upregulated proteins were correctly localised on the cell surface, a prerequisite for them to function as receptors. To facilitate this, immunofluorescence studies were conducted on one of the GABA receptors, GABRG1. The identification of neurotransmitter receptor components on the cell surface using immunofluorescence analysis allows us to confirm the presence of these components on the cell membrane, emphasising their significance in breast-to-brain metastasis and as a potential therapeutic target. The distinct localisation of these receptors on the cell membrane is crucial for their involvement in pseudo-synaptic signalling (Neman *et al.*, 2014b; Barron *et al.*, 2023; Das *et al.*, 2023a). The cells were fixed and stained to see the expression of neurotransmitter receptors on the cell surface using a confocal immunofluorescence microscope, initially focusing on GABA receptor GABRG1. Figure 4.13 shows the immunostaining results of the GABRG1 neurotransmitter receptor in MCF-7 cells. Figures A, B, and C show the ARFGEF3 KO cells, where the GABRG1 is upregulated and predominantly exhibits strong fluorescence localised on the cell membrane, indicating its presence on the cell surface. Conversely, figures D, E, and F represent the control SCR cells, where GABRG1 staining is less pronounced, and its location at the cell surface is not clear. This suggests that GABRG1 is upregulated and present on the cell surface in the absence of ARFGEF3 and expressed at very low levels in cells that express BIG3.

Neurotransmitter receptors are composed of multiple subunits, the number and arrangement of these subunits vary based on their synaptic activity. Glutamate receptors: NMDA receptors consist of four subunits (two NR1 and NR2/NR3 subunits), which allow for complex signalling and contribute to synaptic plasticity (Sanfilippo *et al.*, 2024). AMPA receptors are formed by four subunits (GluA1, Glu A2, GluA3, and GluA4), demonstrate variable calcium permeability

based on the presence of the Glu A2 subunit (Masugi-Tokita and Shigemoto, 2007). GABA_A receptors are composed of five subunits from combinations of α , β , and γ types, influencing synaptic inhibition (Hammond-Weinberger *et al.*, 2020). The subunit composition of AMPA receptors affects synaptic strength and plasticity, while the GABA_A receptor's subunit arrangement influences the inhibitory tone and excitability of neurons. The co-localization of receptor subunits in synapses contributes to the specificity and efficacy of synaptic signalling. The identification of receptor component co-localization is vital for understanding the functional dynamics of neurotransmitter receptors in synaptic contexts. Recent studies have highlighted the complexity of receptor assemblies and their role in modulating synaptic transmission (Sanfilippo *et al.*, 2024). Immunofluorescence studies could provide high-resolution insights into the spatial organization of these receptors at synapses, but more work is required to precisely map the co-localization of receptor components and their integration into distinct synaptic protein complexes.

ARFGEF3KO



SCR

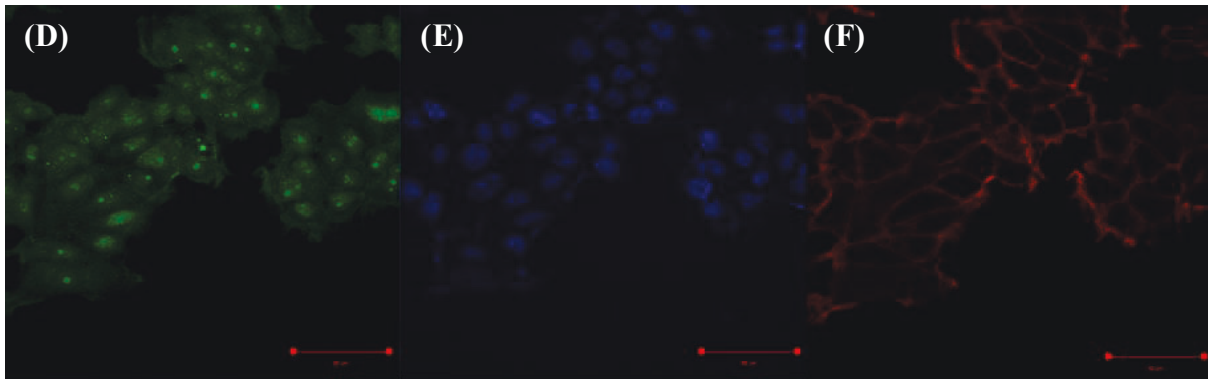


Figure 4.13 Qualitative analysis of expression of neurotransmitter receptors in MCF-7 cell lines.

These images show that ARFGEF3 KO and the control SCR cells were stained with a primary antibody (GABRG1), a secondary antibody (FITC-green fluorescence), DAPI, and Actin-Red. They were viewed and captured using a confocal microscope at 400x magnification. The intense green fluorescence indicated increased expression of GABA receptor GABRG1 in ARFGEF3 KO cells (A-green fluorescence, B-DAPI and C-Actin Red), specifically on the cell surface. On the other hand, the control SCR (D-green fluorescence, E-DAPI and F-Actin Red) shows a faint green fluorescence within the cell's interior but is not prominent on the cell surface.

5. DISCUSSIONS

Breast cancer remains one of the most prevalent cancers worldwide, primarily due to its ability to metastasise to distant organs (Ramamoorthi and Lin, 2011). Most reported cases are caused by the oestrogen receptor alpha (ER α) positive cells, and the cell proliferation is attributed to uncontrolled oestrogen hormone (Berry *et al.*, 2005). Oestradiol, a primary oestrogen hormone produced in females, is seen to activate ER α (Gumireddy *et al.*, 2016b; Gamble *et al.*, 2021). The mechanism of oestradiol and ER α signalling in breast cancer remains incompletely understood. A study by Chen *et al.* 2014 demonstrated that ARFGEF3 (BIG3) is a regulator of oestradiol and ER α signalling in breast cancer. ARFGEF3 was found to be overexpressed in breast cancer cells compared to normal human cells. ARFGEF3 (Brefeldin A-inhibited guanine nucleotide-exchange protein 3, BIG3 is expressed in brain and pancreas in healthy individuals, regulating the secretion of neurotransmitters and insulin (Liu *et al.*, 2016b). PHB2, a multifunctional protein involved in various cellular processes, binds to BIG3 to modulate the transcriptional activity of ER- α . (Chigira *et al.*, 2019a; Toki *et al.*, 2021a). BIG3 functions as an inhibitor of PHB2 nuclear translocation, thus controlling ER- α 's ability to modulate transcription in the nucleus (Kim *et al.*, 2015). The interaction between BIG3 and PHB2 leads to the dephosphorylation of PHB2, resulting in the attenuation of its tumour suppressor function. This activation of the oestradiol (E2)/ER α pathway fosters tumour growth, proliferation, and resistance to breast cancer therapies, including antioestrogen agents like tamoxifen and xanthohumol (Yoshimaru *et al.*, 2014). In the absence of ARFGEF3, PHB2 forms a complex with KPNA proteins, facilitating its translocation to the nucleus, where it binds to the ER α complex and suppresses the ER activity, thereby inhibiting cell growth and proliferation (Kim *et al.*, 2015). In breast cancer, ARFGEF3 expression is upregulated, leading to competitive binding between PHB2 and ARFGEF3 in place of KPNA proteins (Chen *et al.*, 2014). This binding disrupts PHB2's nuclear translocation and results in unmodulated ER α transcriptional activity, ultimately promoting tumour progression (Kim *et al.*, 2009). Although

BIG3 is overexpressed in primary breast cancer and functions as a proto-oncogene, our work suggests that it may also act as a metastasis suppressor.

In addition to glucose, metastatic cancer cells exploit other energy sources in the brain, such as GABA and glutamate. These neurotransmitters, which are abundant in the brain, serve as alternative fuels that cancer cells can utilise to sustain their growth (Neman *et al.*, 2014c; R. Q. Li *et al.*, 2023b). Under adverse circumstances, such as limited oxygen availability, low glucose levels, and the accumulation of waste products, cancer cells can exploit neighbouring non-malignant cells and non-cellular components to sustain their growth and survival (Jahanban-Esfahlan, Seidi and Zarghami, 2017).

The primary cell types of the brain comprise neurons, astrocytes, and microglia, which play a crucial role in supporting the survival and growth of metastatic cells. Neurons and glial are the primary cell types in the brain. Signalling between Neurons is facilitated primarily by two neurotransmitters, excitatory glutamate which initiates an electrical impulse and inhibitory GABA which stops a neural transmission. Astrocytes, being unique to the brain, are particularly important for metastatic cell adaptation. To effectively colonise the brain, metastatic cells undergo significant phenotypic and functional changes, establishing functional gap junctions with astrocytes, allowing them to communicate and transfer signals essential for tumour growth and invasion (Chen *et al.*, 2016; Srinivasan *et al.*, 2021). The study conducted by Wang *et al.* 2013 further demonstrated that these secreted factors from astrocytes significantly increase the migration and invasion capacity of breast cancer cells, establishing astrocytes as key players in the progression of brain metastasis (Chen *et al.*, 2016).

In glioma patients, neuronal stimulation was found to increase the expression of neuroglin-3 (NLGN3), a synaptic protein in neurons. The elevated expression of NLGN3 drives glioma cell proliferation, suggesting that neurons might also aid the progression of brain metastasis in

breast cancer (Venkatesh *et al.*, 2015). The interaction between neurons and tumours via neurotransmitter receptors significantly enhances the survival and proliferation of both primary brain tumours and metastatic brain tumours within the brain microenvironment. In the neuronal environment, neurotransmitters also play a crucial role in gliomas by entering tumour cells and regulating their proliferation, invasion, and cellular differentiation (Huang *et al.*, 2022). This neuron-cancer cell interaction highlights the possibility of neurons not only supporting glioma growth but also contributing to the brain colonization of breast cancer cells. The breast cancer cells that metastasize to the brain exhibit neuronal-like phenotypic adaptations. These metastatic cells express high levels of GABA receptors and transporters, mimicking neuronal properties and enabling them to utilise GABA as an alternative metabolic resource (Neman *et al.*, 2014c; R. Q. Li *et al.*, 2023b). The study by Neman *et al.* demonstrated that breast cancer cells in the brain show elevated GABA catabolism, suggesting that these cells have evolved to use GABA as an energy source to survive and grow in the brain (Neman *et al.*, 2014c; R. Q. Li *et al.*, 2023b). This phenotypic shift towards GABAergic characteristics indicates that breast cancer cells not only adapt to the brain microenvironment but also actively exploit it to meet their metabolic needs.

In addition to GABA, the glutamatergic system is also co-opted by brain metastatic cells. Breast cancer cells upregulate glutamate receptors, further integrating into the brain's neurotransmitter network. This allows them to utilise glutamate signalling for tumour progression and invasion, indicating a broader adaptation to the neurochemical environment of the brain (Sontheimer, 2008; Venkataramani *et al.*, 2019). Metastatic breast cancer cells show features similar to neurons in terms of their receptor expression and metabolic activity, demonstrating how they integrate into the brain's complex cellular interactions to promote their survival. Zheng and colleagues further demonstrated that GRIN2B, a glutamate receptor subunit, is upregulated in over 40% of breast cancer patients with brain **metastasis** (Venkatesh

et al., 2019; Zeng, Zhang, *et al.*, 2019). Knocking out GRIN2B in MDA231 breast cancer cells significantly impaired their ability to colonize the brain, underscoring the importance of glutamate signalling in brain metastasis. Activation of GRIN2B and NMDARs generates a calcium influx that promotes the MEK-MAPK and CAMK pathways, both of which are associated with tumour growth and poor prognosis (Liu *et al.*, 2005; Venkatesh *et al.*, 2015).

The study presented here investigates the role of ARFGEF3 in the regulation of differentially expressed neurotransmitter receptors in breast cancer cells that metastasise and colonise the brain. Gene expression is a key factor in the unregulated growth and spread of tumour cells. In this context, mutations in ARFGEF3 may represent a genetic alteration acquired by breast-to-brain metastatic cells during the metastatic process. Such mutations likely enhance their ability to adapt to the challenging conditions of a secondary site, enabling them to thrive and colonize within the new tumour microenvironment. Characterizing the role of BIG3 in the brain colonization of breast tumour cells provides valuable insights into the complexities of brain metastasis and highlights potential therapeutic targets. BIG3's involvement in regulating neuronal signalling was elucidated by Liu *et al.* (2016), demonstrating that the loss of BIG3 is associated with the increase of GABA activity. Cancer cells that metastasise must adapt to the unique metabolic environment, which often includes nutrient deprivation and metabolic stress (Liu *et al.*, 2016a; Toki *et al.*, 2021a).

Current research has revealed communication between tumour cells and the brain's cellular network. Tumour cells invading the brain exploit neurotransmitter signalling pathways to reprogram the brain microenvironment, fostering tumour adaptation and driving uncontrolled growth and proliferation (Kuol *et al.*, 2018; Jiang *et al.*, 2020). One potential mechanism contributing to this adaptation is the loss of BIG3 function due to mutation, which may play a crucial role in brain metastasis. Furthermore, BIG3, a gene implicated in breast-to-brain

metastasis, has been linked to the regulation of neurotransmitter receptors. In this study, CRISPR-Cas9 editing of MCF7 breast cancer cells was used to investigate the role of BIG3. Knockout of BIG3 revealed differential expression of neurotransmitter receptor subunits, including glutamate and GABA receptor subunits. These findings suggest that mutations in BIG3 may be one mechanism by which breast cancer cells achieve brain colonization.

Whole-exome sequencing of 26 breast-to-brain metastasis (BBM) samples by Dr. Olivares in Dr. Morris's group identified mutations in ARFGEF3, predominantly substitution mutations predicted to inactivate the gene. This evidence suggests that ARFGEF3 loss may play a role in BBM (Figure 4.1). To model this, ARFGEF3 was knocked out in MCF7 breast cancer cells using CRISPR-Cas9, which was performed and confirmed by Dr. Olivares. To ensure the validity of the project, I first revived all the stored cell lines and confirmed that these were the appropriate knockouts before proceeding further. Clone 28 was confirmed as a successful knockout (KO) through PCR and Western blot analyses (Figure 4.2).

This work is the first instance of knocking out BIG3 experimentally in breast cancer cell lines. Initially, I did some preliminary primitive assays, starting with the proliferative assay. The growth trends of MCF-7 cells with ARFGEF3 KO compared to SCR control cells with 7 passages were assessed. The cell number was recorded every seven days to monitor the cumulative population doubling levels. SCR cells are the control cells, which underwent the same procedures. Following the KO of BIG3, BIG3 KO cells demonstrate the same proliferation rates compared to control cells under similar conditions. It is the first experiment of evidence that loss of BIG3 does not change the proliferative rate in breast cancer cells. (Figure 4.3 and 4.4). However, there is a phenotype change, which may require further investigation, as the phenotype appears to look somewhat like mesenchymal cells (Huang, Wu and Xu, 2015; Fedele *et al.*, 2022; Kepuladze, Burkadze and Kokhraidze, 2024). By

proliferating at the same rate, cancer cells may evade chemotherapeutic agents that typically target rapidly dividing cells, thereby increasing the likelihood of dormancy and micro-metastasis formation. Patients with ER-positive breast cancer typically receive tamoxifen therapy to reduce the risk of recurrence. However, in some cases, brain metastases can develop many years after completing treatment. This represents a significant clinical challenge in the UK, as patients who believe they are cured may experience late disease relapse long after discontinuing tamoxifen and other therapies. Emerging evidence suggests that this phenomenon may be driven by specific evolutionary mechanisms, allowing dormant tumor cells to evade treatment and later reactivate in the brain microenvironment. Literature supports the existence of these mechanisms, highlighting the need for further research to improve long-term management strategies for ER-positive breast cancer patients.

The dormancy effect is a crucial factor in the development of breast cancer brain metastases, particularly in patients with ER-positive tumours who have undergone prolonged tamoxifen treatment. While tamoxifen significantly reduces recurrence and mortality rates, a subset of patients experiences late-onset metastases, often years after discontinuing therapy, suggesting a dormancy-driven mechanism (Davies *et al.*, 2013; Rossari *et al.*, 2020). Dormant tumour cells evade treatment by entering a quiescent state through mechanisms such as autophagy, stress-response signaling, and epigenetic modifications, allowing them to survive under unfavourable conditions and later reactivate. (Wang and Lin, 2013). Notably, dormant tumor cells often exhibit stem cell-like properties, rendering them resistant to standard chemotherapy, including tamoxifen (Fehm *et al.*, 2012; Banys-Paluchowski, Reinhardt and Fehm, 2020). This presents a significant clinical challenge, as these cells can remain undetected for extended periods, leading to late recurrences and metastases, particularly in the brain (Rossari *et al.*, 2020; Nisar *et al.*, 2024). Understanding the molecular drivers of dormancy and reactivation is essential for

developing targeted therapeutic strategies to eliminate dormant tumor cells and prevent brain metastases in ER-positive breast cancer patients (Rossari et al., 2020; Robinson et al., 2020).

Following the validation growth curve analysis, the expression of PHB2 was analyzed at both the transcript and protein levels in ARFGEF3 KO and SCR control cells to explore the regulatory dynamics between BIG3 and PHB2. The BIG3-PHB2 complex formation is known to prevent PHB2 from interacting with and inhibiting estrogen receptors, thereby promoting estrogen-dependent breast cancer cell proliferation (Yoshimaru, Aihara, *et al.*, 2017b; Toki *et al.*, 2021a). In the absence of BIG3, PHB2 binds to estrogen receptors, inhibiting their activity and leading to reduced proliferation. PCR analysis revealed similar PHB2 transcript levels in both ARFGEF3 KO and SCR control cells, indicating that BIG3 does not regulate PHB2 transcriptionally. However, Western blot analysis demonstrated a significant upregulation of PHB2 protein in ARFGEF3 KO cells compared to SCR controls, observed in both total cell lysates and the cytoplasmic fraction (Figure 4.5). This upregulation highlights a post-transcriptional or translational regulation of PHB2 expression in the absence of BIG3, potentially enhancing PHB2's ability to inhibit estrogen receptor activity and suppress estrogen signalling (Yoshimaru, Ono, *et al.*, 2017; Toki *et al.*, 2021a).

Recent research has shown that breast cancers that metastasised to the brain showed varied levels of neurotransmitter receptor expression. To investigate the role of ARFGEF3 in neurotransmitter expression, expression assays of some neurotransmitter receptors were carried out. The functional relevance of ARFGEF3 in the context of breast-to-brain metastasis has been elucidated through a series of molecular and functional studies, providing insight into its regulatory role in metastatic progression. I investigated the downstream impact of loss of ARFGEF3 on the differential expression of neurotransmitter receptor genes, particularly focusing on the GABA receptor, AMPA and NMDAR genes. These receptors are pivotal in

mediating neuronal communication and have been increasingly recognized for their role in the brain microenvironment's interactions with metastatic cancer cells. The results showed a significant modulation in the expression of neurotransmitter receptor genes at the mRNA level following ARFGEF3 knockout. Using endpoint PCR and RT-PCR, it shows that loss of ARFGEF3 results in altered transcriptional profiles of key subunits associated with both GABA, AMPA and NMDAR receptors. Specifically, the GABA receptor subunits GABRG1, GABRB3, GABRA5, GABRE, GABBR1 and the NMDA receptor subunits GRIN2C, and GRIN2D demonstrated significant upregulation in ARFGEF3 knockout (KO) clones compared to wild type the control cells (Figure 4.7 and 4.8). In addition to the upregulation of these receptors, we also found a downregulation of GRIN1, GRIA2, GABRG2, and GABRB2. This suggests a potential interaction between breast cancer cells and the GABAergic signalling pathways within the brain microenvironment.

After validating mRNA expression levels, protein-level analysis was conducted to confirm the differential expression of neurotransmitter receptor subunits in ARFGEF3 KO and control (SCR) cells using Western blot, flow cytometry and immunofluorescence. Western blot results revealed a similar expression of GABRB3 in ARFGEF3 KO and control cells, while GABRG1 and GABRA4 were upregulated in ARFGEF3 KO cells, indicating a potential regulatory role of BIG3 in modulating these neurotransmitter receptors (figure 4.10). Flow cytometry analysis further quantified this upregulation, showing significant increases in the expression of GABRG1, GRIN2D, GRIN2B, GRIN2C, GABRA3, and GABRA4 in ARFGEF3 KO cells compared to control cells, with GABRG1 and GRIN2D exhibiting the most pronounced changes. Conversely, GABRB3 showed no significant difference between the KO cells and the control cells (Figures 4.11 and 4.12). Immunofluorescence analysis validated the cell surface localisation of GABRG1 in ARFGEF3 KO cells, highlighting its potential role in pseudo-synaptic signalling and interaction with the brain microenvironment, as suggested by prior

studies (figure 4.13). (Humsa S. Venkatesh, 2017; Venkataramani *et al.*, 2021). The underlying mechanisms driving their differential expression remain unclear; however, the observed alterations in neurotransmitter receptor expression, particularly in these cells, suggest a potential advantage for tumor cells within the brain microenvironment. This confirms our hypothesis that loss of ARFGEF3 results in differential expression of neurotransmitter receptors in breast cancer cells, which may metastasise to the brain.

Breast cancer cells that metastasize to the brain exploit GABA, an inhibitory neurotransmitter, as a metabolic substrate by forming active connections with neurons (Termini, Neman and Jandial, 2014b). These metastatic cells express NMDA receptors, enabling them to form pseudo-synapses with neurons. Tumour cells replace astrocytes within the synaptic cleft, creating pseudo-tripartite synapses that provide access to glutamate. This glutamate-dependent NMDAR signalling enhances calcium influx, promoting tumour proliferation and migration in the brain microenvironment (Zeng, *et al.*, 2019; Gallo, Vitacolonna and Crepaldi, 2023). Connexins, particularly Cx31 and Cx43, facilitate tumour cell adhesion to astrocytes. This interaction promotes focal adhesion kinase (FAK) activation, which triggers NF- κ B signalling. NF- κ B, in turn, enhances laminin deposition and integrin-mediated adhesion, fostering a supportive microenvironment for tumour cell survival (Wang *et al.*, 2021c; Lorusso *et al.*, 2022). NMDAR subunit overexpression, such as NMDAR1 and NMDAR2, has been observed in aggressive metastatic cells, correlating with increased tumour proliferation (García-Gaytán *et al.*, 2022; Galloni *et al.*, 2024).

Astrocytes play a crucial role in modulating synaptic transmission within pseudo-tripartite synapses, significantly influencing both excitatory and inhibitory signalling. Their interactions with pre- and postsynaptic neurons facilitate various mechanisms that enhance or suppress synaptic activity, thereby affecting overall neural communication. Astrocytes release

transmitters in response to neurotransmitter signalling, which can modify synaptic strength. For instance, astrocytic calcium signalling is essential for regulating presynaptic plasticity, where the activation of NMDA receptors leads to a decrease in spontaneous glutamate release, shifting the polarity of synaptic transmission (Letellier and Goda, 2023). Astrocytes are integral in maintaining GABA homeostasis by taking up GABA from the synaptic cleft, metabolizing it, and recycling it back to neurons. This GABA-glutamine cycle is vital for sustaining inhibitory signalling, which is crucial for balanced neural activity (Andersen, Schousboe and Wellendorph, 2023). Tumour cells express synaptic proteins such as neuroligin-3 and glutamate receptors (AMPA, NMDAR), facilitating pseudo-synaptic interactions and leveraging neuronal activity to promote growth and survival (Faulkner *et al.*, 2019; Li *et al.*, 2022).

The interaction between brain tumours and breast cancer cells with the brain microenvironment is pivotal for their survival, adaptation, and proliferation. Tumour cells exploit neurotransmitter receptors, particularly NMDA receptors (NMDARs), to establish synaptic-like connections, known as pseudo-synapses, with neurons. These pseudo-synapses enable tumour cells to acquire neurotransmitters like GABA and glutamate from the synaptic cleft, which serve as critical metabolic substrates to sustain tumour growth and energy demands (Andersen, Schousboe and Wellendorph, 2023; Nguyen *et al.*, 2023). NMDAR activation facilitates calcium signalling pathways, which are crucial for tumour cell proliferation, survival, and progression. This communication is further supported by neurotrophic factors released by tumour cells, which stimulate neuronal infiltration into the tumour microenvironment, creating a feedback loop that promotes tumour growth and neuronal involvement (Das *et al.*, 2023b). The ability of tumour cells to co-opt neuronal signalling underscores the adaptability of metastatic cells in the brain. For instance, in breast-to-brain metastasis, enhanced expression of post-synaptic proteins and neuroligins supports the formation of pseudo-synaptic structures,

replacing astrocyte-mediated interactions and establishing direct communication with neurons. This adaptation not only enhances tumour growth but also highlights the aggressive nature of metastatic cells as they exploit the brain's neural architecture (Zeng, et al., 2019; Das et al., 2023b).

Studies have shown that tumour-neuron communication is enhanced by neurotrophic factors released by tumour cells, which stimulate nerve infiltration into the tumour microenvironment, creating a feedback loop that accelerates tumour expansion. The replacement of astrocytic interactions with direct neuron-tumour communication underscores the aggressive adaptations of metastatic cells within the brain. For instance, in breast-to-brain metastasis, the GluN2B-NMDAR signalling pathway has been implicated in facilitating tumour proliferation. These metastatic cells also exhibit increased expression of post-synaptic signalling proteins and neuroligins, further strengthening pseudo-synapse formation and tumour growth (Zeng, et al., 2019; Das et al., 2023b). The studies by Zeng et al. (2019), Venkatesh et al. (2019), and Venkataramani et al. have significantly advanced our understanding of how brain tumours and breast-to-brain metastatic cells adapt and survive within the brain microenvironment. Zeng et al. specifically highlighted the formation of pseudo-synapses by breast tumours, shedding light on the critical role of NMDAR signalling in facilitating tumour growth and survival. Together, these findings underscore the intricate crosstalk between tumours and neurons, driven by the expression of neurotransmitter receptors.

Building on this foundation, the current study gives a few insights into ARFGEF3 in breast-to-brain metastasis, focusing on its regulation of neurotransmitter receptors. Whole-exome sequencing of 26 breast-to-brain metastases (BBM) identified ARFGEF3 mutations, predominantly loss-of-function substitutions, suggesting a role in metastatic adaptation. The CRISPR CAS9 BIG3 KO cells does not show any alteration of growth rates compared to

control cells, but demonstrates a mesenchymal-like phenotype, potentially may be contributing to dormancy and late-onset metastases in ER-positive breast cancer patients post-tamoxifen therapy. BIG3 loss was associated with increased PHB2. These previous studies by Liu et al. (2016) and Zeng et al. (2019) have provided valuable insights into the link between neuronal synaptic regulation and breast cancer brain metastasis. The formation of pseudo-synapses is a key mechanism for tumour survival and proliferation within the brain microenvironment, as these structures allow tumour cells to exploit neuronal signaling for their growth. This knowledge gap leads to the hypothesis that specific genetic mutations may contribute to brain metastasis by the differential expression of neurotransmitter receptors that enable pseudosynaptic interactions. This mutation identified in breast-to-brain metastatic cells emerges as a potential mechanism underlying this altered expression of neurotransmitter receptors, further enhancing the ability of tumour cells to colonize and thrive in the brain microenvironment. This finding underscores the need for further mechanistic studies to unravel the molecular pathways governing pseudo-synapse formation, which could provide critical insights into the metastatic progression of breast cancer to the brain. Specifically, investigating how BIG3 mutations influence neurotransmitter receptor expression, tumor dormancy, and brain colonization is essential for understanding the mechanisms underlying late-stage metastases. These studies may reveal potential therapeutic targets for preventing the establishment and reactivation of brain metastases, offering new avenues for improving patient outcomes.

6. CONCLUSIONS

Brain metastasis is a complex process in which primary breast cancer cells invade tissues, which leads to poor prognosis and significantly reduces the quality of life for affected patients. This study highlights a potential mechanism by which breast-to-brain metastatic cells colonise the brain. The loss of *ARFGEF3* through mutation is identified as a potential driver of breast cancer cell metastasis and tumour formation in the brain. Furthermore, metastatic breast cancer cells exhibit active signalling with neurons, which supports their survival and proliferation in the brain microenvironment.

Whole genome sequencing of 26 breast-to-brain metastatic patients was conducted to identify genetic alterations shared between primary breast tumours and brain metastasis. Among the findings, *ARFGEF3* mutations were prominently identified. This study demonstrates that loss of *ARFGEF3* impacts the expression of neurotransmitter receptors. *ARFGEF3* appears to regulate certain neurotransmitter receptors, suggesting a potential mechanism contributing to brain metastasis. Neurotransmitter receptor expression plays a crucial role in forming active connections with neurons, enabling breast metastatic cells to form pseudo-synapses and adapt to the brain microenvironment. To achieve this, firstly the knockout of *ARFGEF3* in MCF-7 cells using CRISPR-Cas9, a model previously generated by Ivonne Olivares were validated. Confirmation of gene knockout was performed using RT-PCR and Western blot analysis, ensuring the absence of *ARFGEF3* expression in the KO clones. Subsequently, cell growth assays demonstrated that *ARFGEF3* loss does not affect cell proliferation rates, phenotypic changes resembling mesenchymal-like traits were observed. Furthermore, the loss of *ARFGEF3* results in a significant alteration in the expression of neurotransmitter receptor subunits, particularly those involved in GABAergic and glutamatergic signaling pathways.

Key findings from this study include:

ARFGEF3 knockout breast cancer cells exhibit a mesenchymal-like morphology while maintaining similar proliferation rates compared to control cells.

Loss of ARFGEF3 does not affect PHB2 transcriptionally but leads to its upregulation at the protein level, suggesting post-transcriptional or translational regulation.

ARFGEF3 knockout cells show differential expression of multiple neurotransmitter receptor subunits, including upregulation of GABRG1, GABRB3, GABRA5, GABRE, GABBR1, GRIN2C, and GRIN2D, along with the downregulation of GRIN1, GRIA2, GABRG2, and GABRB2.

Protein-level validation using Western blot, flow cytometry, and immunofluorescence confirmed the upregulation of key neurotransmitter receptor subunits, particularly GABRG1 and GRIN2D, which are implicated in interactions with the brain microenvironment.

The observed alterations in neurotransmitter receptor expression suggest that ARFGEF3 loss may facilitate breast cancer cell adaptation to the brain microenvironment, contributing to metastatic colonization.

While this study provides key insights into the role of ARFGEF3 in breast-to-brain metastases, several questions remain unanswered, necessitating further research:

To uncover the downstream signaling pathways influenced by ARFGEF3, RNA sequencing should be performed on ARFGEF3 KO and control cells. This will help identify differentially expressed genes and pathways involved in neurotransmitter receptor regulation, tumor progression, and metastasis.

To perform co-culture experiments with human neuronal cells and ARFGEF3 KO/control MCF-7 cells. Using gold nanoparticle labeling and electron microscopy, this model could

provide valuable insights into pseudo-synapse formation. These pseudo-synapses facilitate communication and enhance tumour cell survival within the brain, a critical factor in successful colonisation by metastatic cells. Establish mouse models to assess whether ARFGEF3 KO breast cancer cells exhibit increased metastatic potential to the brain. This will provide critical in vivo validation of our findings.

Additionally, expanding the analysis to include other neurotransmitter receptors. These receptors, potentially forming complexes or synapse-like structures with neurons, could reveal intricate signalling mechanisms that ARFGEF3 mutations enable. Investigating their collective role could provide insights into how ARFGEF3 loss alters receptor expression and functionality to promote brain metastasis.

To investigate the role of connexins, which are involved in gap junction formation, in mediating tumor-astrocyte interactions. Understanding these interactions may reveal novel mechanisms of tumor cell adhesion and survival in the brain microenvironment.

Advanced methodologies such as migration and invasion assays, combined with 3D models, would also add valuable data to this investigation. These assays can simulate the dynamic processes of tumour cell migration across the blood-brain barrier (BBB) and subsequent invasion into the brain parenchyma, providing a functional perspective on ARFGEF3's impact.

Identifying these pathways can pave the way for discovering therapeutic targets aimed at disrupting these interactions, offering potential strategies to combat brain metastasis in breast cancer patients. Integrating all these approaches will significantly enhance the understanding of ARFGEF3's role and its implications in the progression of metastatic breast cancer to the brain.

7. REFERENCES

- Adams, J.C. (2001) 'Cell-matrix contact structures', *Cellular and Molecular Life Sciences*, 58(3), pp. 371–392. Available at: <https://doi.org/10.1007/PL00000864>.
- Adamson, E.D. (1987) 'Oncogenes in development', *Development*, 99(4), pp. 449–471. Available at: <https://doi.org/10.1242/dev.99.4.449>.
- Akram, M. *et al.* (2017) 'Awareness and current knowledge of breast cancer', *Biological Research*, 50(1), p. 33. Available at: <https://doi.org/10.1186/s40659-017-0140-9>.
- Albertson, D.G. (2006) 'Gene amplification in cancer', *Trends in Genetics*, 22(8), pp. 447–455. Available at: <https://doi.org/10.1016/j.tig.2006.06.007>.
- Andersen, J.V., Schousboe, A. and Wellendorph, P. (2023) 'Astrocytes regulate inhibitory neurotransmission through GABA uptake, metabolism, and recycling', *Essays in Biochemistry*, 67(1), pp. 77–91. Available at: <https://doi.org/10.1042/EBC20220208>.
- Arem, H. and Loftfield, E. (2018) 'Cancer Epidemiology: A Survey of Modifiable Risk Factors for Prevention and Survivorship', *American Journal of Lifestyle Medicine*, 12(3), pp. 200–210. Available at: <https://doi.org/10.1177/1559827617700600>.
- Arvanitis, C.D., Ferraro, G.B. and Jain, R.K. (2020) 'The blood–brain barrier and blood–tumour barrier in brain tumours and metastases', *Nature Reviews Cancer*, 20(1), pp. 26–41. Available at: <https://doi.org/10.1038/s41568-019-0205-x>.
- Banys-Paluchowski, M., Reinhardt, F. and Fehm, T. (2020) 'Disseminated Tumor Cells and Dormancy in Breast Cancer Progression', in, pp. 35–43. Available at: https://doi.org/10.1007/978-3-030-35805-1_3.
- Barron, T. *et al.* (2023) 'CNSC-01. GABAERGIC NEURON-TO-GLIOMA SYNAPSES IN DIFFUSE MIDLINE GLIOMAS', *Neuro-Oncology*, 25(Supplement_1), pp. i11–i11. Available at: <https://doi.org/10.1093/neuonc/noad073.044>.

- Barzaman, K. *et al.* (2020) ‘Breast cancer: Biology, biomarkers, and treatments’, *International Immunopharmacology*, 84, p. 106535. Available at: <https://doi.org/10.1016/j.intimp.2020.106535>.
- Berry, D.A. *et al.* (2005) ‘Effect of Screening and Adjuvant Therapy on Mortality from Breast Cancer’, *New England Journal of Medicine*, 353(17), pp. 1784–1792. Available at: <https://doi.org/10.1056/NEJMoa050518>.
- Bornman, D.M. *et al.* (2001) ‘Methylation of the E-cadherin Gene in Bladder Neoplasia and in Normal Urothelial Epithelium from Elderly Individuals’, *The American Journal of Pathology*, 159(3), pp. 831–835. Available at: [https://doi.org/10.1016/S0002-9440\(10\)61758-0](https://doi.org/10.1016/S0002-9440(10)61758-0).
- Bos, P.D. *et al.* (2009) ‘Genes that mediate breast cancer metastasis to the brain’, *Nature*, 459(7249), pp. 1005–1009. Available at: <https://doi.org/10.1038/nature08021>.
- Botezatu, A. *et al.* (2016) ‘Mechanisms of Oncogene Activation’, in *New Aspects in Molecular and Cellular Mechanisms of Human Carcinogenesis*. InTech. Available at: <https://doi.org/10.5772/61249>.
- Brastianos, P.K. *et al.* (2015) ‘Genomic Characterization of Brain Metastases Reveals Branched Evolution and Potential Therapeutic Targets’, *Cancer Discovery*, 5(11), pp. 1164–1177. Available at: <https://doi.org/10.1158/2159-8290.CD-15-0369>.
- Breast Cancer Treatment (PDQ®)–Patient Version* (no date).
- Brosnan, E.M. and Anders, C.K. (2018) ‘Understanding patterns of brain metastasis in breast cancer and designing rational therapeutic strategies’, *Annals of Translational Medicine*, 6(9), pp. 163–163. Available at: <https://doi.org/10.21037/atm.2018.04.35>.
- Brown, J.S. *et al.* (2023) ‘Updating the Definition of Cancer’, *Molecular Cancer Research*, 21(11), pp. 1142–1147. Available at: <https://doi.org/10.1158/1541-7786.MCR-23-0411>.
- Cancer Research UK (2024) *Types of cancer*, <https://www.cancerresearchuk.org/about-cancer/what-is-cancer/how-cancer-starts/types-of-cancer>. Available at:

<https://www.cancerresearchuk.org/about-cancer/what-is-cancer/how-cancer-starts/types-of-cancer> (Accessed: 4 July 2024).

Canel, M. *et al.* (2013) 'E-cadherin–integrin crosstalk in cancer invasion and metastasis', *Journal of Cell Science*, 126(2), pp. 393–401. Available at: <https://doi.org/10.1242/jcs.100115>.

Cao, Y. *et al.* (2017) 'Glutamic Pyruvate Transaminase GPT2 Promotes Tumorigenesis of Breast Cancer Cells by Activating Sonic Hedgehog Signaling', *Theranostics*, 7(12), pp. 3021–3033. Available at: <https://doi.org/10.7150/thno.18992>.

Chaffer, C.L. and Weinberg, R.A. (2011) 'A Perspective on Cancer Cell Metastasis', *Science*, 331(6024), pp. 1559–1564. Available at: <https://doi.org/10.1126/science.1203543>.

Chambers, A.F., Groom, A.C. and MacDonald, I.C. (2002) 'Dissemination and growth of cancer cells in metastatic sites', *Nature Reviews Cancer*, 2(8), pp. 563–572. Available at: <https://doi.org/10.1038/nrc865>.

Chen, Q. *et al.* (2016) 'Carcinoma–astrocyte gap junctions promote brain metastasis by cGAMP transfer', *Nature*, 533(7604), pp. 493–498. Available at: <https://doi.org/10.1038/nature18268>.

Chen, S.-H. *et al.* (2019) 'Perineural invasion of cancer: a complex crosstalk between cells and molecules in the perineural niche.', *American journal of cancer research*, 9(1), pp. 1–21.

Chen, Y.-A. *et al.* (2014) 'Brefeldin A-inhibited guanine nucleotide-exchange protein 3 (BIG3) is predicted to interact with its partner through an ARM-type α -helical structure', *BMC Research Notes*, 7(1), p. 435. Available at: <https://doi.org/10.1186/1756-0500-7-435>.

Chigira, T. *et al.* (2019a) 'Biophysical characterization of the breast cancer-related BIG3-PHB2 interaction: Effect of non-conserved loop region of BIG3 on the structure and the interaction', *Biochemical and Biophysical Research Communications*, 518(1), pp. 183–189. Available at: <https://doi.org/10.1016/j.bbrc.2019.08.028>.

Chigira, T. *et al.* (2019b) ‘Biophysical characterization of the breast cancer-related BIG3-PHB2 interaction: Effect of non-conserved loop region of BIG3 on the structure and the interaction’, *Biochemical and Biophysical Research Communications*, 518(1), pp. 183–189. Available at: <https://doi.org/10.1016/j.bbrc.2019.08.028>.

Corti, C. *et al.* (2022) ‘Targeting brain metastases in breast cancer’, *Cancer Treatment Reviews*, 103, p. 102324. Available at: <https://doi.org/10.1016/j.ctrv.2021.102324>.

Courtney, D. *et al.* (2022) ‘Breast cancer recurrence: factors impacting occurrence and survival’, *Irish Journal of Medical Science (1971 -)*, 191(6), pp. 2501–2510. Available at: <https://doi.org/10.1007/s11845-022-02926-x>.

Craene, B. De and Berx, G. (2013) ‘Regulatory networks defining EMT during cancer initiation and progression’, *Nature Reviews Cancer*, 13(2), pp. 97–110. Available at: <https://doi.org/10.1038/nrc3447>.

Cristofalo, V.J. *et al.* (1998) ‘Relationship between donor age and the replicative lifespan of human cells in culture: A reevaluation’, *Proceedings of the National Academy of Sciences*, 95(18), pp. 10614–10619. Available at: <https://doi.org/10.1073/pnas.95.18.10614>.

Dakal, T.C. *et al.* (2024) ‘Oncogenes and tumor suppressor genes: functions and roles in cancers’, *MedComm*, 5(6). Available at: <https://doi.org/10.1002/mco2.582>.

Damrauer, J.S. *et al.* (2014) ‘Intrinsic subtypes of high-grade bladder cancer reflect the hallmarks of breast cancer biology’, *Proceedings of the National Academy of Sciences*, 111(8), pp. 3110–3115. Available at: <https://doi.org/10.1073/pnas.1318376111>.

Das, D. *et al.* (2023a) ‘Breast-to-Brain Metastasis: from Microenvironment to Plasticity’, *Current Breast Cancer Reports*, 15(2), pp. 142–151. Available at: <https://doi.org/10.1007/s12609-023-00488-0>.

Das, D. *et al.* (2023b) ‘Breast-to-Brain Metastasis: from Microenvironment to Plasticity’, *Current Breast Cancer Reports*, 15(2), pp. 142–151. Available at: <https://doi.org/10.1007/s12609-023-00488-0>.

Davies, C. *et al.* (2013) ‘Long-term effects of continuing adjuvant tamoxifen to 10 years versus stopping at 5 years after diagnosis of oestrogen receptor-positive breast cancer: ATLAS, a randomised trial’, *The Lancet*, 381(9869), pp. 805–816. Available at: [https://doi.org/10.1016/S0140-6736\(12\)61963-1](https://doi.org/10.1016/S0140-6736(12)61963-1).

Drell, T.L. *et al.* (2003) ‘Effects of Neurotransmitters on the Chemokinesis and Chemotaxis of MDA-MB-468 Human Breast Carcinoma Cells’, *Breast Cancer Research and Treatment*, 80(1), pp. 63–70. Available at: <https://doi.org/10.1023/A:1024491219366>.

Dubey, A. *et al.* (2023) ‘Breast Cancer and the Brain: A Comprehensive Review of Neurological Complications’, *Cureus* [Preprint]. Available at: <https://doi.org/10.7759/cureus.48941>.

Eduardo Flores-Soto, M. *et al.* (2013) ‘Receptor to Glutamate NMDA-Type: The Functional Diversity of the NR1 Isoforms and Pharmacological Properties’, *Current Pharmaceutical Design*, 19(38), pp. 6709–6719. Available at: <https://doi.org/10.2174/1381612811319380003>.

Fares, J., Kanojia, D., *et al.* (2020) ‘Genes that Mediate Metastasis across the Blood–Brain Barrier’, *Trends in Cancer*, 6(8), pp. 660–676. Available at: <https://doi.org/10.1016/j.trecan.2020.04.007>.

Fares, J., Fares, M.Y., *et al.* (2020) ‘Molecular principles of metastasis: a hallmark of cancer revisited’, *Signal Transduction and Targeted Therapy*. Springer Nature. Available at: <https://doi.org/10.1038/s41392-020-0134-x>.

Faulkner, S. *et al.* (2019) ‘Tumor Neurobiology and the War of Nerves in Cancer’, *Cancer Discovery*, 9(6), pp. 702–710. Available at: <https://doi.org/10.1158/2159-8290.CD-18-1398>.

Fedele, M. *et al.* (2022) ‘The Epithelial–Mesenchymal Transition at the Crossroads between Metabolism and Tumor Progression’, *International Journal of Molecular Sciences*, 23(2), p. 800. Available at: <https://doi.org/10.3390/ijms23020800>.

Fehm, T. *et al.* (2012) ‘Dormancy in breast cancer’, *Breast Cancer: Targets and Therapy*, p. 183. Available at: <https://doi.org/10.2147/BCTT.S26431>.

Friedl, P. and Wolf, K. (2003a) ‘Tumour-cell invasion and migration: diversity and escape mechanisms’, *Nature Reviews Cancer*, 3(5), pp. 362–374. Available at: <https://doi.org/10.1038/nrc1075>.

Friedl, P. and Wolf, K. (2003b) ‘Tumour-cell invasion and migration: diversity and escape mechanisms’, *Nature Reviews Cancer*, 3(5), pp. 362–374. Available at: <https://doi.org/10.1038/nrc1075>.

Gallo, S., Vitacolonna, A. and Crepaldi, T. (2023) ‘NMDA Receptor and Its Emerging Role in Cancer’, *International Journal of Molecular Sciences*, 24(3), p. 2540. Available at: <https://doi.org/10.3390/ijms24032540>.

Galloni, C. *et al.* (2024) ‘Brain endothelial cells promote breast cancer cell extravasation to the brain via EGFR-DOCK4-RAC1 signalling’, *Communications Biology*, 7(1), p. 602. Available at: <https://doi.org/10.1038/s42003-024-06200-x>.

Gamble, P. *et al.* (2021) ‘Determining breast cancer biomarker status and associated morphological features using deep learning’, *Communications Medicine*, 1(1), p. 14. Available at: <https://doi.org/10.1038/s43856-021-00013-3>.

García-Gaytán, A.C. *et al.* (2022) ‘Glutamatergic system components as potential biomarkers and therapeutic targets in cancer in non-neural organs’, *Frontiers in Endocrinology*, 13. Available at: <https://doi.org/10.3389/fendo.2022.1029210>.

- Gumireddy, K. *et al.* (2016a) ‘The mRNA-edited form of GABRA3 suppresses GABRA3-mediated Akt activation and breast cancer metastasis’, *Nature Communications*, 7(1), p. 10715. Available at: <https://doi.org/10.1038/ncomms10715>.
- Gumireddy, K. *et al.* (2016b) ‘The mRNA-edited form of GABRA3 suppresses GABRA3-mediated Akt activation and breast cancer metastasis’, *Nature Communications*, 7(1), p. 10715. Available at: <https://doi.org/10.1038/ncomms10715>.
- Hamester, F. *et al.* (2022) ‘Insights into the Steps of Breast Cancer–Brain Metastases Development: Tumor Cell Interactions with the Blood–Brain Barrier’, *International Journal of Molecular Sciences*, 23(3), p. 1900. Available at: <https://doi.org/10.3390/ijms23031900>.
- Hammond-Weinberger, D.R. *et al.* (2020) ‘Mechanism for neurotransmitter-receptor matching’, *Proceedings of the National Academy of Sciences*, 117(8), pp. 4368–4374. Available at: <https://doi.org/10.1073/pnas.1916600117>.
- Hanahan, D. (2022) ‘Hallmarks of Cancer: New Dimensions’, *Cancer Discovery*, 12(1), pp. 31–46. Available at: <https://doi.org/10.1158/2159-8290.CD-21-1059>.
- Hanahan, D. and Monje, M. (2023) ‘Cancer hallmarks intersect with neuroscience in the tumor microenvironment’, *Cancer Cell*. Cell Press, pp. 573–580. Available at: <https://doi.org/10.1016/j.ccell.2023.02.012>.
- Hanahan, D. and Weinberg, R.A. (2011) ‘Hallmarks of cancer: The next generation’, *Cell*, pp. 646–674. Available at: <https://doi.org/10.1016/j.cell.2011.02.013>.
- Hosonaga, M., Saya, H. and Arima, Y. (2020) ‘Molecular and cellular mechanisms underlying brain metastasis of breast cancer’, *Cancer and Metastasis Reviews*, 39(3), pp. 711–720. Available at: <https://doi.org/10.1007/s10555-020-09881-y>.
- Huang, L., Wu, R.-L. and Xu, A.-M. (2015) ‘Epithelial-mesenchymal transition in gastric cancer.’, *American journal of translational research*, 7(11), pp. 2141–58.

Huang, Qiqi *et al.* (2022) ‘Neurotransmitters: Potential Targets in Glioblastoma’, *Cancers*, 14(16), p. 3970. Available at: <https://doi.org/10.3390/cancers14163970>.

Humsa S. Venkatesh, L.T.T.P.J.W.S.N.S.M.G.J.L.J.N.D.Y.D.P.J.M.J.J.Z.C.J.T.V.O.P.M. (2017) ‘Targeting neuronal activity-regulated neuroligin-3 dependency for high-grade glioma therapy’, *Nature* doi: 10.1038/nature24014 [Preprint].

IncCooper GM. (2000) *The Cell: A Molecular Approach. 2nd edition.* 2nd edition. Edited by Sinauer Associates. Sunderland (MA): Sinauer Associates, Inc.

Ivanova, M. *et al.* (2023) ‘Breast Cancer with Brain Metastasis: Molecular Insights and Clinical Management’, *Genes*, 14(6), p. 1160. Available at: <https://doi.org/10.3390/genes14061160>.

Jahanban-Esfahlan, R., Seidi, K. and Zarghami, N. (2017) ‘Tumor vascular infarction: prospects and challenges’, *International Journal of Hematology*, 105(3), pp. 244–256. Available at: <https://doi.org/10.1007/s12185-016-2171-3>.

Jayachandran, P. *et al.* (2023) ‘Breast cancer and neurotransmitters: emerging insights on mechanisms and therapeutic directions’, *Oncogene*, 42(9), pp. 627–637. Available at: <https://doi.org/10.1038/s41388-022-02584-4>.

Jiang, S.-H. *et al.* (2020) ‘Neurotransmitters: emerging targets in cancer’, *Oncogene*, 39(3), pp. 503–515. Available at: <https://doi.org/10.1038/s41388-019-1006-0>.

Kaleem, M. *et al.* (2022) ‘An Insight into Molecular Targets of Breast Cancer Brain Metastasis’, *International Journal of Molecular Sciences*, 23(19), p. 11687. Available at: <https://doi.org/10.3390/ijms231911687>.

Kaloni, D. *et al.* (2023) ‘BCL-2 protein family: attractive targets for cancer therapy’, *Apoptosis*, 28(1–2), pp. 20–38. Available at: <https://doi.org/10.1007/s10495-022-01780-7>.

Kepuladze, S., Burkadze, G. and Kokhreidze, I. (2024) ‘Epithelial-Mesenchymal Transition Indexes in Triple-Negative Breast Cancer Progression and Metastases’, *Cureus* [Preprint]. Available at: <https://doi.org/10.7759/cureus.68761>.

- Kim, J. *et al.* (2009) ‘Activation of an estrogen/estrogen receptor signaling by BIG3 through its inhibitory effect on nuclear transport of PHB2/REA in breast cancer’, *Cancer Science*, 100(8), pp. 1468–1478. Available at: <https://doi.org/10.1111/j.1349-7006.2009.01209.x>.
- Kim, N.-H. *et al.* (2015) ‘BIG3 Inhibits the Estrogen-Dependent Nuclear Translocation of PHB2 via Multiple Karyopherin-Alpha Proteins in Breast Cancer Cells’, *PLOS ONE*, 10(6), p. e0127707. Available at: <https://doi.org/10.1371/journal.pone.0127707>.
- Koda, S. *et al.* (2023) ‘The role of glutamate receptors in the regulation of the tumor microenvironment’, *Frontiers in Immunology*, 14. Available at: <https://doi.org/10.3389/fimmu.2023.1123841>.
- Kontomanolis, E.N. *et al.* (2021) ‘Basic principles of molecular biology of cancer cell-Molecular cancer indicators’, *JBUON*, 26(5), pp. 1723–1734.
- Krakhmal, N. V *et al.* (2015) ‘Cancer Invasion: Patterns and Mechanisms.’, *Acta naturae*, 7(2), pp. 17–28.
- Kuol, N. *et al.* (2018) ‘Role of the nervous system in cancer metastasis’, *Journal of Experimental & Clinical Cancer Research*, 37(1), p. 5. Available at: <https://doi.org/10.1186/s13046-018-0674-x>.
- Lee, E.Y.H.P. and Muller, W.J. (2010) ‘Oncogenes and Tumor Suppressor Genes’, *Cold Spring Harbor Perspectives in Biology*, 2(10), pp. a003236–a003236. Available at: <https://doi.org/10.1101/cshperspect.a003236>.
- Lei, S. *et al.* (2021) ‘Global patterns of breast cancer incidence and mortality: A population-based cancer registry data analysis from 2000 to 2020’, *Cancer Communications*, 41(11), pp. 1183–1194. Available at: <https://doi.org/10.1002/cac2.12207>.
- Letellier, M. and Goda, Y. (2023) ‘Astrocyte Calcium Signaling Shifts the Polarity of Presynaptic Plasticity’, *Neuroscience*, 525, pp. 38–46. Available at: <https://doi.org/10.1016/j.neuroscience.2023.05.032>.

- Li, H. *et al.* (2014) 'BIG3 inhibits insulin granule biogenesis and insulin secretion', *EMBO reports* [Preprint]. Available at: <https://doi.org/10.1002/embr.201338181>.
- Li, H. *et al.* (2015) 'Increased biogenesis of glucagon-containing secretory granules and glucagon secretion in BIG3-knockout mice', *Molecular Metabolism*, 4(3), pp. 246–252. Available at: <https://doi.org/10.1016/j.molmet.2015.01.001>.
- Li, J. *et al.* (2022) 'The dark side of synaptic proteins in tumours', *British Journal of Cancer*, 127(7), pp. 1184–1192. Available at: <https://doi.org/10.1038/s41416-022-01863-x>.
- Li, N. *et al.* (2023) 'The delta subunit of the GABA_A receptor is necessary for the GPT2-promoted breast cancer metastasis', *Theranostics*, 13(4), pp. 1355–1369. Available at: <https://doi.org/10.7150/thno.80544>.
- Li, R.Q. *et al.* (2023a) 'Exploring neurotransmitters and their receptors for breast cancer prevention and treatment', *Theranostics*, 13(3), pp. 1109–1129. Available at: <https://doi.org/10.7150/thno.81403>.
- Li, R.Q. *et al.* (2023b) 'Exploring neurotransmitters and their receptors for breast cancer prevention and treatment', *Theranostics*, 13(3), pp. 1109–1129. Available at: <https://doi.org/10.7150/thno.81403>.
- Liu, T. *et al.* (2016a) 'Brefeldin A-inhibited guanine nucleotide exchange protein 3 is localized in lysosomes and regulates GABA signaling in hippocampal neurons', *Journal of Neurochemistry*, 139(5), pp. 748–756. Available at: <https://doi.org/10.1111/jnc.13859>.
- Liu, T. *et al.* (2016b) 'Brefeldin A-inhibited guanine nucleotide exchange protein 3 is localized in lysosomes and regulates GABA signaling in hippocampal neurons', *Journal of Neurochemistry*, 139(5), pp. 748–756. Available at: <https://doi.org/10.1111/jnc.13859>.
- Liu, X. *et al.* (2005) 'Nonsynaptic GABA signaling in postnatal subventricular zone controls proliferation of GFAP-expressing progenitors', *Nature Neuroscience*, 8(9), pp. 1179–1187. Available at: <https://doi.org/10.1038/nn1522>.

- Liu, Y. *et al.* (2015) ‘Targeting tumor suppressor genes for cancer therapy’, *BioEssays*, 37(12), pp. 1277–1286. Available at: <https://doi.org/10.1002/bies.201500093>.
- Lorusso, G. *et al.* (2022) ‘Connexins orchestrate progression of breast cancer metastasis to the brain by promoting FAK activation’, *Science Translational Medicine*, 14(661). Available at: <https://doi.org/10.1126/scitranslmed.aax8933>.
- Lynch, H.T., Marcus, J.N. and Rubinstein, W.S. (2008) ‘Stemming the Tide of Cancer for *BRCA1/2* Mutation Carriers’, *Journal of Clinical Oncology*, 26(26), pp. 4239–4243. Available at: <https://doi.org/10.1200/JCO.2008.17.4201>.
- Manore, S.G. *et al.* (2022) ‘IL-6/JAK/STAT3 Signaling in Breast Cancer Metastasis: Biology and Treatment’, *Frontiers in Oncology*, 12. Available at: <https://doi.org/10.3389/fonc.2022.866014>.
- Markowitz, S.D. and Bertagnolli, M.M. (2009) ‘Molecular Basis of Colorectal Cancer’, *New England Journal of Medicine*, 361(25), pp. 2449–2460. Available at: <https://doi.org/10.1056/NEJMra0804588>.
- Masugi-Tokita, M. and Shigemoto, R. (2007) ‘High-resolution quantitative visualization of glutamate and GABA receptors at central synapses’, *Current Opinion in Neurobiology*, 17(3), pp. 387–393. Available at: <https://doi.org/10.1016/j.conb.2007.04.012>.
- Matsui, A. *et al.* (2013) ‘Gene amplification: mechanisms and involvement in cancer’, *BioMolecular Concepts*, 4(6), pp. 567–582. Available at: <https://doi.org/10.1515/bmc-2013-0026>.
- Mattiuzzi, C. and Lippi, G. (2019) ‘Current cancer epidemiology’, *Journal of Epidemiology and Global Health*, 9(4), pp. 217–222. Available at: <https://doi.org/10.2991/jegh.k.191008.001>.
- Maughan, K.L., Lutterbie, M.A. and Ham, P.S. (2010) ‘Treatment of breast cancer.’, *American family physician*, 81(11), pp. 1339–46.

Miricescu, D. *et al.* (2020) ‘PI3K/AKT/mTOR Signaling Pathway in Breast Cancer: From Molecular Landscape to Clinical Aspects’, *International Journal of Molecular Sciences*, 22(1), p. 173. Available at: <https://doi.org/10.3390/ijms22010173>.

Morelli, M.B. *et al.* (2019) ‘Role of the NMDA Receptor in the Antitumor Activity of Chiral 1,4-Dioxane Ligands in MCF-7 and SKBR3 Breast Cancer Cells’, *ACS Medicinal Chemistry Letters*, 10(4), pp. 511–516. Available at: <https://doi.org/10.1021/acsmchemlett.8b00536>.

Motoi, N. *et al.* (2000) ‘Role of ras mutation in the progression of thyroid carcinoma of follicular epithelial origin’, *Pathology - Research and Practice*, 196(1), pp. 1–7. Available at: [https://doi.org/10.1016/S0344-0338\(00\)80015-1](https://doi.org/10.1016/S0344-0338(00)80015-1).

N Kontomanolis, E. *et al.* (2021) ‘Basic principles of molecular biology of cancer cell-Molecular cancer indicators.’, *Journal of B.U.ON. : official journal of the Balkan Union of Oncology*, 26(5), pp. 1723–1734.

Neman, J. *et al.* (2014a) ‘Human breast cancer metastases to the brain display GABAergic properties in the neural niche’, *Proceedings of the National Academy of Sciences*, 111(3), pp. 984–989. Available at: <https://doi.org/10.1073/pnas.1322098111>.

Neman, J. *et al.* (2014b) ‘Human breast cancer metastases to the brain display GABAergic properties in the neural niche’, *Proceedings of the National Academy of Sciences*, 111(3), pp. 984–989. Available at: <https://doi.org/10.1073/pnas.1322098111>.

Neman, J. *et al.* (2014c) ‘Human breast cancer metastases to the brain display GABAergic properties in the neural niche’, *Proceedings of the National Academy of Sciences*, 111(3), pp. 984–989. Available at: <https://doi.org/10.1073/pnas.1322098111>.

Nguyen, T.M. *et al.* (2023) ‘Unveiling the Neural Environment in Cancer: Exploring the Role of Neural Circuit Players and Potential Therapeutic Strategies’, *Cells*, 12(15), p. 1996. Available at: <https://doi.org/10.3390/cells12151996>.

Nisar, I. *et al.* (2024) ‘Extending Tamoxifen Beyond 10years in High Risk Young Breast cancer Patients’, *Journal of Cancer Research and Reviews*, 1(1), p. 14. Available at: <https://doi.org/10.5455/JCRR.20240123070422>.

Nolan, E., Lindeman, G.J. and Visvader, J.E. (2023) ‘Deciphering breast cancer: from biology to the clinic’, *Cell*, 186(8), pp. 1708–1728. Available at: <https://doi.org/10.1016/j.cell.2023.01.040>.

O’Brien, M.A. and Kirby, R. (2008) ‘Apoptosis: A review of pro-apoptotic and anti-apoptotic pathways and dysregulation in disease’, *Journal of Veterinary Emergency and Critical Care*, 18(6), pp. 572–585. Available at: <https://doi.org/10.1111/j.1476-4431.2008.00363.x>.

Olivares, I. (2023) *An investigation into the mechanisms of angiogenesis and breast cancer metastasis*. University of Wolverhampton.

Osswald, M. *et al.* (2015) ‘Brain tumour cells interconnect to a functional and resistant network’, *Nature*, 528(7580), pp. 93–98. Available at: <https://doi.org/10.1038/nature16071>.

Patel, A. (2020) ‘Benign vs Malignant Tumors’, *JAMA Oncology*, 6(9), p. 1488. Available at: <https://doi.org/10.1001/jamaoncol.2020.2592>.

Pei, Z. *et al.* (2020) ‘Pathway analysis of glutamate-mediated, calcium-related signaling in glioma progression’, *Biochemical Pharmacology*, 176, p. 113814. Available at: <https://doi.org/10.1016/j.bcp.2020.113814>.

Pickup, M.W., Mouw, J.K. and Weaver, V.M. (2014a) ‘The extracellular matrix modulates the hallmarks of cancer’, *EMBO reports*, 15(12), pp. 1243–1253. Available at: <https://doi.org/10.15252/embr.201439246>.

Pickup, M.W., Mouw, J.K. and Weaver, V.M. (2014b) ‘The extracellular matrix modulates the hallmarks of cancer’, *EMBO reports*, 15(12), pp. 1243–1253. Available at: <https://doi.org/10.15252/embr.201439246>.

- Pin, J.-P. and Bettler, B. (2016a) ‘Organization and functions of mGlu and GABAB receptor complexes’, *Nature*, 540(7631), pp. 60–68. Available at: <https://doi.org/10.1038/nature20566>.
- Pin, J.-P. and Bettler, B. (2016b) ‘Organization and functions of mGlu and GABAB receptor complexes’, *Nature*, 540(7631), pp. 60–68. Available at: <https://doi.org/10.1038/nature20566>.
- Power, C., Fanning, N. and Redmond, H.P. (2002) ‘Cellular Apoptosis and Organ Injury in Sepsis: A Review’, *Shock*, 18(3), pp. 197–211. Available at: <https://doi.org/10.1097/00024382-200209000-00001>.
- Quail, D.F. and Joyce, J.A. (2013) ‘Microenvironmental regulation of tumor progression and metastasis’, *Nature Medicine*, 19(11), pp. 1423–1437. Available at: <https://doi.org/10.1038/nm.3394>.
- Radin, D.P. and Tsirka, S.E. (2020) ‘Interactions between Tumor Cells, Neurons, and Microglia in the Glioma Microenvironment’, *International Journal of Molecular Sciences*, 21(22), p. 8476. Available at: <https://doi.org/10.3390/ijms21228476>.
- Ramamoorthi, K. and Lin, Y. (2011) ‘The contribution of GABAergic dysfunction to neurodevelopmental disorders’, *Trends in Molecular Medicine*, 17(8), pp. 452–462. Available at: <https://doi.org/10.1016/j.molmed.2011.03.003>.
- Rao, X. *et al.* (2013) ‘An improvement of the $2^{-\Delta\Delta CT}$ method for quantitative real-time polymerase chain reaction data analysis.’, *Biostatistics, bioinformatics and biomathematics*, 3(3), pp. 71–85.
- Roberts, E. (2007) ‘Gamma-aminobutyric acid’, *Scholarpedia*, 2(10), p. 3356. Available at: <https://doi.org/10.4249/scholarpedia.3356>.
- Rossari, F. *et al.* (2020) ‘Tumor dormancy as an alternative step in the development of chemoresistance and metastasis - clinical implications’, *Cellular Oncology*, 43(2), pp. 155–176. Available at: <https://doi.org/10.1007/s13402-019-00467-7>.

Sanfilippo, P. *et al.* (2024) ‘Mapping of multiple neurotransmitter receptor subtypes and distinct protein complexes to the connectome’, *Neuron*, 112(6), pp. 942-958.e13. Available at: <https://doi.org/10.1016/j.neuron.2023.12.014>.

Sarkar, S. *et al.* (2013) ‘Cancer development, progression, and therapy: An epigenetic overview’, *International Journal of Molecular Sciences*, pp. 21087–21113. Available at: <https://doi.org/10.3390/ijms141021087>.

Serrano-Gomez, S.J., Maziveyi, M. and Alahari, S.K. (2016) ‘Regulation of epithelial-mesenchymal transition through epigenetic and post-translational modifications’, *Molecular Cancer*, 15(1), p. 18. Available at: <https://doi.org/10.1186/s12943-016-0502-x>.

Sever, R. and Brugge, J.S. (2015) ‘Signal transduction in cancer’, *Cold Spring Harbor Perspectives in Medicine*, 5(4). Available at: <https://doi.org/10.1101/cshperspect.a006098>.

Sigel, E. and Steinmann, M.E. (2012) ‘Structure, Function, and Modulation of GABAA Receptors’, *Journal of Biological Chemistry*, 287(48), pp. 40224–40231. Available at: <https://doi.org/10.1074/jbc.R112.386664>.

Simsek, M. *et al.* (2022) ‘Breast Cancer Patients with Brain Metastases: A Cross-Sectional Study’, *The Breast Journal*, 2022, pp. 1–5. Available at: <https://doi.org/10.1155/2022/5763810>.

Singh, G., Thakur, N. and Kumar, U. (2023) ‘RAS: Circuitry and therapeutic targeting’, *Cellular Signalling*, 101, p. 110505. Available at: <https://doi.org/10.1016/j.cellsig.2022.110505>.

Sontheimer, H. (2008) ‘A role for glutamate in growth and invasion of primary brain tumors’, *Journal of Neurochemistry*, 105(2), pp. 287–295. Available at: <https://doi.org/10.1111/j.1471-4159.2008.05301.x>.

- Srinivasan, E.S. *et al.* (2021) ‘The microenvironment of brain metastases from solid tumors’, *Neuro-Oncology Advances*, 3(Supplement_5), pp. v121–v132. Available at: <https://doi.org/10.1093/noajnl/vdab121>.
- Suhail, Y. *et al.* (2019) ‘Systems Biology of Cancer Metastasis’, *Cell Systems*, 9(2), pp. 109–127. Available at: <https://doi.org/10.1016/j.cels.2019.07.003>.
- De Talhouet, S. *et al.* (2020) ‘Clinical outcome of breast cancer in carriers of BRCA1 and BRCA2 mutations according to molecular subtypes’, *Scientific Reports*, 10(1), p. 7073. Available at: <https://doi.org/10.1038/s41598-020-63759-1>.
- van Tellingen, O. *et al.* (2015) ‘Overcoming the blood–brain tumor barrier for effective glioblastoma treatment’, *Drug Resistance Updates*, 19, pp. 1–12. Available at: <https://doi.org/10.1016/j.drug.2015.02.002>.
- Terceiro, L.E.L. *et al.* (2023) ‘Navigating the Blood–Brain Barrier: Challenges and Therapeutic Strategies in Breast Cancer Brain Metastases’, *International Journal of Molecular Sciences*, 24(15), p. 12034. Available at: <https://doi.org/10.3390/ijms241512034>.
- Termini, J., Neman, J. and Jandial, R. (2014a) ‘Role of the Neural Niche in Brain Metastatic Cancer’, *Cancer Research*, 74(15), pp. 4011–4015. Available at: <https://doi.org/10.1158/0008-5472.CAN-14-1226>.
- Termini, J., Neman, J. and Jandial, R. (2014b) ‘Role of the Neural Niche in Brain Metastatic Cancer’, *Cancer Research*, 74(15), pp. 4011–4015. Available at: <https://doi.org/10.1158/0008-5472.CAN-14-1226>.
- Toki, S. *et al.* (2021a) ‘The survival and proliferation of osteosarcoma cells are dependent on the mitochondrial BIG3-PHB2 complex formation’, *Cancer Science*, 112(10), pp. 4208–4219. Available at: <https://doi.org/10.1111/cas.15099>.

- Toki, S. *et al.* (2021b) ‘The survival and proliferation of osteosarcoma cells are dependent on the mitochondrial BIG3-PHB2 complex formation’, *Cancer Science*, 112(10), pp. 4208–4219. Available at: <https://doi.org/10.1111/cas.15099>.
- Toki, S. *et al.* (2021c) ‘The survival and proliferation of osteosarcoma cells are dependent on the mitochondrial BIG3-PHB2 complex formation’, *Cancer Science*, 112(10), pp. 4208–4219. Available at: <https://doi.org/10.1111/cas.15099>.
- Torry, D.S. and Cooper, G.M. (1991) ‘Proto-Oncogenes in Development and Cancer’, *American Journal of Reproductive Immunology*, 25(3), pp. 129–132. Available at: <https://doi.org/10.1111/j.1600-0897.1991.tb01080.x>.
- Traynelis, S.F. *et al.* (2010) ‘Glutamate Receptor Ion Channels: Structure, Regulation, and Function’, *Pharmacological Reviews*, 62(3), pp. 405–496. Available at: <https://doi.org/10.1124/pr.109.002451>.
- Upadhyay, A. (2021a) ‘Cancer: An unknown territory; rethinking before going ahead’, *Genes and Diseases*. Chongqing University, pp. 655–661. Available at: <https://doi.org/10.1016/j.gendis.2020.09.002>.
- Upadhyay, A. (2021b) ‘Cancer: An unknown territory; rethinking before going ahead’, *Genes and Diseases*. Chongqing University, pp. 655–661. Available at: <https://doi.org/10.1016/j.gendis.2020.09.002>.
- Venkataramani, V. *et al.* (2019) ‘Glutamatergic synaptic input to glioma cells drives brain tumour progression’, *Nature*, 573(7775), pp. 532–538. Available at: <https://doi.org/10.1038/s41586-019-1564-x>.
- Venkataramani, V. *et al.* (2021) ‘Synaptic input to brain tumors: clinical implications’, *Neuro-Oncology*, 23(1), pp. 23–33. Available at: <https://doi.org/10.1093/neuonc/noaa158>.

Venkatesh, H.S. *et al.* (2015) ‘Neuronal Activity Promotes Glioma Growth through Neuroligin-3 Secretion’, *Cell*, 161(4), pp. 803–816. Available at: <https://doi.org/10.1016/j.cell.2015.04.012>.

Venkatesh, H.S. *et al.* (2019) ‘Electrical and synaptic integration of glioma into neural circuits’, *Nature*, 573(7775), pp. 539–545. Available at: <https://doi.org/10.1038/s41586-019-1563-y>.

Wang, S. and Lin, S.-Y. (2013) ‘Tumor dormancy: potential therapeutic target in tumor recurrence and metastasis prevention’, *Experimental Hematology & Oncology*, 2(1), p. 29. Available at: <https://doi.org/10.1186/2162-3619-2-29>.

Wang, Y. *et al.* (2021a) ‘Breast cancer brain metastasis: insight into molecular mechanisms and therapeutic strategies’, *British Journal of Cancer*, 125(8), pp. 1056–1067. Available at: <https://doi.org/10.1038/s41416-021-01424-8>.

Wang, Y. *et al.* (2021b) ‘Breast cancer brain metastasis: insight into molecular mechanisms and therapeutic strategies’, *British Journal of Cancer*, 125(8), pp. 1056–1067. Available at: <https://doi.org/10.1038/s41416-021-01424-8>.

Wang, Y. *et al.* (2021c) ‘Breast cancer brain metastasis: insight into molecular mechanisms and therapeutic strategies’, *British Journal of Cancer*, 125(8), pp. 1056–1067. Available at: <https://doi.org/10.1038/s41416-021-01424-8>.

Wilhelm, I. *et al.* (2013) ‘Role of the Blood-Brain Barrier in the Formation of Brain Metastases’, *International Journal of Molecular Sciences*, 14(1), pp. 1383–1411. Available at: <https://doi.org/10.3390/ijms14011383>.

Wilkinson, L. and Gathani, T. (2022) ‘Understanding breast cancer as a global health concern’, *The British Journal of Radiology*, 95(1130). Available at: <https://doi.org/10.1259/bjr.20211033>.

- Wu, J. and Crowe, D.L. (2019) ‘Molecular and cellular basis of mammary gland fibrosis and cancer risk’, *International Journal of Cancer*, 144(9), pp. 2239–2253. Available at: <https://doi.org/10.1002/ijc.32000>.
- Yoshimaru, T. *et al.* (2013) ‘Targeting BIG3–PHB2 interaction to overcome tamoxifen resistance in breast cancer cells’, *Nature Communications*, 4(1), p. 2443. Available at: <https://doi.org/10.1038/ncomms3443>.
- Yoshimaru, T. *et al.* (2014) ‘Xanthohumol suppresses oestrogen-signalling in breast cancer through the inhibition of BIG3-PHB2 interactions’, *Scientific Reports*, 4(1), p. 7355. Available at: <https://doi.org/10.1038/srep07355>.
- Yoshimaru, T. *et al.* (2015) ‘Therapeutic advances in <sc>BIG</sc> 3- <sc>PHB</sc> 2 inhibition targeting the crosstalk between estrogen and growth factors in breast cancer’, *Cancer Science*, 106(5), pp. 550–558. Available at: <https://doi.org/10.1111/cas.12654>.
- Yoshimaru, T., Ono, M., *et al.* (2017) ‘A-kinase anchoring protein BIG3 coordinates oestrogen signalling in breast cancer cells’, *Nature Communications*, 8(1), p. 15427. Available at: <https://doi.org/10.1038/ncomms15427>.
- Yoshimaru, T., Aihara, K., *et al.* (2017a) ‘Stapled BIG3 helical peptide ERAP potentiates anti-tumour activity for breast cancer therapeutics’, *Scientific Reports*, 7(1), p. 1821. Available at: <https://doi.org/10.1038/s41598-017-01951-6>.
- Yoshimaru, T., Aihara, K., *et al.* (2017b) ‘Stapled BIG3 helical peptide ERAP potentiates anti-tumour activity for breast cancer therapeutics’, *Scientific Reports*, 7(1), p. 1821. Available at: <https://doi.org/10.1038/s41598-017-01951-6>.
- Zeng, Q., Michael, I.P., *et al.* (2019) ‘Synaptic proximity enables NMDAR signalling to promote brain metastasis’, *Nature*, 573(7775), pp. 526–531. Available at: <https://doi.org/10.1038/s41586-019-1576-6>.

Zeng, Q., Zhang, P., *et al.* (2019) ‘Synaptic proximity enables NMDAR signalling to promote brain metastasis’, *Nature*, 573(7775), pp. 526–531. Available at: <https://doi.org/10.1038/s41586-019-1576-6>.

Zhang, J., Tian, X.-J. and Xing, J. (2016) ‘Signal Transduction Pathways of EMT Induced by TGF- β , SHH, and WNT and Their Crosstalks’, *Journal of Clinical Medicine*, 5(4), p. 41. Available at: <https://doi.org/10.3390/jcm5040041>.

Zhao, H. *et al.* (2023) ‘Biology of breast cancer brain metastases and novel therapies targeting the blood brain barrier: an updated review’, *Medical Oncology*, 40(6), p. 181. Available at: <https://doi.org/10.1007/s12032-023-02047-0>.

APPENDIX

The Ethics Committee at the University of Wolverhampton has approved this project - LSEC/2024-25/MM/52.